Space Mission Design Report

Space Mission Design Course - WS 2025/2026

LICOS
Lunar IoT Constellation System

Authors - matriculation numbers

Fiorenza Ferrante - 03807303
Simone Borzaga - 03805920
Jakub Czerniej - 03818972
Atharva Dhore - 03804621
Gabriel Virto - 03732192
Gonzalo Cuesta - 03698744

February 18, 2026

Table of Contents

Team Members and Roles

Name	Role
Fiorenza Ferrante	Mission Architecture, Payload, TT&C, ADCS
Simone Borzaga	Payload, TT&C, OBDH
Jakub Czerniej	Structure, Cost & Schedule, ConOps, Propulsion, Mass
Atharva Dhore	Power, Ground Segment, Executive Summary, Mass
Gabriel Virto	Thermal
Gonzalo Cuesta	Propulsion, Launch and Deployment

Table 1: Team Responsibilities

List of Tables

List of Figures

List of Abbreviations or Acronyms

IoT	Internet of Things
SLS	Simulated Lunar Surface (with no lumps, valleys or other surface irregularities, covering a Moon that has been approximated as a geometrical sphere)
ISL	Inter-Satellite Link
LFO	Lunar Frozen Orbits
mascons	Mass Concentrations

FSPL	Free-Space Path Loss
wrt	with respect to
RAAN	Right Ascension of Ascending Node
OBDH	On Board Data Handling
ADCS	Attitude Determination and Control System
NRHO	Near Rectilinear Halo Orbit
CPLO	Circular Polar Lunar Orbit
HPBW	Half Power BeamWidth
SFCG	Space Frequency Coordination Group
ITU	International Telecommunication Union
RF	Radio Frequency
LNA	Low Noise Amplifier
PA	Power Amplifier
BPF	Band Pass Filter
OBC	On-Board Computer
TCXO	Temperature Compensated Crystal Oscillator
SF	Spreading Factor
BW	Bandwidth
CR	Coding Rate
TID	Total Ionizing Dose
CSP	Cubesat Space Protocol
ECSS	European Cooperation for Space Standardization
LR-FHSS	Long Range Frequency Hopping Spread Spectrum
TDMA	Time Division Multiple Access
ToA	Time on Air
Tx	Transmitting
Rx	Receiving
SADA	Solar Array Drive Assembly
NF	Noise Figure
CoM	Centre of Mass
CMG	Control Moment Gyroscope
RW	Reaction Wheel
CCSDS	Consultative Committee for Space Data Systems
LICOS	Lunar IoT Constellation System
GS	Ground Segment

List of Symbols

a	Semimajor Axis
e	Eccentricity
i	Inclination
Ω	RAAN
ω	Argument of Periapsis
ν	True Anomaly
P_d	Daylight Power
P_e	Eclipse Power
T_p	Orbital Period
T_e	Eclipse Duration
T_d	Daylight Duration
η_{TJ}	Triple-junction solar cell efficiency
l_d	Degradation loss factor
L_d	Degradation factor
θ	Incidence angle
X_d	Distance factor
X_e	Eclipse fraction
P_{sa}	Required solar array power
P_0	Initial solar cell power
P_{BOL}	Beginning-of-life power
P_{EOL}	End-of-life power
δ	Degradation rate
A_{sa}	Solar array area
$P_{sa,1\ wing}$	Solar array power per wing
$E_{eclipse}$	Energy required during eclipse
$E_{bat,BOL}$	Battery energy at beginning-of-life
η_{rt}	Round-trip battery efficiency
f_{fade}	Battery capacity fade factor
V_{nom}	Nominal bus voltage
C_{pack}	Battery pack capacity
m_{bat}	Battery mass
β	Beta angle
$T_{eclipse}$	Eclipse duration
P_{peak}	Peak spacecraft power
$P_{avg,payload}$	Average payload power
$P_{avg,total}$	Total spacecraft average power

Abstract

The Lunar IoT Constellation (LICOS) mission proposes a scalable satellite network enabling low-data-rate communication between lunar surface assets and Earth using LoRa technology. The system supports sustained lunar operations by providing a distributed communication layer between surface users and terrestrial ground stations, aligned with emerging lunar communication infrastructure concepts [24, 26].

The baseline architecture consists of three orbital planes with twelve satellites per plane in near-polar frozen lunar orbits at approximately 500 km altitude, achieving full instantaneous global coverage. The orbit selection and long-term stability are based on frozen orbit analyses for the lunar environment [35, 14]. Inter-satellite links enable intraplanar and interplanar routing, while a relay segment forwards aggregated data to Earth via X-band communication, consistent with lunar relay system architectures [26].

Subsystem sizing confirms feasibility within nanosatellite-class constraints. The spacecraft average power demand is approximately 155 W, supported by deployable triple-junction solar arrays [6] and an EPS–battery configuration based on commercial space-qualified units [18, 17]. The design methodology follows established spacecraft power system practices [55]. A five-year operational lifetime with controlled lunar disposal ensures sustainable constellation management.

1 Introduction

1.1 Background

There is a growing international excitement about exploring the Moon, thanks to projects such as NASA's Artemis program and efforts by other governments and private companies. Upcoming missions are establishing the foundation for sustained human and robotic presence on the Moon [39], and they aim not only to revisit the lunar surface but to establish long-term infrastructure, including rovers, scientific instruments, resource utilization systems, and power networks.

As lunar operations become more complex and geographically distributed, reliable and scalable communication architectures will be essential. NASA's LunaNet concept and ESA's Moonlight initiative propose interoperable communication and navigation services in lunar orbit [24]. While these architectures primarily target high-data-rate links, there is an emerging need for low-power, low-data-rate communication networks to connect distributed sensors and infrastructure elements. This challenge aligns with the concept of the Internet of Things (IoT), where multiple autonomous devices exchange data efficiently over long distances with minimal power consumption.

LoRa technology, widely deployed on Earth through LoRaWAN networks, offers an attractive solution for lunar IoT applications. LoRa modulation enables long-range communication with very low power consumption, robust link margins, and simplified network topology. However, the lunar environment introduces unique challenges, including vacuum conditions, radiation exposure, large temperature variations, line-of-sight constraints, and the absence of terrestrial communication infrastructure. Adapting LoRa-based communication to the lunar domain, therefore, requires careful mission design and system analysis.

1.2 Scope and Objectives

This project evaluates the feasibility of a Lunar IoT Constellation using LoRa technology. The mission involves small satellites in Low Lunar Orbit serving as nodes between lunar surface assets and Earth.

The scope of the study includes:

- Definition of an orbital communication architecture enabling continuous surface coverage;
- Link budget evaluation for LoRa transmission under lunar constraints;

- Selection of antenna configuration and communication parameters;
- Spacecraft subsystem design with emphasis on propulsion, thermal, power and structure;
- Assessment of scalability toward future lunar infrastructure expansion.

The primary objective is to show that a LoRa-based system can deliver reliable, low-power lunar IoT connectivity and remain compatible with new lunar communication frameworks.

1.3 Previous Studies

Current lunar communication initiatives, such as NASA's LunaNet and ESA's Moonlight program, aim to establish standardized relay and navigation services in lunar orbit [12]. While these systems support high-bandwidth missions, they do not address the needs of low-power distributed IoT networks.

On Earth, LoRa networks provide robust long-range communication with minimal energy use, enabling large-scale sensor deployments. Recent research confirms that LoRa modulation is suitable for satellite-enabled IoT systems, especially for low-data-rate applications.

This mission design applies these concepts to the lunar environment by integrating LoRa-based communication with an orbital CubeSat relay architecture. Unlike terrestrial systems, the proposed approach must consider orbital dynamics, beta-angle-dependent illumination, Doppler shifts, and the lack of atmospheric propagation. This work bridges terrestrial IoT principles with lunar mission engineering.

2 Executive Summary - Author: Atharva Dhore

The LICOS is conceived to provide continuous, low-power communication coverage for distributed assets on the lunar surface. By leveraging LoRa technology, the system establishes a structured and energy-efficient communication layer that connects lunar surface devices to Earth via an orbital relay. The architecture is designed to support long-term lunar exploration and infrastructure development through reliable and scalable data exchange.

2.1 Requirements and Design Drivers

The system requirements are driven by the need for high global coverage, reliable link margins, and compliance with international frequency regulations. Key design drivers include maintaining stable frozen lunar orbits, ensuring communication continuity during eclipse phases ($T_{eclipse}$), managing limited Earth visibility, and satisfying power and thermal constraints over a five-year operational lifetime. Scalability and compatibility with future lunar missions are also fundamental considerations.

2.2 System Baseline Summary

The baseline architecture consists of three orbital planes with twelve satellites per plane at an altitude of approximately 500 km, supported by a dedicated relay satellite. Each spacecraft integrates LoRa-based S-band communication, an X-band Earth link, electric propulsion for station-keeping, deployable solar arrays, and battery storage sized for eclipse survival based on $E_{eclipse}$. The GS relies on deep-space X-band stations operating in a store-and-forward mode to accommodate non-continuous contact periods.

2.3 Technical Conclusions

The analysis demonstrates that the selected configuration can achieve full lunar surface coverage while maintaining acceptable power, thermal, and communication margins. The system satisfies operational requirements under nominal and worst-case conditions. Although limitations exist in terms of data

rate and Earth visibility constraints, the proposed architecture is technically feasible and provides a structured foundation for future expansion of lunar IoT services.

3 Mission Objectives and Deliverables

3.1 Mission Statement

As humanity prepares for sustained lunar presence, the need for interconnected surface elements becomes critical. The Internet of Things Constellation addresses this challenge by establishing a global lunar IoT network using LoRa technology, offering a simple, low power solution which is ideal for distributed, low data rate communication. A system of satellites ensures data transfer between Earth and LoRa enabled assets on the Moon and delivers a scalable communication layer that supports the development of future lunar infrastructure.

3.2 Mission Objectives

Primary Objectives:

- To provide and sustain IoT communication coverage across the lunar surface using LoRa technology.
- To establish a bidirectional data relay path between the Lunar IoT network and Earth ground stations.
- To establish comunication links for lunar assets supporting all mission data transfer requirements.

Secondary Objectives:

- To ensure compatibility between the LoRa network and all existing or planned LoRa integrated lunar mission assets.
- To ensure that the Lunar IoT network design supports future scalability of data throughput and user capacity.

3.2.1 Mission Success Criteria

Table 2: Mission Success Criteria

Criterion	Minimum Success	Medium Success	Full Success
Global Coverage & Reliability	80% lunar surface coverage with 90% link availability during visibility windows.	95% lunar surface coverage with 95% link availability during visibility windows.	99% lunar surface coverage with 99% link availability during visibility windows.
Earth Data Relay Path	Bidirectional relay demonstrated for 24 cumulative hours.	Bidirectional relay sustained for 7 consecutive days.	Bidirectional relay with 99% uptime over 30 days.
Network Throughput & Stability	200 users/satellite, 500 bps, 60 s latency, 2 h outage.	350 users/satellite, 500 bps, 30 s latency, 1 h outage.	450 users/satellite, 500 bps, 10 s latency, 10 min outage.
Lunar Interoperability	Link with 1 non-mission LoRa asset.	Links with 3 non-mission LoRa assets.	Links with all available LoRa assets in coverage.

Criterion	Minimum Success	Medium Success	Full Success
Design Scalability	50% user capacity increase via orbital plane additions.	100% user capacity increase via constellation expansion.	200% capacity and throughput increase via modular upgrades.

3.3 Mission Requirements and Design Drivers

The LICOS mission architecture is shaped by several fundamental design drivers that establish the technical approach and constrain subsystem design decisions:

- **Multi-Hop Relay Architecture**
  The four-segment communication pathway (Surface → Constellation → Relay → Earth) spans distances from 1,170 km to 391,000 km, requiring distinct frequency allocations, modulation schemes, and antenna configurations for each link.
- **LoRa Technology for Low-Power IoT Connectivity**
  LoRa enables low-power, long-range communication for distributed lunar IoT assets, driving S-Band frequency allocation (2025–2290 MHz), LR-FHSS modulation for high-density user access, and kilobit-per-second data rates.
- **Lunar Orbital Environment Constraints**
  The absence of lunar magnetic field and atmosphere eliminates magnetorquers and atmospheric drag, requiring reaction wheels with thruster desaturation, active station-keeping, radiation-tolerant components, and thermal/power systems capable of sustaining 70-minute eclipse periods.
- **High-Capacity User Support and Scalability**
  Supporting hundreds of concurrent users per satellite requires frequency division between orbital planes, multi-receiver relay architecture, and modular system design enabling capacity expansion through constellation augmentation.
- **Autonomous Operation and Fault Tolerance**
  Extended communication delays and infeasibility of on-orbit servicing necessitate autonomous fault detection, time-tagged command execution, and redundancy strategies (dual star trackers, pyramid reaction wheels, triple firmware storage) for 5-year mission continuity.

The mission requirements establish the baseline design constraints and performance targets that guide all subsystem designs. Requirements are categorized by prefix: MR (Mission/Functional), PR (Performance), ER (Environmental), and OR (Operational).

Table 3: Mission Requirements

ID	Requirement Statement
MR-001	The system shall provide LoRa-based communication coverage across at least 90% of the lunar surface to support distributed IoT assets.
MR-002	The system shall establish a bidirectional data relay path between lunar surface assets and Earth ground stations with a maximum latency of 1 minute when Earth is in visibility.
MR-003	The system shall support inter-satellite communication links to enable data routing within the constellation.
MR-004	The system shall implement communication protocols compatible with LoRa-enabled lunar assets and Earth ground networks.

ID	Requirement Statement
MR-005	The system shall be designed to support scalable expansion to at least 5000 user capacity and data throughput through constellation augmentation.
PR-001	The system shall support simultaneous communication sessions for at least 400 concurrent users per constellation satellite.
PR-002	The system shall achieve a minimum of 90% lunar surface coverage with at least 90% link availability during satellite visibility windows.
PR-003	The system shall provide a minimum guaranteed data rate of 400 bps for uplink transmissions from lunar surface assets.
PR-004	The system shall provide end-to-end data latency not exceeding 60 seconds under nominal relay visibility conditions.
PR-005	All communication links shall maintain a minimum link margin of 2 dB under worst-case geometric and operational conditions.
PR-006	The system shall allocate channel bandwidth at least four times wider than the maximum expected Doppler shift to ensure reliable packet reception.
PR-007	The system shall operate for a minimum mission lifetime of 5 years from initial orbital deployment.
PR-008	The constellation satellites shall comply with the mass and volume constraints of commercially available lunar-capable launch vehicles.
ER-002	All spacecraft components shall operate within the thermal range of -180°C to +120°C encountered in lunar orbit.
ER-003	The system shall maintain operational capability during eclipse periods of up to 70 minutes duration through onboard energy storage.
ER-004	All electronic components shall be selected or shielded to withstand the cumulative radiation dose of 2 krad expected in lunar orbit over the 5-year mission lifetime.
ER-005	The spacecraft structure shall withstand launch loads of 6g axial compression, 2g axial tension, and 2.5g lateral acceleration.
ER-006	The system shall implement frequency allocation and protocol strategies to mitigate interference between constellation satellites and external RF sources.
OR-001	The system shall be designed to enable safe decommissioning and disposal at end of mission life in compliance with space debris mitigation guidelines.
OR-002	Constellation satellites shall execute autonomous station-keeping maneuvers to maintain orbital parameters within defined tolerances.
OR-003	The system shall implement autonomous fault detection and recovery mechanisms to restore nominal operations without ground intervention.
OR-004	All spacecraft shall support remote firmware updates and configuration changes via ground commanding.

4 Mission Analysis - Author: Fiorenza Ferrante

The following analysis validates the utility of the proposed lunar network, confirming its ability to deliver continuous and reliable IoT connectivity across the Moon. Through literature studies, models and simulations, the architecture is verified to meet defined requirements and overcome environmental constraints.

4.1 Design Drivers

Design drivers for mission architecture are divided into two categories: Constellation and Relay.

Constellation:

- **Orbital Altitude Selection**
  The constellation altitude is constrained to an operational window between 300 km and 600 km. The lower bound (300 km) is established to mitigate orbital instability caused by lunar mascons, reducing station-keeping ΔV requirements. The upper bound (600 km) is driven by the link budget. Limiting altitude minimizes Free-Space Path Loss, ensuring communication links can be closed with low-complexity surface assets and satellite equipment. This altitude range balances orbital stability with communication performance and coverage, ensuring that the constellation can provides at least 90% of SLS coverage using relatively low-gain antennas and less satellites.

- **Global Coverage**
  The Constellation architecture has to be designed to achieve global coverage on most of the lunar surface, considering a k-fold redundancy of 2. This ensures that any point on the SLS has simultaneous visibility of at least two satellites, providing critical link redundancy and efficient data transfer for surface assets.

- **Constellation Efficiency & Cost Optimization**
  To minimize mission cost and operational complexity, the constellation architecture will to be optimized for the minimum viable number of satellites. This can be achieved by regulating key orbital parameters as altitude, footprint size, and orbital plane distribution, while balancing system redundancy. The final design will be selected to reduce launch mass and complexity of satellite and ground assets equipment, without compromising the required link availability or coverage performance.

- **Inter-Satellite Connectivity**
  The constellation architecture will be selected to support ISLs either inter and/or intra-planar. The selected architecture will ensure a continuous and effective communication network between satellites across the constellation.

- **Footprint Sizing**
  The satellite antenna footprint is the fundamental driver for both global coverage and redundancy. The variation of the footprint size requests the optimization of other parameters as orbital altitude, inclination and number of satellites. This iterative tuning ensures that the final configuration achieves at least 90% of continuous SLS coverage while maintaining the required overlap for redundancy.

- **Collision Avoidance**
  To mitigate the risk of inter-planar collisions, the constellation architecture, specifically the Phase Parameter, has to be optimized for passive orbital safety. The selected phasing needs to ensure

that satellites in intersecting planes maximize their minimum separation distance at crossing nodes (orbital intersections). The geometric configuration will guarantee that no two satellites occupy the same volume of space simultaneously during nominal operations, eliminating collision risk during nominal operations.

- **Orbital Stability & Station-Keeping**
  To minimize station-keeping ΔV requirements, the constellation will utilize LFOs. These orbital parameters are specifically selected to mitigate the dominant gravitational perturbations present in the operational altitude band. By minimizing the argument of periapsis (ω) and eccentricity (e) mean drifts, the design can achieve passive stability, significantly reducing propellant consumption and operational workload.

Relay:

- **Earth visibility**
  The relay orbit should be specifically dimensioned to maximize geometric visibility between the relay satellite and designated terrestrial ground stations. This will ensure bidirectional data transfer, for both the downlink of telemetry and payload data from the lunar constellation and surface assets and the uplink of commands and control signals from Earth. The orbit selection is driven by the requirement to minimize occultation periods where the Moon blocks the line-of-sight to Earth.

- **Orbital Stability & Station-Keeping Efficiency**
  The relay orbit will be selected to be as stable as possible. This design reduces the frequency of station-keeping maneuvers, preserving the satellite's propellant budget for the duration of the mission.

- **Link Closure**
  The relay orbit has to be designed to ensure reliable link closure, satisfying link budget requirements for communication with both Earth and the constellation around the Moon.

4.2 Requirements

Table 4: Constellation and Relay Requirements

ID	Requirement Statement
Constellation Requirements	
REQ-CONST-001	The constellation shall achieve coverage of at least 90% of the lunar surface area.
REQ-CONST-002	The constellation shall ensure that any point on the lunar surface has simultaneous visibility to at least 2 satellites for at least 90% of one orbital period.
REQ-CONST-003	The constellation satellites shall maintain a minimum separation distance of 30 km radius from any other constellation satellite at all times during nominal operations.

ID	Requirement Statement
REQ-CONST-004	The constellation shall operate at orbital altitudes between 300 km and 600 km above the lunar surface.
REQ-CONST-005	Each satellite's altitude shall provide a minimum footprint radius of 900 km at the lunar surface.
REQ-CONST-006	The constellation geometry shall support at least one ISL path between any adjacent satellite during nominal operations.
REQ-CONST-007	The constellation orbital configuration shall maintain relative satellite phasing within ±50 km of nominal positions throughout the mission lifetime.
REQ-CONST-008	The total station-keeping ΔV for each constellation satellite shall not exceed 150 m/s over 1 year.
REQ-CONST-009	The constellation geometry shall maintain link closure with with a minimum margin of 2 dB for all designated worse case geometry proximity links during nominal operations.
Relay Requirements	
REQ-RELAY-001	The relay satellite shall maintain line of sight visibility to at least one Earth ground station for at least 90% of each orbital period.
REQ-RELAY-002	The relay satellite shall maintain line of sight visibility to at least one constellation satellite for at least 90% of each orbital period.
REQ-RELAY-003	The relay satellite station-keeping ΔV shall not exceed 150 m/s over 1 year.
REQ-RELAY-004	All relay communication links shall close with a minimum link margin of 2 dB under worst case geometry during nominal operations.

Verification is done via Analysis and Inspection for Phase A and B. Status ✓indicates that the requirement has been successfully verified.

Table 5: Constellation & Relay Requirements Traceability and Verification Matrix

Req. ID	Req. Description	Objective/Driver	Method	Status
Constellation				
REQ-CONST-001	90% Lunar Surface Coverage	**Obj:** Primary 1 (IoT Coverage) **Driver:** Global Coverage	A	✓
REQ-CONST-002	Simultaneous 2 Sat Visibility	**Obj:** Primary 1 (IoT Coverage) **Driver:** Global Coverage	A / I	✓
REQ-CONST-003	30 km Min. Separation	**Driver:** Collision Avoidance	A	✓
REQ-CONST-004	Altitude 300–600 km	**Driver:** Orbital Altitude Selection **Driver:** Stability	A	✓

Req. ID	Req. Description	Objective/Driver	Method	Status
REQ-CONST-005	900 km Footprint Radius	**Driver:** Footprint Sizing **Obj:** Primary 1 (IoT Coverage)	A	✓
REQ-CONST-006	Support 1 ISL Path	**Driver:** Inter-Satellite Connectivity **Obj:** Primary 3 (Comm. Links)	A / I	✓
REQ-CONST-007	Phasing ±50 km	**Driver:** Collision Avoidance **Driver:** Efficiency	A	✓
REQ-CONST-008	$\Delta V \leq 150$ m/s	**Driver:** Stability & Station-Keeping	A	✓
REQ-CONST-009	Link Margin ≥ 2 dB	**Obj:** Primary 3 (Comm. Links) **Driver:** Link Closure	A	✓
Relay				
REQ-RELAY-001	Earth Visibility (90%)	**Obj:** Primary 2 (Relay Path) **Driver:** Earth Visibility	A / I	✓
REQ-RELAY-002	Constellation Visibility (90%)	**Obj:** Primary 2 (Relay Path) **Driver:** Link Closure	A / I	✓
REQ-RELAY-003	Relay $\Delta V \leq 150$ m/s	**Driver:** Orbital Stability (Relay)	A	✓
REQ-RELAY-004	Link Margin ≥ 2 dB	**Obj:** Primary 3 (Comm. Links) **Driver:** Link Closure	A	✓

4.3 Assumptions and trade-off

Assumptions:

- The Moon is considered to be a perfect sphere.
- Station-keeping maneuvers computed in propulsion section regarding the constellation are assumed to be performed correctly and thoroughly.
- For MATLAB simulations, lunar mascons and other perturbing forces (e.g. Earth's influence) are not taken into account.
- For GMAT simulations, degree and order for the lunar potential expansion considered was 25, for an orbital altitude of $\simeq 540$ km [35].

Constellation Trade-offs:

- **Orbital Stability vs. Link Budget**
  The constellation altitude selection was constrained to an operational window between 300 km and 600 km. The lower bound of 300 km is established to mitigate the destabilizing effects of lunar mascons. While the fundamental gravitational acceleration scales with the inverse square of the

altitude, as described by Newton's Law of Universal Gravitation in Equation 1, the perturbative forces arising from the Moon's heterogeneous mass distribution are significantly more pronounced at lower altitudes.

Below 300 km, these perturbations dominate the orbital evolution, requiring frequent station-keeping maneuvers to maintain the constellation geometry. Uncorrected deviations from a LFO at low altitudes lead to rapid orbital decay, with estimated impact times at approximately 4 weeks from 30 km and 4 months from 100 km [14]. By setting the floor at 300 km, the system minimizes the ΔV required to counteract these perturbations while maintaining a stable LFO configuration.

The upper limit of 600 km is driven by the link budget constraints of the surface assets and satellites payload. As altitude increases, FSPL increases, degrading the received signal strength. The 600 km threshold ensures that the link can be closed using low-power, low-complexity IoT equipment (specifically LoRa technology) without requiring high-gain directional antennas on the surface or on board of the satellites.

This final selected altitude of ~ 540 km (slightly different for every plane) represents the optimal compromise, balancing the stability of the lunar gravitational environment with the communication limits of the payload.

$$g(h) = \frac{G \cdot M_M}{(R_M + h)^2} \tag{1}$$

- **Number of Satellites and Planes vs. Cost and Coverage**
  The constellation architecture was optimized to minimize total system cost while satisfying the critical performance requirements: a minimum of 90% coverage of the SLS and a k-fold redundancy of $k = 2$ (dual-satellite visibility).

  Numerical simulations performed in MATLAB were used to iterate the constellation parameters. By coupling the payload selection with the chosen final orbital altitude, an effective footprint radius of $R_{fp} \approx 1000$ km was established, considering an elevation margin of 7°. Initial optimization runs identified a minimum of 35 satellites distributed across 5 orbital planes (35/5) or 7 planes (35/7) to meet the coverage mandate. However, the final design trade-off favored a configuration of 36 satellites distributed across 3 planes (36/3). Although this architecture increases the space segment mass by one satellite, the reduction of two orbital planes significantly decreases the launch and the station-keeping complexity, required to maintain the constellation geometry.

  Furthermore, the selection of the architecture 36/3 still includes an inclination span over a range of $78° \leq i \leq 90°$ as shown in Figure 1 (analyzed with a 2° step resolution). This operational envelope is crucial, as it permits the selection of a specific 'frozen' inclination, required to counteract the perturbing effects of the lunar mascons and maintain a stable LFO without compromising the constellation's geometry. The final inclination was chosen to be 84° for all three planes [35], according with the analysis found in literature for the selected Walker Delta 36/3 configuration.

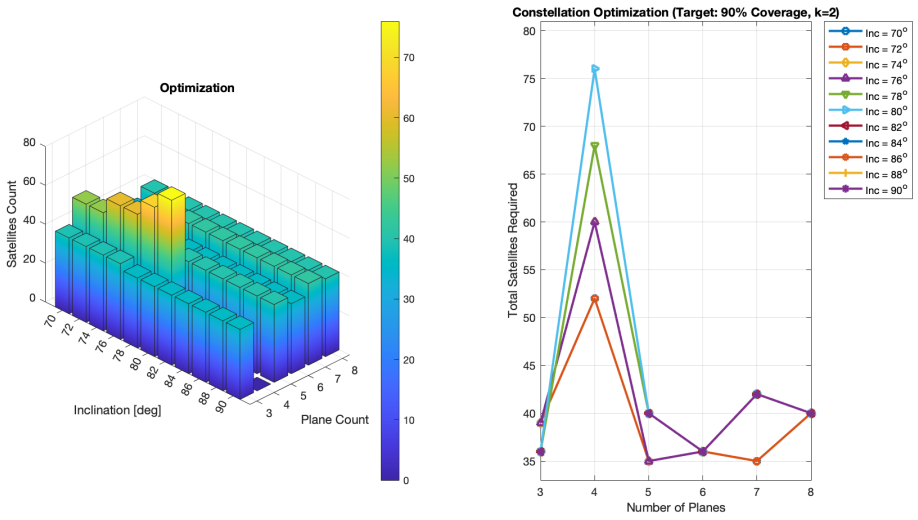

Figure 1: Constellation Optimization via MATLAB Simulation.

- **Inter vs. Intra-planar Communication (Walker Star vs. Delta)**
  A critical trade-off was performed to select the constellation's geometry based on ISL connectivity requirements. The choice laid between Walker Star and Walker Delta configurations.

  A Walker Star architecture typically facilitates continuous inter-planar communication links because satellites in adjacent planes maintain stable relative positions and low Doppler shifts, except near the polar crossing. On the other hand, a Walker Delta configuration distributes orbital planes evenly over 360° of RAAN. This geometry results in satellites in adjacent planes having high relative velocities and complex pointing requirements for inter-planar links, particularly at lower latitudes.

  However, since the OBDH subsystem and communication payload were designed to prioritize robust intra-planar links to minimize pointing complexity, a Walker Delta configuration was selected. This architecture supports stable intra-planar link chains while permitting inter-planar links at the lunar poles, where orbital planes converge and relative range minimizes.

Relay Trade-offs:

- **Earth Visibility vs. Orbit Stability and Link Budget**
  A critical parameter in defining the relay orbit is the Earth visibility (Line of Sight).

  Initially, a Halo orbit around the Earth-Moon L1 Lagrange point was considered. While this configuration offers 100% Earth visibility, the orbit is dynamically unstable, requiring significant station-keeping ΔV to prevent departure from the selected trajectory [10, 38].

  Subsequently, a Southern L2 NRHO was evaluated [11]. While the NRHO provides superior stability and continuous Earth visibility, the high apolune altitude (up to 75,000 km) introduces excessive FSPL. Closing the link budget from such distances would necessitate impressively high gain antennas, driving up size, weight, power, cost and complexity of the relay satellite.

  Consequently, the final selection was a Circular Polar Lunar Orbit. Although this orbit introduces periodic Earth occultations, it drastically reduces the communication range, allowing for reliable link closure with less complex payloads [26]. Literature confirms that communication blackouts are restricted to a maximum duration of approximately 69 minutes twice a year [26]. These eclipse times are mitigated via store and forward, where data is accumulated onboard the relay and downlinked once Earth Line of Sight is reestablished.

4.4 Baseline Design

Constellation:

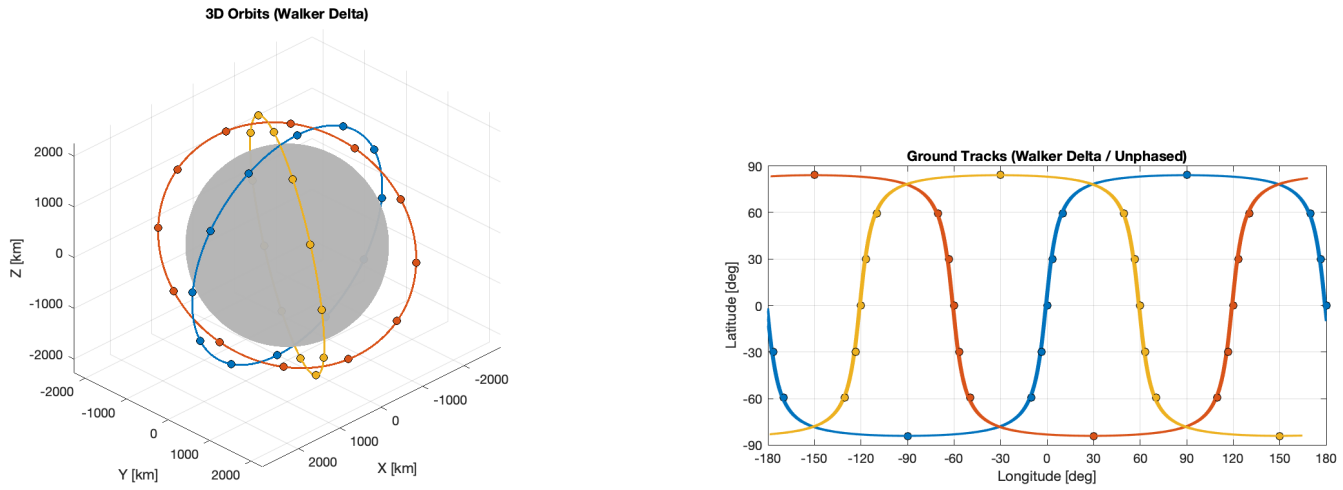

(a) 3D MATLAB Plot of Walker Delta 36/3/0.

(b) 2D MATLAB Plot of Walker Delta 36/3/0.

Figure 2

Table 6: Orbital Elements: Constellation Configuration (Walker Delta 36/3/0)

Orbital Element	**Plane 1**	**Plane 2**	**Plane 3**
a	2250 km	2286 km	2277 km
e	$4.350 \cdot 10^{-3}$	$5.285 \cdot 10^{-3}$	$5.251 \cdot 10^{-3}$
i	84°	84°	84°
Ω	0°	120°	240°
ω	90°	97°	99°
ν	12 Satellites per plane, separated by 30°		

The finalized lunar constellation architecture employs a Walker Delta 36/3/0 configuration, Figure 2. The detailed orbital elements for each plane are listed in Table 6 [35]. This architecture follows Design Drivers and satisfies Requirements by validating the following system performance metrics:

- **Global Coverage:** Achieves a minimum coverage of the SLS of 99.94% every orbital period, assuming a satellite footprint radius of 1000 km corresponding to a 7° elevation mask (Figure 3) and a sample every $\simeq$1.6 min (100 samples per orbit).

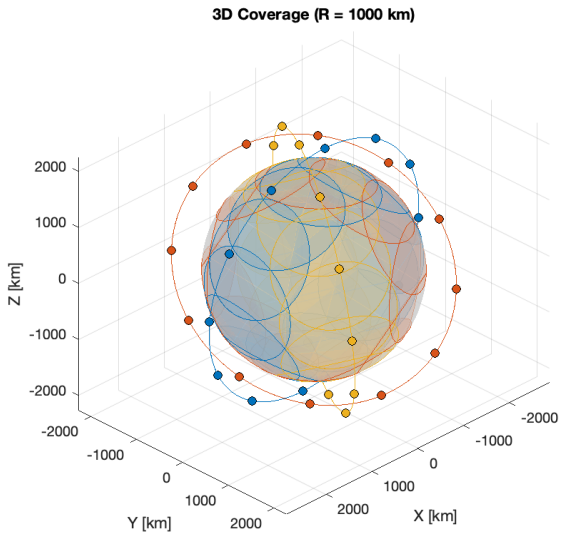

(a) 3D MATLAB Plot of Satellites' Footprints.

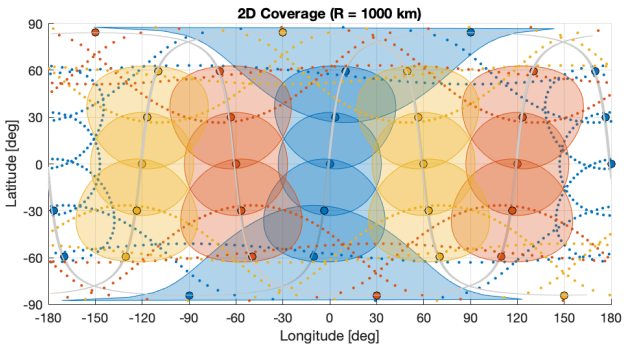

(b) 2D MATLAB Plot of Satellites' Footprints.

Figure 3

- **Redundancy:** Guarantees a minimum k-fold redundancy of 2, ensuring dual satellite visibility for robust service availability.
- **Optimization:** Balances the number of satellites and orbital planes to minimize costs and station-keeping complexity, Figure 1.
- **Connectivity:** Supports continuous intra-planar ISL and inter-planar connectivity at the lunar poles.
- **Safety:** Ensures passive orbital safety with no collision risks detected during nominal operations phase.

  Figure 4 illustrates the baseline collision avoidance analysis performed in MATLAB under idealized Keplerian conditions (two-body dynamics). This model is validated against the high fidelity GMAT simulation presented in Figure 5, which incorporates full lunar environmental perturbations, including non-spherical gravity terms and third-body effects.

  Despite the orbital element drift induced by these perturbations, the collision-free result from the MATLAB analysis remains valid. As demonstrated in the GMAT data, the uncorrected variation of the semi-major axis (a) remains below 2 km over the simulation period of 1 year. Given that this natural drift is significantly smaller than the minimum separation distance, and that monthly station-keeping maneuvers will actively correct these deviations, the constellation's passive safety is confirmed.

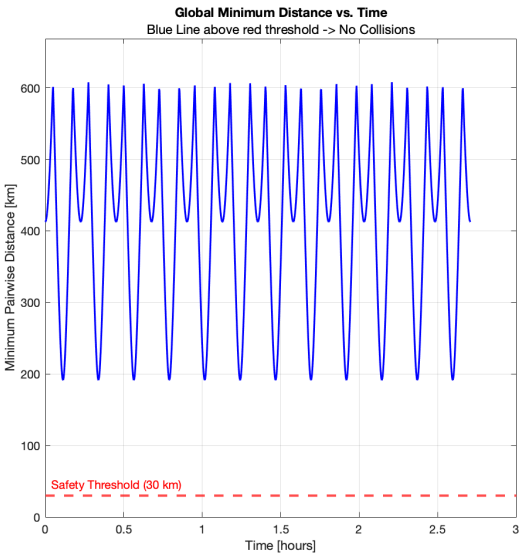

(a) MATLAB Plot of Global Minimum Distance between Satellites of the constellation over one Orbital Period.

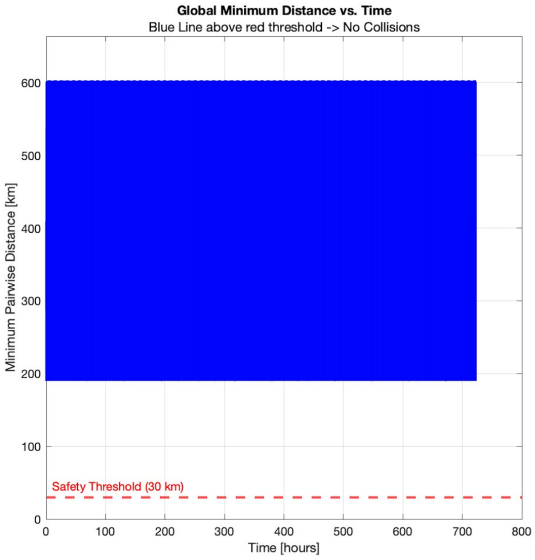

(b) MATLAB Plot of Global Minimum Distance between Satellites of the constellation over one year.

Figure 4

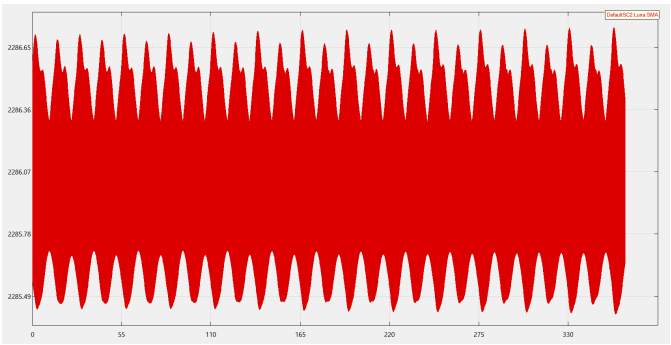

Figure 5: GMAT Simulation: Yearly Drift of Semimajor Axis of Plane 2 in km (y-axis) vs. days (x-axis). Similar result for the other two planes.

- **Stability:** Leverages LFO parameters to minimize the station-keeping ΔV required to counteract lunar gravitational perturbations.

  High-fidelity simulations conducted in GMAT confirm that periodic station-keeping maneuvers are required monthly to counteract lunar gravitational perturbations [35].

  Figure 6 presents the orbital evolution of Plane 2, which serves as a representative result since similar drifts were obtained for the other two planes. The analysis focuses on two critical stability metrics:

  – The Eccentricity-Argument of Perigee drift (e vs. ω), which monitors the stability of the frozen orbit condition.

  – The Inclination variation (i), which is one of the primary drivers for maintaining consistent surface coverage patterns over the mission lifetime.

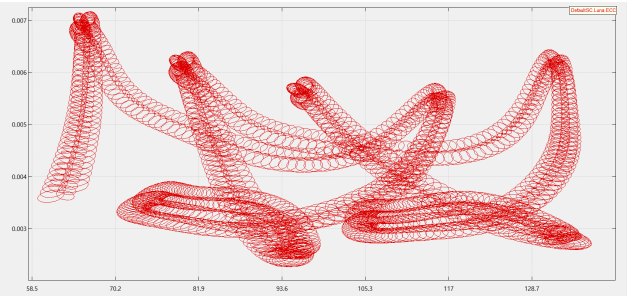

(a) GMAT Simulation of e vs. ω drift over 2 months (e on y-axis and ω on x-axis in degrees).

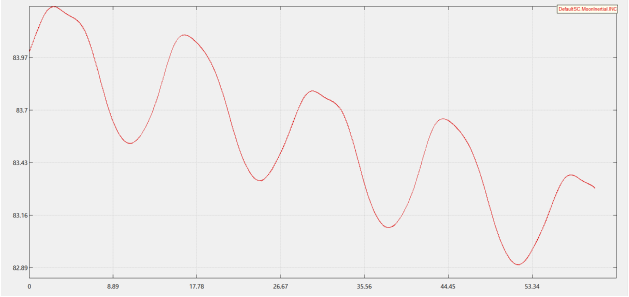

(b) GMAT Simulation of i drift over 2 months (i on y-axis in degrees and time on x-axis in days).

Figure 6

Relay:

The final Design of the relay architecture consists of a Lunar Circular Polar Orbit with one relay satellite. Orbital plane parameters are listed in Table 7 [26].

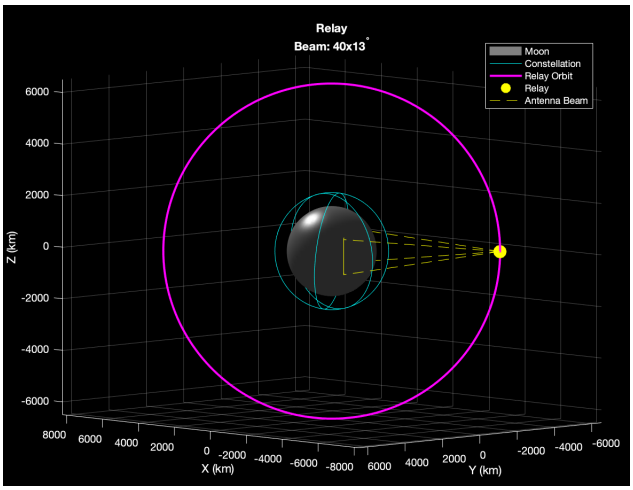

Figure 7: Representative image of the Relay Orbit, obtained via MATLAB code.

a	6500 km
e	0
i	90°
Ω	45°
ω	0°
ν	145°

Table 7: Orbital Elements Relay Plane.

The selected orbital configuration ensures robust link closure with positive margins, even at the antenna's Edge of Coverage defined by the HPBW.

Furthermore, the high stability of this plane significantly reduces propellant consumption, requiring a station-keeping budget of only $\Delta V \approx 4$ m/s per year to counteract perturbations [26].

Regarding Earth visibility, the relay maintains continuous Line-of-Sight for the majority of the mission. Communication outages are confined to two distinct occultation periods per year, each lasting approximately one month. During these intervals, the Earth occultation duration per orbit initiates at ∼20 minutes, peakes at a maximum of 69 minutes, and recedes to 20 minutes [26]. Even at it's maximum, the eclipse time doesn't exceed 10% of the orbital period of 13.1 hours [26].

5 System Design

5.1 General Design - Authors: Jakub Czerniej

5.1.1 General Configuration

The proposed spacecraft is a microsatellite platform designed for a lunar constellation to provide high-speed internet connectivity.

The configuration consists of a central cuboid bus housing the payload and avionics, with deployable solar arrays and antennas. The physical architecture is designed to transition from a compact "Stowed" state during launch to a fully "Deployed" operational state in the lunar orbit environment.

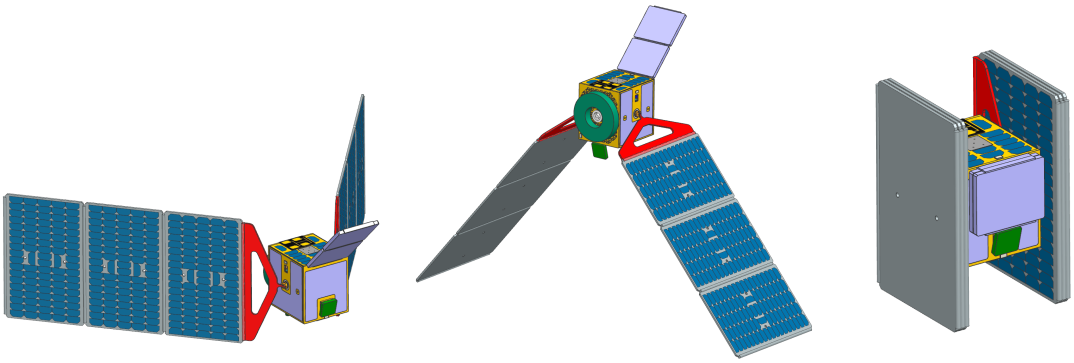

Figure 8: Spacecraft Configuration. Left: Deployed (default) Configuration. Center: Deployed (Adjusting Solar Arrays to the Sun) Configuration. Right: Stowed (Launch) Configuration.

5.1.2 Physical Characteristics

The physical envelope and mass budget of the satellite are summarized below. These dimensions are driven by the dynamic constraints of the surface area required for power generation.

Table 8: Spacecraft Physical Characteristics

Parameter	**Stowed (Launch)**	**Deployed (Orbit)**
Length (X)	446 mm	2410 mm
Width (Y)	460 mm	1750 mm
Height (Z)	750 mm	880 mm
Wet Mass	$\approx 55,6$ kg	
Dry Mass	$\approx 52,1$ kg	

5.1.3 Subsystems Organization

The satellite integrates all critical subsystems required for the mission, including the Structure, Electrical Power System (EPS), Propulsion, Attitude Determination and Control (ADCS), TELECOM, Onboard Data Handling (ODH), Thermal System and Telecommunications Payload.

A detailed technical description of these subsystems, including their design requirements, trade-offs, and performance specifications, is provided in the subsequent chapters of this report.

5.2 Payload - Authors: Fiorenza Ferrante & Simone Borzaga

The Payload subsystem is the core functional element of the LICOS constellation, responsible for establishing and maintaining all links between lunar surface IoT assets, constellation satellites and the relay satellite. Built around commercial LoRa technology adapted for the lunar S-Band frequency allocation, the payload architecture must simultaneously satisfy stringent link budget requirements, support high user capacity and survive the harsh radiation environment of lunar orbit over a 5-year mission lifetime.

5.2.1 Design Drivers

Following are the Design Drivers for the Payload Subsystem:

- **LoRa Technology Adoption & Frequency Constraints**
  The primary payload driver is to validate the feasibility of a space-based IoT network around the Moon, utilizing LoRa technology. Consequently, the core payload subsystem must be built around the selection of LoRa hardware. The chip choice is constrained by the specific lunar frequency allocation, set by recommendation restrictions [5][19].
- **Link Budget Closure**
  The selection of the LoRa transceiver specifications is primarily driven by the necessity to close all communication links with a safety margin. Since standard LoRa hardware is optimized for terrestrial low-power networks, the payload architecture can integrate components, including Low-Noise Amplifiers (LNA) and Power Amplifiers (PA), compensating for the significant FSPL of the lunar environment.
- **Data Flow**
  Hardware configuration must support sufficient data throughput to prevent network saturation, ensuring that latencies remain within defined operational limits.
- **Components Selection**
  To ensure the operational feasibility of the payload analysis, the design is driven by the selection of commercial off the shelf components. Reference to existing market hardware is required to estimate and validate system performance against realistic benchmarks.
- **Radiation Hardening**
  Due to the intense radiation levels in lunar orbit, ensuring hardware survival is a critical design driver. For components not radiation hardened already, the design must incorporate a protective structural shield to reduce radiation exposure to safe levels and prevent short circuits, ensuring the payload remains operational throughout the mission duration.

5.2.2 Payload Requirements

Table 9: Payload Subsystem Requirements

ID	Requirement Statement
REQ-PAY-001	The payload shall transmit and receive signals with LoRa chips within the allocated SFCG and ITU S-Band frequency recommendations for the lunar region (2025-2110 MHz / 2200-2290 MHz).
REQ-PAY-002	The payload shall close all communication links with a minimum link margin of 2 dB at HPBW edge.

ID	Requirement Statement
REQ-PAY-003	The payload shall operate with a channel bandwidth at least 4 times larger than the maximum expected Doppler shift.
REQ-PAY-004	The payload shall support a minimum data rate of 500 bps on the ground uplink to prevent network saturation under nominal user load.
REQ-PAY-005	The payload shall provide Earth-to-Moon coverage within a minimum footprint radius of at least 900 km at the baseline altitude.
REQ-PAY-006	The payload shall switch between Receiving (Rx) and Transmitting (Tx) modes within 200 microseconds.
REQ-PAY-007	The payload electronics shall be shielded to withstand a Total Ionizing Dose (TID) of at least 2 krad over the mission lifetime.
REQ-PAY-008	The payload shall implement Single Event protection capable of cutting power to the affected rail within 100 microseconds of over-current detection.
REQ-PAY-009	The payload shall meet all performance specifications within an operating temperature range of -40°C to +85°C.
REQ-PAY-010	The payload shall survive without permanent degradation within a non-operating temperature range of -55°C to +95°C.
REQ-PAY-011	The payload shall consume a maximum of 50 Watts during peak transmission mode.
REQ-PAY-012	The total mass of the payload shall not exceed 3 kg.

5.2.3 Assumptions and trade-off

Assumptions

- **Compatibility of Components**
  It is assumed that the chosen components are fully compatible and will integrate seamlessly, functioning together without causing electrical, software or RF interference.
- **Exclusion of Secondary Components**
  The payload design is restricted to primary functional units critical to meeting the performance requirements. Secondary components, including but not limited to connectors, cabling, mountings and thermal materials are excluded in this analysis. Consequently, their delays are not considered to affect chip synchronization.
- **Nominal Component Performance**
  Performance analysis relies on nominal datasheet specifications. Factors for worst-case thermal extremes, radiation induced degradation, or End-of-Life aging are not applied at this preliminary design stage.
- **Operating Ranges** The Payload receives stable regulated voltage from the power subsystem and operates within temperature ranges throughout all mission phases.

Trade-offs

- **LoRa Chip Selection:**
  Compliance with ITU and SFCG recommendations strictly limits the operational frequency to the S-band, specifically within the bands of 2025–2110 MHz and 2200–2290 MHz [5, 19]. While the lunar

environment supports higher frequency bands, current commercial LoRa technology is not capable of communicating with frequencies higher than 2.4 GHz bands. Consequently, the hardware selection was restricted to the Semtech LR1121 transceiver, which is uniquely capable of supporting these specific S-band frequencies [46].
A critical design trade-off arises from the transceiver's inherent half-duplex capabilities. Two options were taken into account:

1. **Single-Transceiver Architecture:** Utilizing a single chip with Time Allocation, which minimizes power but requires sequential link handling, increasing latency.
2. **Multi-Transceiver Architecture:** Integrating multiple chips to enable parallel processing of multiple communication streams, thereby reducing latency and maximizing network throughput at the cost of increased power load.

Since LoRa data rate is naturally very low, the second option was chosen for the final design, with 3 chips handling three different tasks: satellite-ground, ISL and satellite-relay communications.

- **Antenna Selection & Gain Optimization:**
  As preliminary design, it was evaluated the feasibility of utilizing low-gain omnidirectional antennas to minimize ADCS pointing requirements, handle multiple communication links with one antenna and maximize the instantaneous surface footprint.
  However, a shift to multiple directional antennas architecture was preferred because it satisfies the required link closure. Indeed, omnidirectional gain levels were insufficient to close the link over the network distances with the limited transmit power of the payload, while directional antennas also help mitigate signal interference, which is critical for maintaining communication integrity in the lunar environment.
  The final configuration employs:
  – **Medium-Gain Antennas (7.5 dBi):** Selected for the Space-Ground and ISL communication.
  – **High-Gain Antenna (13 dBi):** Design choice for the Constellation-to-Relay link.
- **Transmit Power vs. User Constraints:**
  A critical trade-off evaluated the optimal distribution of link margin resources between the space segment and the ground user segment. The architectural decision lay between:

  1. **Low-Power Satellite Architecture:** Relying solely on the native LoRa transceiver output (13 dBm) coupled with a LNA and BPF. This minimizes satellite Size, Weight, and Power but necessitates high-gain, high-power user terminals on the lunar surface to close the link.
  2. **High-Power Satellite Architecture:** Integrating a dedicated PA into the satellite payload. This increases the satellite's power budget and thermal load but significantly relaxes the user constraints, enabling smaller, lower-power surface devices.

  The final design favors the second option, High-Power Architecture. By shifting the complexity to the constellation, the system minimizes the burden on the user segment, ensuring that small, resource-constrained surface assets can reliably access the network without requiring large, high power consuming antennas.
- **Clock Selection**
  High-precision timing is critical for the LoRa chips synchronization. Initially, a dedicated Temperature Compensated Crystal Oscillator was chosen to guarantee frequency stability of ± 0.5 ppm [45] independent from the other satellite components.
  The dedicated TCXO was discarded in favor of utilizing the master clock signal provided by the OBC. This architecture reduces the payload's component count by handling OBDH, ADCS and clock tasks all together, it reduces power consumption and eliminates the need for a separate clock, simplifying the payload design. While this removes hardware complexity, it shifts the burden to software and

protocol design. The payload must now implement a rigorous Time Synchronization Protocol to compensate for the OBC clock's potential jitter or drift due to its lower frequency stability wrt TCXO.

5.2.4 Baseline Design

The satellite payload consists of three independent RF chains, each dedicated to one communication interface: the lunar ground link, the ISL, and the relay link. Each chain is built around the same core hardware but configured for its specific link requirements. The common components of each chain are:

- **Semtech LR1121 Transceiver [46]:** Figure 9 shows the selected chip, the core processing unit of each RF chain, selected for its native S-Band capability and dual-mode LoRa/LR-FHSS modulation support. The ground link chain operates with SF12, BW = 250 kHz and CR = 4/5, providing a receiver sensitivity of −130 dBm and a data rate of 586 bps, optimized for closing the link with low-power surface assets. The ISL and relay chains operate at SF7, BW = 125 kHz and CR = 4/5, providing 5.5 kbps throughput to optimize data flow.

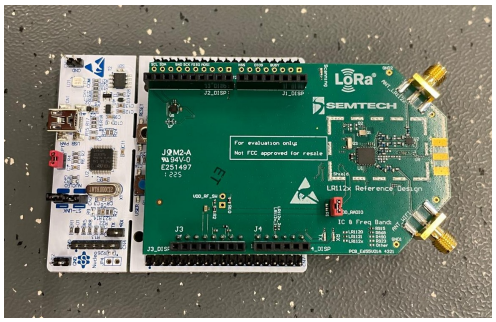

Figure 9: Semtech LR1121 transceiver with NUCLEO microprocessor board. Additionally, an antenna operating at S-Band frequency was connected to the LoRa chip, this configuration was used during laboratory tests, confirming non-degrading performance of the signal when the theoretical datasheet limit of 2.2 GHz is surpassed [46], up to 2.2005 GHz, maximum frequency selected for the mission.

- **Skyworks SKY67151 Low Noise Amplifier [48]:** Placed on the receive paths, with a noise figure of approximately 0.25 dB, it amplifies the incoming signal before it reaches the transceiver, maximizing the effective receiver sensitivity of the system.
- **Triad RF TA1295 Power Amplifier [53]:** Placed on the transmit paths, it boosts the chip +13 dBm max output (that can be lowered to +1 dBm to make the PA work) to +34 dBm, providing the additional gain required to close the lunar communication links against the significant FSPL of the lunar environment.
- **Qorvo QPC1022 RF Switch [44]:** For each chain swaps between the LNA receive path and the PA transmit path in accordance with the chip half-duplex operation. The switching time is 1500 ns, well below the 200 μs requirement.
- **Mini-Circuits CBP-2150AN+ Bandpass Filter [36]:** Placed at the antenna ports, it suppresses out-of-band signal interference across the 2000–2300 MHz frequencies, protecting the LNA from saturation and ensuring compliance with the allocated S-Band frequency ranges.
- **TI TPS25982 Current-Limiting Power Switch [52]:** Six units are distributed across the payload between the battery and the following active components: one per LR1121 chip on the low-power line and one per PA on the high-power line. Each switch provides an adjustable over-current trip point with microsecond-level response time and event reporting to the OBC, implementing Single Event protection by preventing short circuits.

The following component has been selected for only the Ground and ISL chains:

- **S-Band Patch Antenna, 7.5 dBi [57]:** It provides sufficient gain to maintain link closure across the footprint and beamwidth to achieve global coverage from the baseline orbital altitude.

The following component has been selected for only the Relay chain:

- **Space Inventor S-Band 2×2 Array Antenna, 13 dBi [50]:** It provides the additional gain required to close the more demanding constellation-to-relay link. It also guarantees a beamwidth large enough have the relay in visibility for enough time.

All three RF chains interface directly with the On-Board Computer [49], which handles data routing, protocol encapsulation, timing coordination and radiation fault recovery for the payload. Additionally, all non radiation hardened components are encapsulated in an aluminum plate with a thickness of 7 mm [43], considering a TID of 2 krad during the mission lifetime of 5 years (0.3 rad per day) [20].

5.3 Power - Author: Atharva Dhore

5.3.1 Power Requirements and Design Drivers

Power Subsystem Requirements

Table 10: Power Subsystem Requirements

Req. ID	Requirement Statement
REQ-PWR-001	The Electrical Power Subsystem (EPS) shall generate electrical power using deployable solar arrays during sunlight periods.
REQ-PWR-002	The solar array shall provide sufficient End-of-Life (EOL) power to sustain the average spacecraft load of 155 W.
REQ-PWR-003	The solar array shall provide a minimum effective area of 1.56 m^2 to satisfy EOL power requirements.
REQ-PWR-004	The EPS shall ensure positive power balance during sunlight, accounting for power path efficiencies and battery charging.
REQ-PWR-005	The EPS shall store sufficient energy to supply all spacecraft loads during the maximum eclipse duration.
REQ-PWR-006	The battery shall provide a minimum usable energy capacity of 484.35 Wh.
REQ-PWR-007	The battery Depth of Discharge (DoD) shall not exceed 30% under nominal operations to ensure compliance with a 5-year mission lifetime.
REQ-PWR-008	The EPS shall regulate and distribute power to all spacecraft subsystems within allowable bus voltage limits.
REQ-PWR-009	The EPS shall recharge the battery during sunlight while simultaneously supplying spacecraft loads.
REQ-PWR-010	The EPS shall maintain bus voltage stability during peak load events, including high-rate transmission and propulsion modes.
REQ-PWR-011	The EPS shall prevent simultaneous high-power operations that could result in bus collapse or battery overstress.

Req. ID	Requirement Statement
REQ-PWR-012	The EPS shall support autonomous load shedding in Safe Mode to preserve critical spacecraft functions.
REQ-PWR-013	The EPS components shall operate within defined thermal limits for the lunar orbital environment.
REQ-PWR-014	The EPS shall tolerate radiation exposure consistent with a 5-year lunar mission lifetime.
REQ-PWR-015	The Solar Array Drive Assembly (SADA) shall orient the solar panels to minimize solar incidence angle during sunlight periods.

Power Subsystem Design Drivers

The design of the Electrical Power Subsystem (EPS) is governed by the mission architecture, lunar orbital environment, operational concept, and lifetime objectives of the LICOS lunar IoT constellation. The EPS must ensure uninterrupted, regulated, and fault-tolerant power delivery across all mission phases while maintaining adequate design margins at End-of-Life (EOL).

Average Power Demand

The spacecraft average power demand of approximately 155 W represents the primary sizing driver for both the solar array and battery system. The EPS must sustain this load at End-of-Life (EOL), accounting for degradation effects and power path inefficiencies [55].

Eclipse Duration

The selected Circular Polar Lunar Orbit introduces periodic eclipse intervals. The EPS must supply uninterrupted power during the maximum eclipse duration, directly driving battery capacity sizing and Depth of Discharge (DoD) limits [26].

Lifetime and Degradation Effects

The five-year mission lifetime introduces progressive degradation mechanisms that directly affect EPS performance. Solar cells experience radiation-induced efficiency loss, while battery systems undergo capacity fade and increased internal resistance due to charge–discharge cycling.

To ensure long-term reliability, the solar array is sized based on EOL performance rather than Beginning-of-Life (BOL) output. Battery sizing includes margins for capacity degradation and respects conservative Depth of Discharge (DoD) limits to extend cycle life. These lifetime considerations are critical to maintaining uninterrupted power availability throughout the operational phase of the LICOS constellation.

Lunar Environmental Conditions

The lunar orbital environment presents:

- High solar flux (≈ 1361 W/m^2) [55],
- Absence of atmospheric attenuation,
- Extreme thermal cycling [20],
- Radiation exposure over a 5-year lifetime.

These conditions drive solar cell selection (triple-junction), degradation margins, and battery chemistry constraints.

Solar Incidence and Pointing Strategy

Power generation is strongly dependent on solar incidence angle. Since the spacecraft maintains a nadir-pointing attitude for communication requirements, solar tracking must be achieved via a Solar

Array Drive Assembly (SADA) [9]. This drives the need for:

- Single-axis solar tracking capability,
- Sun sensor integration,
- Closed-loop motor control,
- Mechanical rotation limits.

Power Budget Overview and Load Breakdown Structure

Table 11: Electrical Power Budget and Load Breakdown for Lunar IoT Constellation Spacecraft

Item No.	Subsystem / Equipment	Qty	Operational Mode	Electrical Operating Point	Nominal Power per Unit [W]	Peak Power per Unit [W]	Config ID / Mode ID	Duty Cycle [-]	Mode Avg Power per Unit [W]	Config Averaged Power [W]
1	Semtech LR1121 chip	3	RX (LoRa SF7, S-Band 125 kHz)	6.7 mA × 3.3 V	0.0221	0.20295	2	0.5	0.01105	0.1228
							3	0.5	0.01105	
			RX (LoRa SF12, S-Band 250 kHz)	7.41 mA x 3.3 V	0.0244		1	0.8	0.01952	
			TX (S-Band +1 dBm)	20.5 mA x 3.3V	0.06765		1	0.2	0.01353	
							2	0.5	0.033825	
							3	0.5	0.033825	
2	Power Amplifier (34 dB)	3	TX (PA ON)	7 V × 2.3 A	16.1	48.3	1	0.2	3.22	19.446
							2	0.5	8.05	
							3	0.5	8.05	
			Disabled / OFF (quiescent disabled)	7 V × 0.010 A	0.07		1	0.8	0.056	
							2	0.5	0.035	
							3	0.5	0.035	
3	Low Noise Amplifier around 0.5 dB NF	3	RX (LNA ON, IDQ typ)	5 V × 70 mA	0.35	1.05	1	0.8	0.28	0.81
							2	0.5	0.175	
							3	0.5	0.175	
			RX (LNA ON, IDQ min)	5 V × 30 mA	0.15		1	0.2	0.03	
							2	0.5	0.075	
							3	0.5	0.075	
4	RF Switch to change between PA and LNA in transmit and receive mode	3	Active (EN=High, switching TX/RX path)	5.0 V × 52 µA	0.00026	0.00078	1,2,3	1	0.00026	0.00026
6	Current Limiting Power Switch as radiation hardening	5	ON (enabled)	5 V x 1.0 mA	0.005	0.025	1,2,3,4,5	1	0.025	0.025
7	Propulsion	1	ON	20.45 A x 22V	450	450	1	0.25	112.5	112.5
8	Star Tracker	1	initialization	5.0 V x 200 mA	1	1	1	0.0125	0.0125	0.605
			Tracking	3.65V x 164 mA	0.6			0.9875	0.5925	
9	Sun sensor	6	idle	5v x 0.3mA	0.0015	0.24	1,2,3,4,5,6	0.01	0.00009	0.23769
			sampling	5V x 8mA	0.04			0.99	0.2376	
10	Reaction Wheels (MODEL RW1)	4	at max momentum	22 V x 0.636 A	14	56	1,2,3,4	0.1	5.6	20
			zero momentum	22 V x 0.182 A	4			0.9	14.4	
11	Thrusters	1	Standby	9V x 0.02 A	0.25	7.11	1	0.95	0.2375	0.593
			Active	9V x 0.79A	7.11			0.05	0.3555	
12	OBC/ADCS Computer	1	Active	3.3 V x 0.3A	1	1	1	1	1	1
13	IMU	1	Normal	3V x 5.150mA	0.01545	0.01545	1	0.9374	0.01448283	0.0144880884
			Suspended	3V x 0.028mA	0.000084			0.0626	0.0000052584	
14	Solar Array Drive Assembly	2	Active	14V x 0.25A	3.5	7	1,2	0.01	0.07	0.07

Table 11 presents the detailed power budget of the spacecraft, including all subsystems, operational modes, duty cycles, and configuration-dependent averaging. Each component is evaluated at its electrical operating point, and both nominal and peak power per unit are calculated. Duty cycles are applied per operational mode to obtain the mode-averaged and configuration-averaged power consumption[55].

The total spacecraft peak power requirement is: $P_{peak} = 571.94$ W

This value is dominated by propulsion (450 W) and reaction wheel momentum management (56 W peak combined), representing worst-case concurrent operation. Such peak events are transient and operationally scheduled to prevent bus overstress[55].

The average payload power consumption is: $P_{avg,payload} = 42.92$ W

This includes LoRa transceivers, power amplifiers, LNAs, RF switches, and associated electronics under duty-cycle-weighted operation. The total spacecraft average power consumption is:

$$P_{avg,total} = 155.42 \text{ W}$$

This value represents the primary sizing driver for the solar array and battery system. Solar array sizing is performed to sustain this load at End-of-Life (EOL), while the battery capacity is dimensioned to support eclipse operations under the defined Depth of Discharge (DoD) constraints. Peak power events are managed through operational scheduling, ensuring that propulsion, high-rate transmission, and battery recharge are not executed simultaneously unless sufficient power margin is available[55].

5.3.2 Assumptions and trade-off

Solar Array Sizing: Assumptions, Methodology, and Trade-Offs

Table 12 summarizes the solar array sizing workflow used to dimension the deployable solar panels for the LICOS spacecraft. The sizing is based on an energy-balance approach, where the solar array must (i) directly support the spacecraft load during sunlight and (ii) provide additional power to recharge the battery energy depleted during eclipse. The average spacecraft load is assumed equal in sunlight and eclipse, i.e., $P_d \approx P_e \approx 155.4$ W, and the baseline orbit parameters (T_p, T_e, T_d) are taken from the selected lunar constellation geometry.

Key assumptions: The conversion from incident solar flux to usable electrical power is computed using a triple-junction (TJ) cell efficiency of $\eta_{TJ} = 30\%$ [6]and the solar constant $S = 1361$ W/m^2. To represent realistic assembly effects, a deployment/mismatch derating factor of $l_d = 0.85$ is applied at Beginning-of-Life (BOL). End-of-Life (EOL) performance is modeled using a degradation rate of 0.5%/yr over a 5-year lifetime, yielding a life degradation factor $L_d = (1 - 0.005)^N$ with $N = 5$. Since solar incidence is not always normal, a worst-case incidence angle of $\theta = 50^\circ$ is assumed, reducing effective BOL power density by a $\cos\theta$ factor. Power path efficiencies are included to account for regulation and battery cycling losses: a daylight (direct) path efficiency of $X_d = 0.8$ and an eclipse (battery) path efficiency of $X_e = 0.6$.

Required solar array power: During sunlight, the array must provide power for the instantaneous daylight load and also the additional power needed to "pay back" the eclipse energy by charging the battery. Using the SMAD-style energy balance, the required solar array output during sunlight is:

$$P_{sa} = \frac{P_d}{X_d} + \frac{P_e\, T_e}{T_d\, X_e} \tag{2}$$

where P_d is the average daylight load, P_e is the average eclipse load, T_e is the eclipse duration, T_d is the sunlight duration, and X_d, X_e are the power-path efficiencies for daylight and eclipse operation, respectively.

Table 12: Solar sizing and orbital analysis overview

(a) Solar Array Energy Balance Methodology

Step 1			
Define power needs & mission constraints	Average load power during daylight and eclipse = Pe = Pd	155.4242381	W
	Orbit altitude (O1)	2250	km
	Orbit period = Tp	9577.05	s
	Eclipse duration = Te	2689.55	s
	Sunlight duration = Td	6887.5	s
	Mission lifetime	5	yr
Step 2			
Compute required solar array power	Psa = solar array power required during sunlight	295.4348674	W
Step 3			
Ideal power per area (normal incidence)	P0 = eta S=	408.3	W/m^2
Step 4			
BOL power density (ld,BOL = assembly & mismatch derating factor)	PBol = P0 ld cosTheta	223.0826539	W/m^2
Step 5			
EOL degradation over n yrs' (Ld = life degradation factor)	Ld = (1 − degradation rate)^N)	0.9752487531	
	PEol= PBOL · Ld	217.56108	W/m^2
Step 6			
Required solar array area	Asa=Psa / PEOL	1.357939882	m^2
	Margin	15	%
	Asa,with margin=	1.561630864	m^2
	Baseline sizing target Approx	1.56	m^2
		15600	cm^2
Step 7			
30% Triple-Junction (TJ) solar array (8x8)	std assemly	61.46	cm^2
	Usable solar area	60.35	cm^2
	mass	7.1	gms per asmbly
	Total panels req	259	Qty
	total mass	1838.9	gms

(b) Solar Array Design Assumptions and Efficiencies

Inputs/Assumptions		
Power Path efficiencies (Xd, Xe)		
Xd Daylight (direct) power path efficiency	0.8	
Xe Eclipse (battery) power path efficiency	0.6	
Solar const = s =	1361	W/m^2
triple-junction XTJ Prime average BOL efficiency Eta =	30	%
Assembly + mismatch derating (BOL) ld =	0.85	
Worst-case incidence angle Theta =	50	deg
Degradation rate	0.5	%/yr

(c) Orbital Parameters and Eclipse Analysis

Orbit Radius [km]	**Orbit Period**		**Eclipse Period**	
	[s]	[hr]	[s]	[min]
2250	9577.05	2.66	2689.55	44.83
2286	9807.81	2.72	2695.28	44.92
2277	9749.95	2.71	2693.76	44.9

BOL power density: The ideal electrical power-per-area at normal incidence is:

$$P_0 = \eta_{TJ} S \tag{3}$$

Applying assembly/mismatch derating and the worst-case incidence angle yields the BOL effective power density:

$$P_{BOL} = P_0 l_d \cos\theta \tag{4}$$

This formulation captures both manufacturing/assembly losses and the reduction due to non-normal solar incidence.

EOL degradation and required area: The EOL power density is obtained using the life degradation factor L_d:

$$P_{EOL} \;=\; P_{BOL}\, L_d \qquad \text{with} \qquad L_d = (1-\delta)^N \tag{5}$$

where δ is the annual degradation rate and N is the mission lifetime in years.

The required solar array area then follows as:

$$A_{sa} \;=\; \frac{P_{sa}}{P_{EOL}} \tag{6}$$

A design margin is subsequently applied (15%) to account for modeling uncertainty, pointing errors, thermal effects, and operational variability, leading to the selected baseline area $A_{sa} \approx 1.56$ m^2.

Trade-offs: The solar array sizing is primarily driven by the geometric relationship between the Sun vector and the spacecraft attitude. In the selected near-polar lunar orbit, the spacecraft maintains a nadir-pointing attitude to satisfy communication requirements. When the orbital beta angle approaches 90°, the Sun vector becomes nearly parallel to the orbital plane. Due to attitude locking, the spacecraft body cannot freely rotate to maintain normal solar incidence. In the worst-case configuration, the solar rays become nearly parallel to the nominal array mounting plane, resulting in $\theta \approx 90°$ and therefore negligible power generation ($P \propto \cos\theta$).

To mitigate this geometric limitation, the solar panels are mounted with an additional cant angle of approximately 40° relative to the spacecraft body. This ensures that even under worst-case beta angle conditions, the effective solar incidence angle is reduced from 90° to approximately 50°. Consequently, the conservative sizing assumption uses $\theta = 50°$ as the worst-case incidence angle in the power-per-area calculation.

This approach increases the required array area but significantly reduces the risk of power shortfall during high-beta seasons or constrained attitude operations. Similarly, selecting higher design margins increases structural mass and stowed volume, yet improves robustness against End-of-Life degradation and uncertainties in efficiency assumptions. The selected daylight and eclipse power path efficiencies (X_d and X_e) reflect a realistic representation of regulator and battery cycling losses; lower efficiencies increase required solar array power, but yield a more conservative and reliable design point for the 5-year lunar mission.

Inter-panel shadowing considerations:

In the worst-case configuration where the beta angle approaches 90°, only one deployable solar wing is effectively illuminated due to spacecraft attitude locking and array cant geometry. The opposite wing is oriented away from the Sun and therefore does not generate power. Since the non-illuminated wing is not positioned between the Sun and the active surface, no inter-panel umbra or self-shadowing occurs.

In this high-β scenario, battery charging is intentionally not performed, and the generation requirement is reduced to supplying the average spacecraft load only. Because the total deployable area is equally distributed between two identical wings, the single illuminated wing provides approximately:

$$P_{sa,1\ wing} \approx \frac{P_{sa}}{2} = \frac{295.43}{2} = 147.72 \text{ W}.$$

The resulting power difference with respect to the spacecraft average demand is:

$$\Delta P = P_{avg,total} - P_{sa,1\ wing} = 155.42 - 147.72 = 7.70 \text{ W}.$$

This remaining shortfall (approximately 8 W depending on instantaneous pointing and conversion efficiency) is compensated by additional body-mounted solar cells located on the spacecraft top surface.

Therefore, even under the $\beta \approx 90°$ worst-case geometry, the spacecraft maintains energy balance without inter-panel shadowing, while deferring battery recharge during this condition.

Battery Sizing: Assumptions, Methodology, and Trade-Offs

Table 13: Battery Sizing Methodology and Design Assumptions

(a) Battery Sizing Methodology

Step 1 Identify Energy Storage Requirement	Eeclipse = Pe Te = Eclipse energy req=	418021.2596 J 116.1170165 Wh
Step 2 Select Battery Technology	Tradeoffs	
Step 3 Required battery capacity at BOL (sized for EOL)	Required battery energy Ebat=	483.8209023 Wh
Step 4 Select Battery Capacity (Baseline)	Selected battery capacity (BOL) =	500 Wh
Step 5 Convert Energy to Capacity (Ah)	8S5P = EBat = EBat Nominal =	17.5 Ah 504 Wh 500 Wh
Step 6 Estimate Battery Mass	Mass battery = Baseline battery mass =	2.5 kg 2.7 kg
Step 7 Lithium-ion Battery Pack	Single module mass = Dimension =	0.5 kg 93x86x41 mm

(b) Battery Design Assumptions and Parameters

Inputs/Assumptions		
Eclipse power load Pe =	155.4242381	W
Eclipse Duration Te =	2689.55	s
Maximum allowable DoD	40	%
Battery round-trip efficiency	0.9	
Capacity fade factor	0.8	
Sizing margin	20	%
Qty	5	
Capacity:	3.5	Ah
Vnom:	28.8	V
Specific energy	200	Wh/kg
Pack-level battery mass (incl. BMS + harness)	0.2	kg

Table 13 summarizes the battery sizing process used to dimension the spacecraft energy storage system. The battery is sized to fully support the eclipse energy requirement while respecting Depth of Discharge (DoD), round-trip efficiency, degradation, and mission lifetime constraints.

Eclipse Energy Requirement:

The required eclipse energy is computed from the average eclipse load and eclipse duration:

$E_{eclipse} = P_e \cdot T_e$, $E_{eclipse} = 155.42 \text{ W} \times 2689.55 \text{ s} = 4.18 \times 10^5 \text{ J} = 116.12 \text{ Wh}$.

This represents the minimum usable energy that must be delivered by the battery during each eclipse period.

Battery Capacity Sizing:

To ensure End-of-Life (EOL) compliance, the battery is sized at Beginning-of-Life (BOL) while accounting for:

The required battery capacity at BOL is therefore:

$$E_{bat,BOL} = \frac{E_{eclipse}}{\text{DoD} \cdot \eta_{rt} \cdot f_{fade}} \rightarrow E_{bat,BOL} = \frac{116.12}{0.4 \times 0.9 \times 0.8} \approx 483.82 \text{ Wh}.$$

A 500 Wh baseline battery is selected to include additional sizing margin and provide operational robustness.

- Maximum allowable DoD ($\text{DoD}_{\max}$) = 40%
- Design margin = 20%
- Round-trip efficiency (η_{rt}) = 0.90
- Capacity fade factor (f_{fade}) = 0.8

Capacity Conversion and Configuration:

The battery configuration (8S5P) yields:

$V_{nom} = 28.8$ V, $C_{pack} = 17.5$ Ah,

corresponding to approximately 500 Wh nominal stored energy.

Mass Trade-Off:

Using a specific energy of 200 Wh/kg, the estimated battery mass is:

$m_{bat} \approx \frac{500}{200} = 2.5$ kg.

Including packaging, Battery Management System (BMS), and harness, the baseline mass increases to approximately 2.7 kg.

Design Trade-Offs:

The battery sizing is primarily driven by the trade-off between allowable DoD and system mass. A lower DoD increases cycle life and mission robustness but requires larger capacity and higher mass. The selected 40% DoD represents a balance between lifetime reliability and mass efficiency for a 5-year lunar mission [17].

Similarly, incorporating round-trip efficiency and capacity fade ensures conservative sizing at EOL, preventing energy shortfall during extended eclipse seasons or high-load operational modes. The selected 500 Wh capacity therefore provides sufficient margin while remaining compatible with spacecraft mass and volume constraints.

5.3.3 Baseline Design

The baseline Electrical Power Subsystem (EPS) architecture consists of two deployable solar wings equipped with AZUR SPACE 30% triple-junction (TJ3G30) solar cells, providing the required 1.56 m^2 effective area at End-of-Life (EOL)[6],[18]. Solar array orientation is achieved through two Solar Array Drive Mechanisms (SADM) supplied by COMAT (qty: 2), enabling single-axis tracking to mitigate high-beta angle losses in the polar lunar orbit. Power conditioning, regulation, and distribution are performed by the GomSpace NanoPower P80 EPS unit, selected for its flight heritage, compatibility with 28 V-class buses, and suitability for medium-power CubeSat-class missions.

Energy storage is provided by a GomSpace NanoPower BPX lithium-ion battery module, sized to 500 Wh at Beginning-of-Life (BOL) to satisfy eclipse energy requirements while respecting Depth of Discharge (DoD), round-trip efficiency, and lifetime degradation constraints. Vendor quotations have been obtained for the EPS, battery, and solar cells, confirming commercial availability and compatibility within the system architecture. At the time of writing, the SADM procurement is pending quotation; however, the selected COMAT unit satisfies torque, rotation range, and space qualification requirements consistent with the mission power and attitude profile.

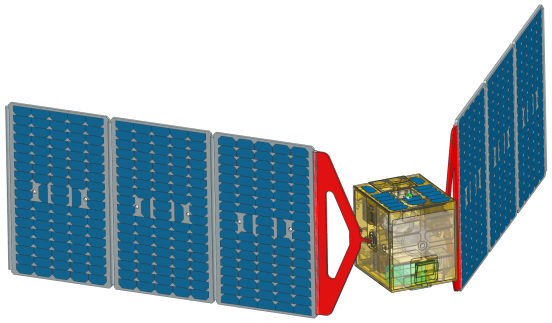

Figure 10: LICOS spacecraft deployed configuration with cant-mounted solar arrays and internal power subsystem layout

Figure 10 illustrates the deployed configuration of the spacecraft, showing the two cant-mounted solar wings with an approximate 40° inclination relative to the spacecraft body. The body-mounted solar cells on the top panel are also visible and provide supplementary power during high-β conditions when only one deployable wing is illuminated. The Solar Array Drive Assemblies (SADA) are located at the wing roots (red interface brackets), while the NanoPower P80 EPS and BPX battery modules are integrated within the internal spacecraft structure.

5.4 Thermal Control - Author: Gabriel Virto

The thermal control system (TCS) ensures each spacecraft component remains within safe temperature limits during lunar orbit. In the vacuum of space, heat transfer occurs only through radiation or conduction within the spacecraft's structure. The main factors affecting temperature are direct sunlight, sunlight reflected from the lunar surface, and thermal emissions from the Moon. [15]

This chapter outlines how the spacecraft manages heat and protects critical systems, such as electronics and batteries. Components like the LR1121 chip require stable thermal conditions for reliable performance. These are therefore given particular attention. Robust thermal control measures are vital for mission success and for maintaining communication during the orbital phase.

5.4.1 Design Objectives and Requirements

Thermal Environment in Lunar Surface and Orbit

Unlike Earth, the Moon doesn't have an atmosphere. Because of this, heat in lunar orbit can only be radiated or within the spacecraft itself. Without an atmosphere, the Moon's surface temperature varies dramatically, with sunlit areas reaching approximately 390 – 400 K and shadowed regions decreasing to nearly 90 - 100K [31]. These big differences create a challenging environment for thermal engineers and set the main rules for how spacecraft must be designed to handle temperature.

A spacecraft flying close to the Moon encounters three main external heat sources: direct sunlight, sunlight reflected from the lunar surface, and heat emitted by the Moon as infrared radiation. These fluxes are summarized below:

Parameter	Hot Case	Cold Case
Solar Radiation q_{solar}	1361 W/m^2	0 W/m^2
Lunar albedo (7%)	$\sim$100W/m^2 absorbed	0 W/m^2
Lunar IR	Up to $\sim$120-150 W/m^2	Minimal (<10 W/m^2)

Table 14: Thermal Modeling Boundary Conditions (Worst Case Scenarios)

For the thermal analysis, two bounding conditions are considered: the hot case and the cold case. In the hot case, corresponding to sunlit orbital conditions, the spacecraft is exposed to direct solar radiation, lunar albedo and lunar infrared emission. This configuration produces the maximum external heat input and therefore governs the sizing of the radiative heat rejection system. In the cold case, corresponding to eclipse or shadow conditions, the spacecraft receives minimal external heating, with no direct solar contribution and significantly reduced. This scenario represents the minimum heat input condition and is critical for preventing excessive cooling of temperature-sensitive components.

These two limiting cases establish the spacecraft's thermal design envelope. Under hot conditions, the primary risk is overheating of electronics and batteries, which is mitigated by using high-emissivity coatings and deployable radiators to enhance heat rejection. In cold conditions, the main risks are component freezing and battery performance degradation, addressed by applying multilayer insulation (MLI) to reduce radiative heat losses and stabilize internal temperatures.

Thermal Requirements

Each of the internal instruments mentioned in Table 11 has a specific temperature range within which it can operate without issues. The temperature limits summarized in Table 15 define the allowable operational and non-operational ranges for each spacecraft subsystem. These limits are derived from manufacturer specifications and mission requirements [46]. Although several components can tolerate significantly higher maximum temperatures, the thermal control system is conservatively designed to maintain the internal structure below 35°C during nominal operation. This value is selected to protect temperature-sensitive elements while also providing a margin against local hot spots and material degradation.

	Allowable Temperature [°C]				**Design** [°C]	
	Operational		Non-operational			
COMPONENTS	Min	Max	Min	Max	Min	Max
Semtech LR1121 chip	−55	125	−40	85	−35	80
Power Amplifier	−55	100	−40	85	−35	80
Low Noise Amplifier	−40	150	−40	105	−35	100
RF switch	−65	150	−40	100	−35	95
Power switch	−65	150	−40	125	−35	120
Propulsion	n/a	n/a	−20	40	−15	35
Star tracker	n/a	n/a	−55	125	−50	120
Sun sensor	−30	70	−20	60	−15	55
Reaction wheels	n/a	n/a	0	60	5	55
IMU	n/a	n/a	−104	150	−100	145

Table 15: Design temperature ranges of the spacecraft components

5.4.2 Assumptions and trade-off

External heat fluxes

The MATLAB CubeSat Toolbox was used to calculate the sun visibility flag and the solar beta angle over one orbital period, which defines the time-dependent external radiative boundary conditions applied in the thermal model.

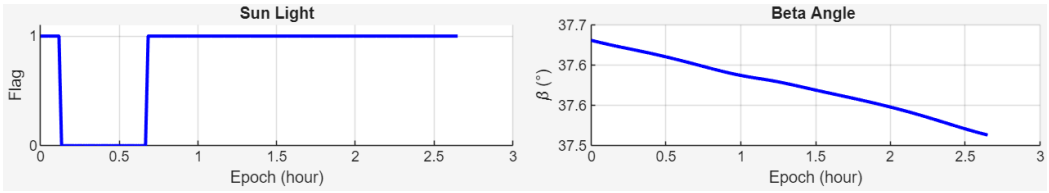

(a) Orbital Plane 1: Eclipse phase present.

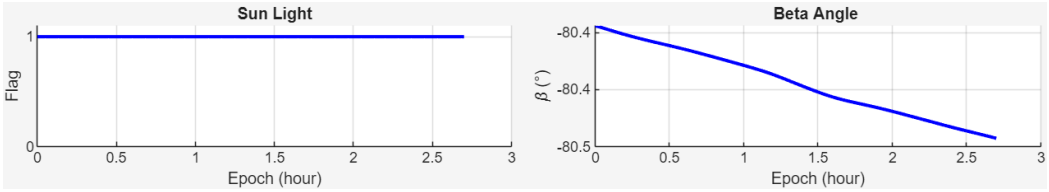

(b) Orbital Plane 3: Continuous solar illumination

Figure 11: Sun visibility flag and beta angle evolution for two different orbital planes

Three orbital plane configurations with different RAAN values were analyzed, as shown in Figure 11. In Plane 1 shown in Table 6, eclipse intervals occur when the Moon blocks the Sun, resulting in zero direct solar input during those periods. In contrast, Plane 3 (see Table 6) maintains continuous solar illumination due to a high absolute beta angle, preventing eclipse. This configuration produces the maximum external heat load and defines the hot-case condition for radiator sizing.

The thermal model includes three external radiative heat sources. The MATLAB code of [25] was implemented and modified for our case. Figures 12 and 13 illustrate the orbital variation of solar and albedo heat fluxes of Plane 1. Solar radiation dominates during illuminated phases, while lunar IR remains a secondary but non-negligible contribution for nadir-facing surfaces.

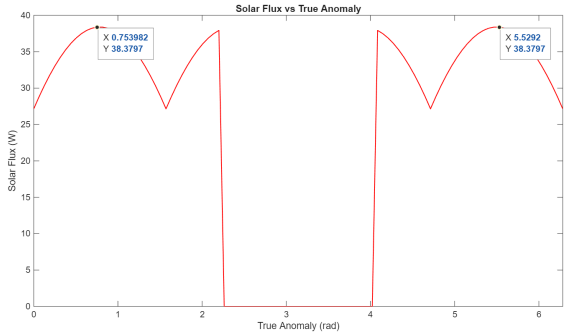

Figure 12: Absorbed solar heat flux

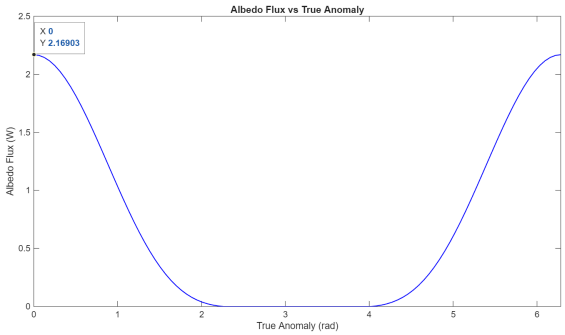

Figure 13: Absorbed lunar albedo heat flux

Face	Hot Case	Cold Case
-X	0.5572 W	0.0022 W
+X	0.5572 W	0.0022 W
-Y	0 W	0 W
+Y	2.2787 W	0.0089 W
-Z	0.4776 W	0.0019 W
+Z	0.4776 W	0.0019 W
Total	4.3483 W	0.0170 W

Table 16: Lunar IR boundary conditions for hot and cold cases.

Radiator sizing

The spacecraft must reject approximately 166 W, including internal dissipation and external heat. Radiative heat rejection to deep space is governed by $Q = \varepsilon\sigma AT^4$. The maximum allowable radiator temperature is limited to 35°C (308 K).

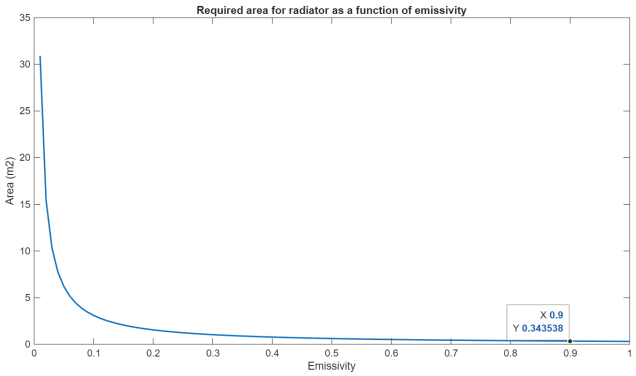

Figure 14: Required radiator area as a function of emissivity for a limit of 35°C.

Figure 20 illustrates the strong dependence of required radiator area on surface emissivity. Selecting an OSR coating with $\varepsilon \approx 0.9$ significantly reduces the required area and enables a compact design. In conclusion, the radiator surfaces are coated with OSR and the required area will be $0.34m^2$. Passive thermal control is implemented using body-mounted Optical Solar Reflectors (OSR) and a deployable radiator panel.

Lumped Parameter Model

The spacecraft thermal behavior is modeled using a lumped parameter network, as illustrated in Figure 15. Individual subsystems (e.g., structure, propulsion, EPS, tank, payload, AOCS) are represented as thermal nodes connected through conductive thermal resistances R_i. Internal heat dissipation from electronics and propulsion units is modeled as heat flow sources applied to the corresponding nodes. External heat inputs, including solar radiation and lunar infrared radiation, are applied to the outer structural node. [1]

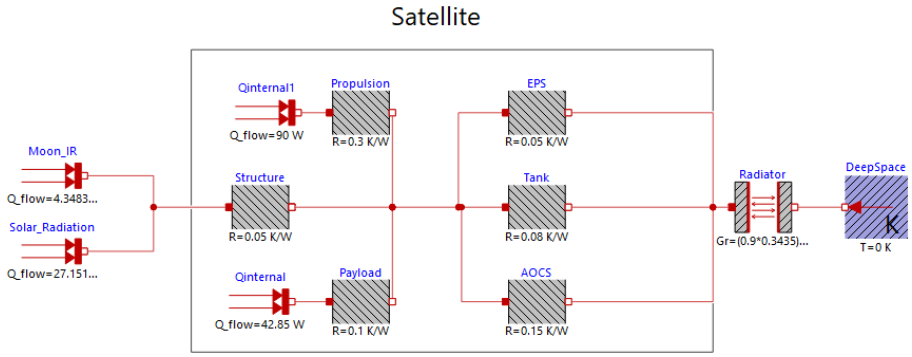

Figure 15: Lumped parameter thermal network of the spacecraft

Radiative heat rejection to deep space is modeled as a thermal radiation element connected to a $T = 0$ K sink. The deployable radiator is represented as an additional radiative branch, which can be enabled or disabled depending on the hot or cold case configuration. By solving the nodal energy balance equations, the final temperature of each component can be determined under the specified environmental conditions.

5.4.3 Baseline Design

Spacecraft Geometry

The spacecraft is a rectangular satellite with external dimensions of $30\text{cm} \times 35\text{cm} \times 35\text{cm}$, corresponding to a cuboid.

For thermal control, a total area of 0.16 m^2 of the spacecraft body is covered with Optical Solar Reflectors (OSR), distributed across the most suitable external faces for radiative heat rejection. In addition, a deployable radiator panel provides an extra 0.20 m^2 of effective radiating area. The total radiative area available for heat rejection is therefore $A_{\text{radiator}} = 0.16 + 0.20 = 0.36$ m^2

Deployable Radiator

To ensure adequate heat rejection and maintain the spacecraft below the 35°C temperature limit, a deployable radiator panel is implemented. The deployable radiator provides an effective area of $A_{\text{dep}} = 0.2$ m^2 and complements the body-mounted OSR surfaces.

The radiator is a lightweight aluminum honeycomb sandwich panel with aluminum face sheets bonded to a core approximately 10–15 mm thick. This structure offers a high stiffness-to-mass ratio and mechanical stability during launch and deployment. The panel is attached to the spacecraft bus with a hinged mechanism.

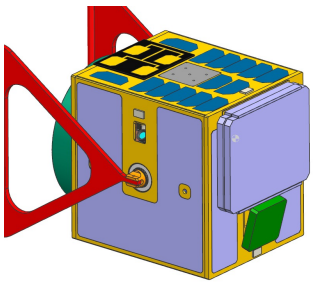

Figure 16: Deployable Radiator

Both sides of the deployable panel are coated with OSR. The double-sided configuration increases radiative efficiency when both surfaces maintain a high view factor to deep space. Heat transport from internal components to the radiator surface is ensured through embedded aluminum heat pipes. These passive two-phase devices operate without electrical power and distribute heat uniformly, reducing temperature gradients and enhancing overall thermal performance.

Thermal Results

The hot-case temperature is obtained from the steady-state radiative energy balance, considering the total effective radiating area, including the deployable radiator:

$$T_{\text{hc}} = \left(\frac{Q_{\text{total,hc}}}{\sigma \left(\varepsilon_{\text{eff}} A_{\text{eff}} + \varepsilon_{\text{OSR}} A_{\text{dep}} \right)} \right)^{1/4}, \tag{7}$$

where σ is the Stefan–Boltzmann constant, A_{eff} represents the body-mounted radiating area (OSR and exposed surfaces), and A_{dep} corresponds to the deployable radiator area.

Evaluating the hot case condition, the internal temperature is $T_{\text{hc}} = 305.64$ K (32.5°C) which remains below the allowable structural limit of 35°C.

For the cold-case condition, the deployable radiator is thermally decoupled by switching off the heat pipes. In this configuration, the radiator does not contribute to heat rejection, reducing the effective

radiative area to the body-mounted OSR and insulated (MLI-covered) surfaces only. The steady-state cold-case temperature is therefore computed as

$$T_{\mathrm{cc}} = \left(\frac{Q_{\mathrm{total,cc}}}{\sigma \varepsilon_{\mathrm{eff}} A_{\mathrm{eff}}} \right)^{1/4}. \tag{8}$$

The resulting cold-case temperature is $T_{\mathrm{cc}} = 263.58$ K $\quad (-9.6^{\circ}\mathrm{C})$

After determining the global internal temperature of the spacecraft, a more detailed analysis was performed using the lumped parameter thermal model. As shown in the network representation in Figure 15, the principal internal heat sources are localized within the payload and propulsion subsystems, representing the worst-case internal dissipation scenario. Figure 17 presents the steady-state temperatures obtained from the lumped parameter thermal model under the hot-case configuration.

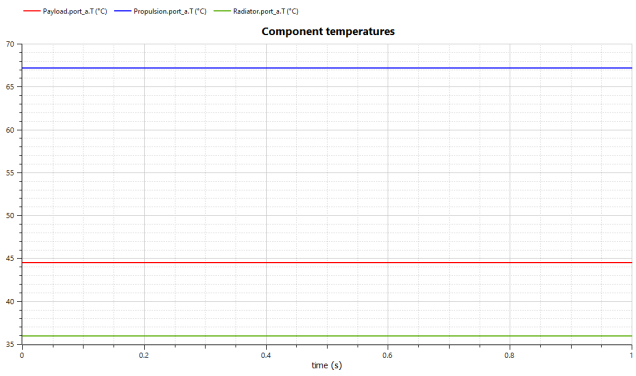

Figure 17: Component temperatures under hot-case conditions.

The resulting temperatures indicate that the payload stabilizes at approximately 44°C, the propulsion subsystem reaches about 67°C and the radiator node maintains a temperature of 35.9°C. These values remain within the allowable operational limits of the respective components. The radiator temperature closely approaches the design constraint of 35°C, confirming that the radiative area and emissivity selection are appropriately sized for the imposed thermal load.

These results demonstrate that the proposed thermal control architecture effectively regulates subsystem temperatures under maximum heat input conditions. The combination of body-mounted OSR surfaces and a deployable radiator, coupled with controllable heat-pipe operation, provides a balanced, robust passive thermal solution for Low Lunar Orbit. Furthermore, the configuration maintains adequate thermal margin in the hot case while preserving the ability to mitigate excessive cooling during eclipse phases.

5.5 Structure - Author: Jakub Czerniej

5.5.1 Structure Requirements and Design Drivers

The structural subsystem is critical for the survival of the spacecraft during the launch phase and for maintaining the geometrical integrity of the constellation satellite payload.

Unlike typical Low Earth Orbit (LEO) missions where mass optimization is the primary constraint, this design prioritizes robustness and long-term reliability. Since the Neutron launch vehicle provides a significant performance margin, we did not focus on aggressive weight reduction. Instead, the structure was designed to be substantial enough to endure the harsh deep-space environment for a 5-year mission duration.

The primary design driver was to create a rigid, thermally stable chassis that naturally shields internal avionics from the high radiation levels found in lunar orbit. Consequently, we selected thicker aluminum gauges to ensure the safety of the electronics and the longevity of the mission, rather than minimizing structural mass.

Table 17: Structure Subsystem Requirements

ID	Requirement Statement
REQ-STR-001	The spacecraft structural subsystem shall ensure that the total spacecraft mass remains within the microsatellite class envelope.
REQ-STR-002	The structure shall be compliant with the ultimate launch loads, including static, dynamic, acoustic and shock environment of the launcher.
REQ-STR-003	The structure shall withstand loads induced during translunar injection, mid-course correction maneuvers, and lunar orbit insertion burns. the
REQ-STR-004	The structure shall maintain mechanical integrity, dimensional stability, and alignment under repeated deep-space thermal cycling conditions characteristic of lunar orbit.
REQ-STR-005	The structure shall tolerate micrometeoroid impacts expected in lunar space.
REQ-STR-006	The structure shall provide mechanical interface to other vehicle
REQ-STR-007	The structure shall accommodate thrust loads, pressure loads, and dynamic coupling associated with the propulsion subsystem.
REQ-STR-008	The structure shall allow safe handling, integration, and accessibility for Assembly, Integration and Testing, including vibration, shock, and thermal vacuum campaigns.
REQ-STR-009	The structure shall provide standardized mounting provisions for all spacecraft subsystems.
REQ-STR-010	The structure shall maintain mechanical integrity, dimensional stability, and alignment under repeated deep-space thermal cycling conditions.

5.5.2 Assumptions and Design Trade-offs

During the preliminary design phase, the structural architecture was defined through a trade-off analysis balancing mass efficiency, manufacturability, and assembly accessibility (AIT). While mass optimization remains a critical driver for lunar transfer capability, the design strategy prioritized technologies feasible for a university-class project.

Structural Architecture Selection

Three primary architectural concepts were evaluated: a Monocoque shell, Aluminum Honeycomb panels, and a modular "Cage" (Plate-and-Standoff) frame.

The Monocoque concept, machined from a single block, was rejected early in the trade-off process. Despite its high potential for stiffness, it severely restricts access to internal components, making the integration of the avionics stack and propulsion system operationally high-risk.

Subsequently, Aluminum Honeycomb Sandwich panels were considered due to their industry-standard stiffness-to-weight ratio. However, this option was also deemed unsuitable for the current design phase. The manufacturing complexity associated with potting inserts for every mounting point, combined

with high fabrication costs and lead times, did not justify the mass savings for a 55 kg satellite with a launch margin.

Ultimately, a Modular "Cage" Architecture was selected as the baseline. This design features two primary load-bearing decks connected by structural rails and enclosed by removable side panels. This solution offers the optimal balance for the mission requirements: it allows for significant mass reduction through aggressive CNC pocketing (lightweighting) of the solid plates, while ensuring that side panels can be removed for maintenance without compromising the primary load path.

Material Selection

For the primary structure, Aluminum 7075-T7351 was selected. While standard Al-6061 is easier to machine, Al-7075 offers a superior yield strength, allowing for thinner wall sections and reduced overall mass. Crucially, the T7351 temper was chosen over the more common T6. Given the 5-year mission duration in the deep-space environment, the T7351 temper provides essential resistance to Stress-Corrosion Cracking (SCC), ensuring long-term structural integrity where T6 might be susceptible to brittle failure.

5.5.3 Baseline Design Description

The proposed structural configuration, shown in Figure **??**, represents the preliminary baseline with overall dimensions of [INSERT DIMS] mm and a current structural mass of approximately 11 kg. At this early design stage (Phase 0), the geometry focuses on defining the primary load paths and volumetric constraints rather than detailed mass or manufacturing optimization. Consequently, minor features such as fastener holes, cable routing interfaces, and specific CNC tooling features have been omitted to simplify the initial Finite Element Analysis. This model serves as the reference baseline, establishing the stiffness and strength margins required before proceeding to detailed mechanical design and further weight reduction iterations.

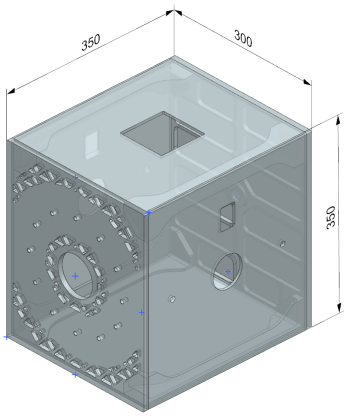

Figure 18: LICOS structure with general dimensions

5.5.4 Structural (FEM) Analysis

Introduction and Methodology

The structural integrity of the satellite was verified using the Finite Element Method (FEM) implemented in **Siemens Simcenter 3D (Nastran)**. The primary objective of these analyses is to demonstrate that the design meets the stiffness requirements defined by the launch vehicle provider and possesses sufficient strength to withstand the maximum expected launch loads.

To ensure the validity of this preliminary design, conservative modeling assumptions were applied throughout the simulation process. Specifically, a Safety Factor (SF) of **1.5** was imposed on all yield and ultimate strength checks to account for design maturity margins and modeling uncertainties. Furthermore, while a specific mass margin was added to the simulation to account for non-modeled hardware such as cabling and fasteners, the bolted joints were idealized as rigid connections for the global analysis.

Modal Analysis

Objectives and Verification Criteria

The primary objective of the Finite Element Analysis (FEA) was to verify the structural integrity of the satellite design under launch conditions. Specifically, the analysis aimed to determine the fundamental natural frequencies (Modal Analysis) and the stress distribution under peak loads.

According to the *Rocket Lab Neutron Payload User's Guide*, specific stiffness requirements are typically defined via a Coupled Loads Analysis (CLA) tailored to the specific mission profile. However, in the absence of a launch vehicle coupled model for this preliminary design phase, industry-standard stiffness targets for medium-lift launch vehicles were adopted as conservative acceptance criteria:

- **Lateral Frequency (X, Y):** > 10 Hz.
- **Axial Frequency (Z):** > 25 Hz.

Meeting these targets ensures that the spacecraft is dynamically decoupled from the launcher's control system frequencies.

Finite Element Model (FEM) Setup

The numerical analysis was performed using SOL 103 Module in Nastran. The mesh generation strategy was optimized to balance computational efficiency with result accuracy for the complex geometry.

Mesh Properties:

- **Element Type:** The entire structure was discretized using higher-order 3D Tetrahedral elements (**CTETRA10**).
- **Element Sizing:**
  - **Primary Structure:** A fine mesh size of **5 mm** was applied to the two decks (Top/Bottom) and the 4 structural pillars to capture high stress gradients in the load path.
  - **Secondary Structure:** A coarser mesh size of **10 mm** was applied to the outer side.
- **Mesh Quality:** A mesh scaling factor (growth rate) of **1.3** was utilized to ensure smooth transitions between detailed features and the bulk volume.

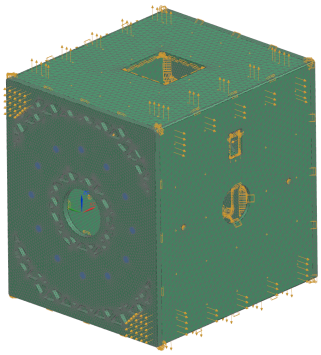

Figure 19: Mesh of the structure

Boundary Conditions and Connections

To simulate the launch configuration, the following boundary conditions and connections were applied:

1. **Constraints:** The model was constrained at the mounting holes of the bottom interface ring. A **Fixed Constraint** (locking all 6 Degrees of Freedom: TX, TY, TZ, RX, RY, RZ) was applied to these surfaces to simulate the bolted connection to the separation ring.
2. **Component Connections:** To simulate the assembly of the "Cage" structure, individual parts were connected using **Surface-to-Surface Gluing**. This method ensures continuous displacement continuity between the mating surfaces of the pillars and decks.
3. **Propellant Tank Modeling (RBE3 + CONM2):** Since the internal propellant tank was not modeled as a 3D solid to reduce complexity, it was represented as a 0D Lumped Mass element (**CONM2**) positioned at the tank's Center of Gravity.
    - **Connection:** The CONM2 element was connected to the structural mounting points using **1D RBE3 (Interpolation)** elements. Unlike rigid RBE2 elements, RBE3 elements distribute the mass load without adding artificial stiffness to the structure, ensuring the modal results remain realistic.
4. **Non-Structural Mass (NSM):** The mass of avionics, batteries, and cabling was accounted for by applying Non-Structural Mass area loads directly to the side panels.

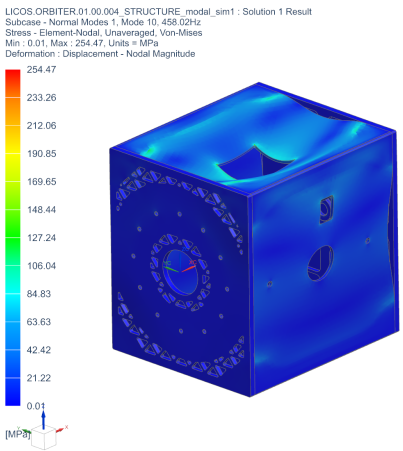

Figure 20: von Mises stressess of the Mode number 10

Modal Analysis Results

The first 10 natural frequencies were extracted to evaluate the stiffness. The results are summarized in Table 18.

Table 18: Natural Frequencies of the Spacecraft Structure (Modes 1-10)

Mode	**1**	**2**	**3**	**4**	**5**	**6**	**7**	**8**	**9**	**10**
Freq. [Hz]	107.9	120.8	235.0	295.8	319.4	334.3	427.6	434.0	438.8	458.0

Interpretation

The first fundamental frequency is observed at **107.9 Hz**. This value is significantly higher than the 25 Hz requirement, indicating an exceptionally stiff structure. While this confirms the design is safe from resonance issues, it should be noted that the high stiffness suggests the structure may be over-designed in terms of mass. Furthermore, as this is a preliminary simplified model (Phase 0), real-world values may decrease once detailed fastener flexibility and tolerance gaps are introduced in later design phases.

Stress Verification (Example Case)

To verify strength, the Von Mises stress distribution was analyzed. For example, in the high-frequency domain (referencing Mode 10 at approx. 458 Hz), significant nodal stress concentrations were observed.

As shown in the analysis, the peak Von Mises stress recorded was **255 MPa**. To validate structural safety, the Margin of Safety (MoS) was calculated against the yield strength of Aluminum 7075-T7351 ($R_{p0.2} = 435$ MPa) using a Safety Factor (SF) of 1.5.

Margin of Safety Calculation:

$$\sigma_{allow} = \frac{R_{p0.2}}{SF} = \frac{435 \text{ MPa}}{1.5} = 290 \text{ MPa} \qquad MoS = \frac{\sigma_{allow}}{\sigma_{max}} - 1 = \frac{290 \text{ MPa}}{255 \text{ MPa}} - 1 = \mathbf{+0.137}$$

Since the Margin of Safety is positive ($MoS > 0$), the structure is considered safe for this load case, although the margin is tight, suggesting that local reinforcement or mesh refinement may be required in the detailed design phase.

Quasi-Static Loads Analysis

Load Factors and Cases Definition

The structural strength verification is based on the Quasi-Static Load Factors specified in the *Neutron Payload User's Guide* for light payloads. The document specifies the following limit loads:

- **Axial Compression:** $6g$
- **Axial Tension:** $2g$
- **Lateral:** $\pm 2.5g$

Based on these limits, two critical design load cases were defined to simulate the worst-case combined loading scenarios during the launch phase:

1. **Load Case 1 (Max Compression):** Combination of $6g$ axial compression (Z-axis) and $2.5g$ lateral acceleration applied away from the OTV mounting interface (simulating the maximum bending moment on the pillars).

2. **Load Case 2 (Max Tension):** Combination of $2g$ axial tension (Z-axis) and $2.5g$ lateral acceleration applied along the longitudinal axis of the OTV.

FEM Setup and Boundary Conditions

This time numerical analysis was performed using SOL 101 Module in Nastran. General configuration remains identical to the one used for the Modal Analysis to ensure consistency.

- **Mesh:** The same CTETRA10 mesh with 5 mm (primary) and 10 mm (secondary) element sizing was utilized.
- **Boundary Conditions:** The structure is fixed at the separation ring interface holes.
- **Load Application:** The inertial loads were applied to the entire structure (including the non-structural mass and propellant tank) using a global acceleration function.

Results

The linear static analysis was performed for both load cases. The Von Mises stress distributions are presented below.

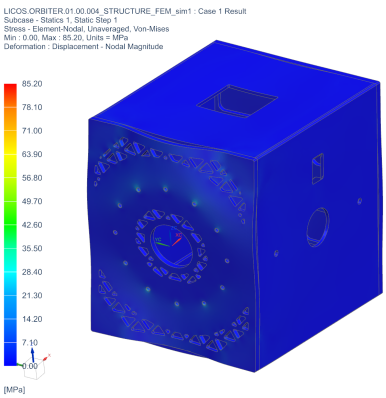

(a) Load Case 1 (6g Compression + 2.5g Lateral)

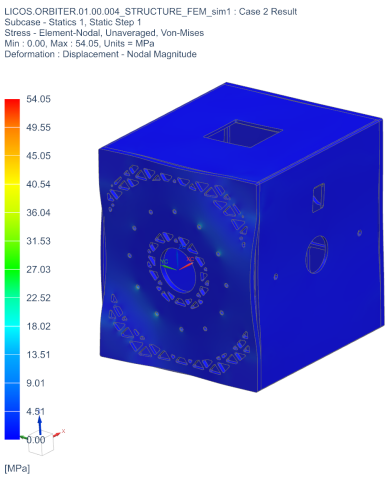

(b) Load Case 2 (2g Tension + 2.5g Lateral).

Figure 21

Strength Verification and Margin of Safety

The structural analysis confirms that the design withstands both load cases without failure. A comparison of the results reveals that Load Case 1 (Max Compression) is more dangerous scenario, inducing significantly higher stress concentrations in the lower pillars and the baseplate interface due to the combined compressive and bending loads.

Critical Results (Load Case 1):

- **Maximum Von Mises Stress:** 85 MPa
- **Location:** Walls of the mounting holes to spearation ring

To verify the structural integrity, the Margin of Safety (MoS) was calculated against the yield strength of Aluminum 7075-T7351 ($R_{p0.2} = 435$ MPa) using a conservative Safety Factor (SF) of 1.5.

Calculation:

$$\sigma_{allow} = \frac{R_{p0.2}}{SF} = \frac{435 \text{ MPa}}{1.5} = 290 \text{ MPa} \qquad MoS = \frac{\sigma_{allow}}{\sigma_{max,LC1}} - 1 = \frac{290 \text{ MPa}}{85 \text{ MPa}} - 1 = \mathbf{2.4}$$

Conclusion

The positive Margin of Safety indicates that the preliminary structural design possesses sufficient strength to withstand the maximum expected quasi-static launch loads with the required safety margins.

5.6 Propulsion - Authors: Jakub Czerniej & Gonzalo Cuesta

5.6.1 Propulsion Requirements and Design Drivers

Each satellite in the constellation needs to perform some maneuvers during the lifetime of the mission. The maneuvers the satellite should do are the following: initial positioning, station keeping, maintaining separation, collision avoidance, and disposal. The mass of the propulsion system should also be as low as possible, as a higher mass would increase the launch costs. The power requirements of the propulsion system should also be optimized.

The delta-v that the propulsion system must provide is at least 1017.6 m/s. A more detailed breakdown of the delta-v requirements can be found in the following section.

Propulsive maneuvers:

- **Satellite separation**
  Immediately after the satellites are separated from the Orbiter Transfer Vehicle, they must perform a maneuver to separate themselves in orbit. The separation is done by a method called orbit phasing. For this method, a burn is performed to change the semi-major axis of the orbit slightly. The burns are done so that the satellite's orbits' semi-major axis differ slightly. This means that the satellites end up having relative angular velocities, so that they start separating. Once they have separated equally around the orbit, another burn is done so that the satellites return to their correct orbit for the mission.

  The necessary delta-v necessary for the initial separation of the satellites was determined as 8 m/s. The delta-v for maintaining this separation over the mission was calculated to be 90 m/s. [27, 28]

- **Station-keeping**
  Periodic station-keeping maneuvers are necessary to counter the non-uniform lunar gravity field. For conservative planning, a worst-case allocation of 10 m/s per month was considered. This approach results in an annual station-keeping budget of approximately 120 m/s. Over a five-year operational lifetime, the total allocated delta-v amounts to 600 m/s, increasing to 1,200 m/s for a ten-year mission. [42]

- **Collision avoidance**
  Additional delta-v allocation is required for collision avoidance. Although the lunar orbital environment is significantly less congested than Earth orbit, collision risk may arise. Due to the use of low-thrust electric propulsion, avoidance maneuvers must be initiated several days in advance of the predicted closest approach to allow sufficient time to complete the avoidance maneuver.

A delta-v amount of 6 m/s has been determined to be necessary to allocate for collision avoidance for a year through conservative assumptions. This corresponds to 30 m/s for a five year mission and 60 m/s for a 10 year mission.

Final delta-v budget:

From the previous delta-v calculations, the final delta-v budget for a 5-year mission duration is calculated:

- Initial positioning = 8 m/s
- Station-keeping = 600 m/s
- Maintaining separation = 90 m/s
- Collision avoidance = 30 m/s
- Disposal = 120 m/s
- Margin = 20%
- **Total = 1017.6 m/s**

The delta-v budget requires 1017.6 m/s of delta-v for the targeted mission lifetime of five years. This delta-v value was used for the following design and sizing of the propulsion system.

5.6.2 Assumptions and trade-off

There are multiple propulsion options for this type of CubeSats. The most commonly used are cold gas systems, chemical propulsion systems, and electric propulsion systems, among others. Each of these options has its advantages and its drawbacks.

Cold gas systems

One of the propulsion types that was considered is the cold-gas thruster. These thrusters have the main advantages of low complexity, low cost, and ease of integration. The main disadvantage of cold-gas thrusters is their low specific impulse, resulting in low efficiency. The resulting required propellant mass is relatively large for the type and size of satellite used for this mission, due to the large delta-v requirements for the long mission duration. For this reason, cold-gas thrusters were not chosen for the propulsion system.

Chemical propulsion systems

Chemical propulsion systems were also observed due to their high technological maturity. These types of engines are reliable, have the ability to restart, and provide a higher efficiency than cold-gas thrusters. Unfortunately, the specific impulse of these systems is still not sufficient for the mass and size restrictions needed for this mission.

Electrical propulsion systems

Electric engines are characterized by low thrust and high efficiency. Hall-effect thrusters are a popular electrical propulsion system for small satellites. These thrusters are characterized by their high efficiency. The specific impulse of these systems normally lies between 1000 and 1600s, and they operate at a power range of 20-620W. The high efficiency of these systems results in a low propellant mass, which is very appropriate for CubeSats. This technology is also characterized by its low thrust level. Most hall-effect thrusters for CubeSats only archive thrust values between 4 and 40mN. Nonetheless, these values can still be enough for their usual use case.

5.6.3 Baseline Design

The "ExoTerra Halo" (Figure 22) by the manufacturer ExoTerra was the thruster chosen for the constellation satellite. This is a compact hall-effect thruster that uses Xenon as its propellant. This

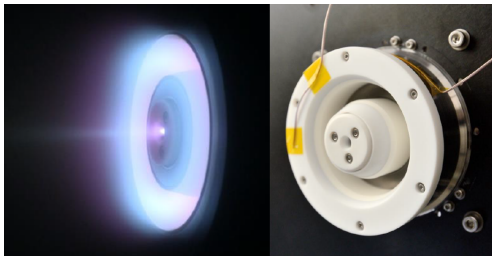

Figure 22: The "ExoTerra Hallo" thruster

thruster has many qualities that made it appropriate for this mission. The "ExoTerra Hallo" has a relatively low mass of 0.85kg for the thruster, which is a very good value for the mass requirements of the satellite. It also fits within an envelope of 80mm diameter by 75 mm length. These dimensions make it comfortably fit a 1U volume, if the propellant tank is not included. [13]

In terms of performance, the thruster can operate within a thrust range of 4-30mN. These values are sufficient for the maneuvers that the satellite must perform, as more thrust-intensive maneuvers are performed by the Orbiter Transfer Vehicle (OTV) (see Chapter 8). [13]

The main characteristic that decided this thruster is its high efficiency. The engine has a total specific impulse of 600 to 1400s[13]. This efficiency, among other characteristics were used to calculate the mass and volume needed for the propellant:

- Required delta-v = 1017.6 m/s
- Estimated wet mass of satellite (for the purposes of propellant-mass calculations) = 50kg
- Calculated propellant mass = 3.45kg (rounded up to 3.5kg)
- **Propellant tank mass = 2.36kg**
- Total propellant tank wet mass = 5.81kg
- Tank pressure = 150 bar
- Density of Xenon = 1.6 kg/l
- Resulting propellant volume = 2.1875 l
- **Tank volume = 2.297 l**

These calculations give out values of mass and volume that were acceptable for the desired dimensions of the satellite. Due to this combination of capable thrust and great efficiency, the "ExoTerra Halo" thruster is capable of fulfilling the requirements for this satellite.

5.7 Telecommunication (Authors: Simone Borzaga & Fiorenza Ferrante)

The Telecommunication subsystem establishes the complete pathways of data across the network, implementing a multi-hop relay architecture across four distinct communication links. This subsystem is the mission's primary enabling technology, directly fulfilling the core objective of providing global IoT connectivity across the lunar surface.

5.7.1 Design Drivers

Following are the Design Drivers for the Telecommunication Subsystem:

- **Link Closure over Multiple Distances**
  The telecom subsystem must close multiple independent communication links operating at fundamentally different distances: the lunar surface-to-constellation link (up to 1,444 km at the horizon), the intersatellite link (approximately 1,170 km between satellite on the same plane), the constellation-to-relay link (approximately 4,240 km in the selected relay orbit) and the relay-to-Earth link (up to

391,000 km). Each link imposes distinct FSPL constraints, requiring a tailored combination of transmit power, antenna gain, and modulation sensitivity to achieve the minimum required link margin across all operational scenarios.

- **Frequency Regulation and Interference Avoidance**
  All lunar communication links must comply with ITU and SFCG frequency recommendations for the lunar region, restricting S-Band operations to the 2025–2110 MHz and 2200–2290 MHz bands [5, 19]. Within these constraints, frequency allocation must further prevent interference between constellation satellites and avoid signal collisions at the relay receiver, where multiple satellites transmit simultaneously. The relay-to-Earth link must also operate following frequencies recommendations, ensure compatibility with selected ground networks and avoid interference with the S-Band constellation links.
- **Doppler Shift Tolerance**
  The orbital velocity of constellation satellites in low lunar orbit induces significant Doppler shifts on all active links. The channel bandwidth of each link must be selected to be at least four times wider than the maximum expected Doppler shift, ensuring reliable packet reception without requiring complex real-time frequency compensation hardware.
- **Protocol and Modulation for High-Density Traffic**
  The constellation must support a high number of surface users transmitting data simultaneously. Protocol and modulation must therefore be selected to handle high density traffic of concurrent users, while remaining compatible with the half-duplex constraints of the selected transceiver hardware.

5.7.2 Telecommunication Requirements

Table 19: Telecommunication Subsystem Requirements

ID	Requirement Statement
REQ-TTC-001	The telecommunication subsystem shall operate all S-Band links within the ITU and SFCG allocated lunar frequency ranges: 2025–2110 MHz and 2200–2290 MHz.
REQ-TTC-002	The telecommunication subsystem shall support bidirectional communication between constellation satellites and lunar surface assets using LoRa modulation with a minimum link margin of 2 dB at the edge of the HPBW.
REQ-TTC-003	The telecommunication subsystem shall support communication between constellation satellites via Inter-Satellite Link using LoRa modulation with a minimum link margin of 2 dB at the edge of the HPBW.
REQ-TTC-004	The telecommunication subsystem shall support bidirectional communication between constellation satellites and the relay satellite using LoRa modulation with a minimum link margin of 2 dB at the edge of the HPBW.
REQ-TTC-005	The telecommunication subsystem shall support bidirectional communication between the relay satellite and Earth using LoRa modulation with a minimum link margin of 2 dB at the edge of the HPBW.
REQ-TTC-006	The telecommunication subsystem shall receive updates and telecommands from Earth ground stations in the X-Band uplink frequency range 7190–7235 MHz.

ID	Requirement Statement
REQ-TTC-007	The telecommunication subsystem shall transmit telemetry and payload data to Earth ground stations in the X-Band downlink frequency range 8450–8500 MHz.
REQ-TTC-008	The telecommunication subsystem shall allocate a channel bandwidth for each link at least four times wider than the maximum expected Doppler shift on that link.
REQ-TTC-009	The surface-to-constellation uplink shall support concurrent reception from at least 5,000 surface users constellation-wide within a single visibility window.
REQ-TTC-010	The telecommunication subsystem shall implement a minimum channel spacing of 500 kHz between adjacent carrier frequencies.

5.7.3 Assumptions and trade-off

Assumptions

- **Link Budget Analysis**
  All link budget calculations assume a conservative system loss allocation of 3 dB to account for cable losses, connector losses, polarization mismatch, and pointing inaccuracies. This margin is applied uniformly across all communication links unless otherwise specified.
- **Worst-Case Design Margins**
  The telecommunication architecture is designed to meet all requirements under worst-case geometric conditions. Any operational scenario with more favorable conditions (e.g. shorter distances, higher antenna gain, reduced Doppler) is assumed to satisfy the link closure requirement with additional margin.
- **Component Performance Specifications**
  Performance analysis relies on typical datasheet specifications for all RF components. Variations due to thermal extremes, radiation-induced degradation, or aging are not applied at this preliminary design stage.
- **Lunar Environment**
  The telecommunication subsystem operates in the vacuum of space around the Moon. No atmospheric attenuation, ionospheric scintillation, tropospheric delay, or weather-related signal degradation is considered in the link budget analysis, as these effects are absent in the lunar environment.
- **User Terminal Compliance**
  All lunar surface users are assumed to comply with the defined transmission protocol, respecting frequency allocations, duty cycle constraints, packet size limits, and the required transmitted power specifications. Non-compliant terminals may experience degraded link quality or inability to establish communication with the constellation.

Trade-off

Relay Orbit Selection

The relay satellite orbit directly determines the feasibility of the constellation-to-relay link and the availability of the Earth connection. Three candidate orbits were evaluated:

1. **L1 Halo Orbit:** A halo orbit around the Earth-Moon L1 Lagrange point provides continuous Earth visibility. However, analysis revealed that L1 halo orbits are inherently unstable, requiring continuous station-keeping maneuvers with prohibitive propellant consumption over the 5-year mission lifetime [38]. Additionally, the long distances from the Moon would necessitate adaptive large power

and antenna gain to maintain link closure.

2. **Near Rectilinear Halo Orbit (NRHO):** NRHO architectures offer improved stability compared to L1 halos and have heritage from the Artemis program [41]. However, the highly elliptical geometry introduces extreme distance variation. Closing the S-Band LoRa link at apolune (75000 km) would require either a massive deployable reflector antenna (30 dB) on the relay satellite or reducing the LoRa data rate to gain sensitivity, severely limiting throughput and introducing network congestion.
3. **Medium Lunar Orbit (6,500 km altitude):** A circular polar orbit at 6,500 km altitude was selected as the baseline. This orbit is orbitally stable with manageable station-keeping requirements and maintains a nearly constant distance from the constellation of approximately 4,240 km, enabling the link to be closed with commercially available S-Band antenna arrays without requiring deployable structures [26]. The trade-off is that the orbit introduces periodic eclipse periods during which Earth visibility is lost. This latency is acceptable compared to the cost and complexity of the alternative architectures.

LoRa Technology for ISL Relay Link

The selection of LoRa modulation for inter-satellite communication and the constellation-to-relay link required evaluation against alternative solutions:

1. **Alternative: Different Modulation and Frequency Bands:** Standard modulation could provide higher data rates and more mature space heritage. However, implementing this solution would require the selection of a new transceiver and extensive development and the receiver sensitivity of standard FSK/PSK at comparable data rates is significantly worse than LoRa's chirp spread spectrum, increasing the required transmit power or antenna gain to close the link. Higher frequency bands recommended for lunar operations [19] were also evaluated but discarded due to increased FSPL, required transmit power and antenna gain.
2. **LoRa (Selected):** LoRa was retained for the ISL and relay links to maintain architectural consistency with the ground link, enabling the use of the same LR1121 transceiver hardware across the entire network. This reduces component count, simplifies procurement, and allows the OBDH to implement a unified communication stack. The trade-off is that LoRa's inherent low data rate constrains the maximum user capacity and introduces latency in multi-hop routing scenarios, but this was deemed acceptable given the mission's emphasis on low-power, long-range communication rather than high-speed data transfer.

Frequency Allocation Between Orbital Planes

To prevent signal interference at the relay satellite, where multiple constellation orbital planes transmit simultaneously, two multiple access strategies were evaluated:

1. **Time Division Multiple Access (TDMA):** Sequential time allocation would allow all orbital planes to share a single frequency channel, simplifying frequency coordination. However, TDMA introduces significant queuing delays when the relay satellite is simultaneously visible to satellites from multiple planes. With a maximum data rate of 5.5 kbps per LoRa channel, strict time coordination would create a bottleneck, preventing the relay from receiving data in parallel and increasing latency.
2. **Frequency Division (Selected):** Each orbital plane was assigned a unique S-Band frequency channel within the allocated 2025–2110 MHz band, separated by sufficient guard bands to prevent adjacent channel interference. This architecture allows the relay satellite to receive simultaneous transmissions from all three orbital planes using three independent LR1121 receivers connected to a common antenna via an RF splitter. While the splitter introduces a 5 dB signal loss, the frequency division approach eliminates queuing delays, enabling the relay to process the data flow three times faster.

Inter-Satellite Link Topology: Intra-Plane vs Inter-Plane

The ISL architecture must balance network connectivity with link complexity and antenna pointing requirements:

1. **Inter-Plane ISL:** A fully connected network where satellites can communicate directly with any neighbor would minimize routing hops and reduce latency. However, inter-plane ISL require cross-link antennas with continuous pointing capability, significantly increasing ADCS complexity and power consumption. Additionally, the geometry of crossing planes introduces highly variable link distances and Doppler shifts, making link closure more challenging.
2. **Intra-Plane Only (Selected):** The baseline architecture implements ISLs only between satellites within the same orbital plane (forward and backward neighbors). This allows the use of fixed-pointing directional antennas with stable link geometry, simplifying the payload and ADCS design. Data transfer is achieved by routing packets in the selected frequency along the orbital plane in the forward direction. The only cross-plane hop happens for user requests that, if needed, can reach the polar regions, where all three planes converge, and satellites can transfer data via the right plane frequency.

5.7.4 Baseline Design

Communication Link Architecture

The LICOS telecommunication architecture implements four distinct communication links, each optimized for its specific distance, data rate, and operational requirements. Table 20 summarizes the complete link budget analysis for all operational links.

Table 20: Link Budget Summary for All Communication Links

Parameter	**Surface → Const.**	**Const. → Surface**	**ISL**	**Const. → Relay**	**Relay → Const.**	**Relay → Earth**
Distance (km)	1,444	1,444	1,170	4,240	4,240	391,000
Frequency (MHz)	2,200	2,100	2,100	2,025	2,028.5	8,450
EIRP (dBm)	29	34	38.5	44	45	53
FSPL (dB)	-162.5	-161.1	-160.3	-171.1	-171.1	-222.8
Rx Gain (dBi)	9.25	4	9.25	14.75	14.25	62.7
System Loss (dB)	-3	-3	-3	-3	-3	-3
Rx Power (dBm)	-127.3	-126.1	-115.5	-115.4	-114.9	-110.1
Sensitivity (dBm)	-130	-130	-118	-118	-118	-113
Link Margin (dB)	**2.7**	**3.9**	**2.5**	**2.6**	**3.1**	**2.9**

All links meet the minimum 2 dB link margin requirement. The Tx Gain and Rx Gain values shown are composite system gains that include all component contributions: PA gain, LNA gain, BPF insertion loss, antenna edge-of-coverage loss, and RF splitter loss where applicable. The surface-constellation bidirectional link margins are achieved through the user terminal gain constraints: 29 dBi combined transmit gain and 4 dBi receive gain. The Earth-relay uplink is not shown in this table as it operates on a separate X-Band frequency (7.2 GHz) with significantly higher margin (> 50 dB) due to ground station capabilities.

LoRa Configuration Parameters

Each S-Band link is configured with specific LoRa parameters to balance sensitivity, data rate, and Doppler tolerance:

Table 21: LoRa Modulation Parameters per Link

Link	SF	BW (kHz)	CR	Sensitivity (dBm)	Data Rate (bps)
Surface → Constellation	12	250	4/5	-130	488 (LR-FHSS)
Constellation → Surface	12	250	4/5	-130	586
ISL (Intra-Plane)	7	125	4/5	-118	5,469
Constellation → Relay	7	125	4/5	-118	5,469
Relay → Constellation	7	125	4/5	-118	5,469

The bandwidth selections satisfy the Doppler tolerance requirement with positive margin. Maximum Doppler shift is approximately 1.6 km/s at 540 km altitude. For the S-Band links operating near 2.1 GHz, the maximum Doppler shift is calculated as $\Delta f = (v/c) \times f = (1600/3 \times 10^8) \times 2.1 \times 10^9 \approx 11.2$ kHz. The selected 125 kHz bandwidth for ISL and relay links ($125/4 = 31.25$ kHz > 11.2 kHz) and the 250 kHz bandwidth for ground links ($250/4 = 62.5$ kHz > 11.2 kHz) provide both large margin, ensuring reliable packet reception without requiring real-time frequency compensation.

The ground uplink uses LR-FHSS modulation to support high-density concurrent user access, while all other links use standard LoRa. The selection of SF12 for the ground link prioritizes sensitivity over data rate, enabling link closure with low-power surface assets, while SF7 is used for ISL and relay links to increase throughput and prevent network congestion.

Frequency Allocation Plan

To prevent inter-plane interference at the relay satellite and enable simultaneous multi-plane reception, each orbital plane is assigned a unique frequency channel within the allocated S-Band spectrum:

Orbital Plane	ISL (MHz)	Uplink to Relay (MHz)	Downlink to Surface (MHz)
Plane 1	2,101	2,025.5	2,100
Plane 2	2,102	2,026.5	2,099
Plane 3	2,103	2,027.5	2,098
Common Frequencies			
Surface Uplink	2,200.25 MHz (all planes)		
Relay Downlink	2,028.5 MHz (beacons to constellation)		

Figure 23: S-Band Frequency Allocation by Orbital Plane

Each plane is separated by 1 MHz guard bands (four times the size of the maximum channel bandwidth) to prevent adjacent channel interference. The relay satellite transmits coordination beacons and updates on a shared downlink broadcast frequency of 2,028.5 MHz, separate from the constellation uplink frequencies.

Constellation Satellite Telecommunication Architecture

Each constellation satellite implements three independent RF chains built around Semtech LR1121 transceivers [46], each optimized for its communication interface:

- **Ground Link Chain:** Connected to a nadir-pointing 7.5 dBi S-Band patch antenna [57], the ground chain operates in LR-FHSS mode for uplink reception (2,200.25 MHz) and standard LoRa SF12 for downlink transmission (orbital plane-specific frequency). The receive path includes a LNA (0.25 dB NF) [48] and a BPF (1 dB insertion loss) [36]. The transmit path uses a PA (+34 dBm output) [53]. A RF switch [44] toggles between receive and transmit modes.

- **ISL Chain:** Connected to a velocity-vector-pointing 7.5 dBi S-Band patch antenna for transmitting and the same antenna in the opposite direction for receiving (both tilted 15° towards the Moon for easier link). The ISL chain operates in standard LoRa SF7 mode for communication with neighbors within the orbital plane with higher data rate. The RF chain architecture mirrors the ground link (LNA, BPF, PA, switch). Frequency allocation is plane-specific to prevent cross-plane interference.
- **Relay Link Chain:** Connected to a anti-nadir-pointing 13 dBi S-Band antenna array [50], the relay chain operates in standard LoRa SF7 mode for uplink transmission to the relay satellite in the plane-specific frequency and reception of relay coordination beacons on the shared downlink band. The high-gain antenna compensates for the longer 4,240 km constellation-to-relay distance.

Relay Satellite Telecommunication Architecture

The relay satellite implements a dual-band architecture to aggregate S-Band traffic from the constellation and relay it to Earth via X-Band:

- **S-Band Array:** Three Semtech LR1121 receivers [46] are connected to a common 18 dBi S-Band antenna array [50] (Space Inventor 4×1 configuration) via a 3-way RF splitter. Each receiver is tuned to one orbital plane frequency (2,025 MHz, 2,055 MHz, 2,085 MHz), enabling simultaneous reception from all three planes without time-division between planes. The splitter introduces approximately 5 dB insertion loss, which is compensated by the high-gain antenna and LNA [48]. A single BPF [36] is placed at the antenna port. One of LR1121 transceivers at times is used to broadcast relay coordination beacons, visibility windows, and telecommands to the constellation on the shared downlink band. Operates at reduced duty cycle (<10%) to maximize receive time.
- **X-Band Subsystem:** An IMT X-Band transponder [22] (+41 dBm output power) is connected to a 15 dBi X-Band patch antenna [4] with a dedicated X-Band BPF [37]. The subsystem receives updates and commands from Earth ground stations (7,190–7,235 MHz) at 4 kbps and transmits aggregated telemetry and payload data (8,450–8,500 MHz) at 800 kbps using QPSK modulation. The high data rate will enable the relay to dump the entire 69-minute eclipse buffer (83.2 Mb) in approximately 104 seconds upon Earth line-of-sight re-acquisition.

The components of the Constellation and of the Relay together allow the network to achieve the link margins shown in Table 20 and to send the data from end to end.

User Terminal Requirements

To close the surface-to-constellation link, lunar surface users must comply with the following hardware and protocol constraints:

Table 22: User Terminal Requirements for Network Access

Parameter	Requirement
Transceiver	Semtech LR1121 or future S-Band LoRa-compatible chip
Transmit Frequency	2,200.25 MHz
Receive Frequency	Plane-specific: 2,025.5 / 2,026.5 / 2,027.5 MHz
Transmit Chain Gain	29 dB minimum
Receive Chain Gain	4 dB minimum
Modulation	LR-FHSS uplink, LoRa SF12 downlink
Protocol	CSP 2.x with 6-byte header
Packet Size	User data ≤36 bytes, Requests ≤18 bytes
Transmission Interval	≥90 seconds between telemetry packets

These constraints distribute the link budget responsibility between the space and ground segments. User terminals must provide sufficient gain to compensate for the 1,444 km worst-case distance, while

the constellation maintains medium-gain fixed antennas to avoid difficult pointing requirements and allow every user on the footprint to be received.

5.8 Attitude Determination and Control - Author: Fiorenza Ferrante

(ADCS) is a mission-critical subsystem responsible for estimating the spacecraft's orientation in space and applying the necessary torques to achieve and maintain a desired pointing state. For the proposed lunar IoT constellation, ADCS is a primary driver of overall mission feasibility and network performance.

5.8.1 Design Drivers

Following are the Subsystem Design Drivers:

- **Nominal Attitude Acquisition & Link Pointing**
  The primary operational driver for the ADCS is to maintain precise 3-axis stabilization to support the communication payload. The system must ensure continuous nadir-pointing for surface IoT coverage and constellation-relay communications, and continuous velocity pointing for ISL. The required pointing accuracy and maximum allowable jitter are strictly dictated by the HPBW of the selected antennas. Any deviation beyond these limits will result in pointing losses that compromise the link budget closure.
- **Power Maximization & Sun-Tracking**
  To support the high-power requirements necessary for Propulsion and Payload, the ADCS must maximize the efficiency of the spacecraft's power generation. This requires the implementation of dedicated sensors and, if necessary, continuous steering capabilities.
- **Lunar Environment & Hardware Constraints**
  The physical realities of the lunar orbital environment strictly dictate the selection of ADCS sensors and actuators. Unlike Low Earth Orbit missions, the Moon lacks a global magnetic field and an atmosphere. Consequently, standard terrestrial components such as magnetorquers for momentum dumping or atmosphere sensitive horizon sensors are entirely ineffective. The subsystem architecture is therefore forced to rely exclusively on celestial references or Moon tailored horizon sensors for attitude determination, and a combination of Reaction Wheels and Thrusters for momentum exchange and desaturation.

5.8.2 Requirements

Table 23: ADCS Subsystem Requirements

ID	Requirement Statement
REQ-ADCS-001	The ADCS shall maintain nadir-pointing attitude with a 3-sigma pointing accuracy of $\pm 1.0^\circ$ for surface and relay communication operations.
REQ-ADCS-002	The ADCS shall maintain velocity-vector pointing attitude with a 3-sigma pointing accuracy of $\pm 1.0^\circ$ for Inter-Satellite Link operations.
REQ-ADCS-003	The ADCS shall limit attitude jitter to less than $0.01^\circ/s$ during all communication operations.
REQ-ADCS-004	The ADCS shall provide 3-axis attitude knowledge with an accuracy of $\pm 0.5^\circ$ (3-sigma) during nominal operations.

ID	Requirement Statement
REQ-ADCS-005	The ADCS shall orient the solar arrays to maintain Sun incidence angle within $\pm 20^\circ$ of normal during nominal operations to maximize power generation.
REQ-ADCS-006	The ADCS shall acquire and track the Sun vector with an accuracy of $\pm 2^\circ$ for optimal solar power pointing.
REQ-ADCS-007	The ADCS shall acquire nominal 3-axis stabilized attitude within 3 hours of orbital insertion.
REQ-ADCS-008	The ADCS shall perform reaction wheel desaturation maneuvers using thrusters when stored angular momentum exceeds 90% of the maximum wheel capacity.
REQ-ADCS-009	The ADCS shall maintain the same required attitude knowledge and pointing accuracy during orbital eclipse periods.

5.8.3 Assumptions and trade-off

Assumptions

- The exact statistical noise metrics (e.g. thrust variance) are not published in the thrusters datasheet [54]. Therefore, a normally distributed thrust error profile is assumed, characterized by a 3σ deviation of 0.6 mN along the three axis.
- For attitude calculations and simulation, the moment arm defined as the distance from the thrust vector application point (nozzle) to the spacecraft CoM is assumed to be the same for all five thrusters.
- Thrusters actuations are modeled as ideal step functions, assuming the system delivers nominal thrust instantaneously and continuously during all commanded firing windows.
- All components are considered to operate at their typical performance values and they are considered to be compatible with each other and with the rest of the satellite.
- The analysis assumes that the Power System and Thermal Control System are adequately sized to handle the peak power loads and thermal dissipation requirements of the ADCS hardware.
- The ADCS simulation and performance analysis is conducted for a single representative spacecraft. The results and validated performance margins are assumed to be applicable to all identical satellites within the constellation.

Trade-offs

Actuator Selection

The choice of primary attitude control actuators directly impacts system complexity, mass, and pointing performance:

1. **Control Moment Gyroscopes (CMGs):** CMGs provide extremely high torque output and precise control, making them ideal for agile platforms requiring frequent large-angle slews. However, CMG systems are too heavy and complex. Additionally, the precision offered by CMGs (sub-arcsecond pointing) far exceeds the $\pm 1^\circ$ dedicated requirement, representing significant over-design and wasted mass budget.
2. **Thrusters Only:** Using thrusters as attitude control actuators would eliminate the need for reaction wheels, reducing hardware complexity and cost. However, thruster-only control suffers from several critical drawbacks: minimum impulse bit limitations prevent fine pointing (typical precision ± 5–10°), propellant consumption for continuous attitude maintenance would deplete reserves within

months, and the thrust level is insufficient to provide rapid attitude control for a 50 kg spacecraft.
3. **Reaction Wheels with Thruster Desaturation:** Commercial off the shelf reaction wheels provide sufficient torque to maintain the required pointing accuracy while offering lower mass, higher reliability and significantly lower cost. A four-wheel pyramid configuration was selected to provide full three-axis control with single-wheel failure redundancy. Reaction wheels need to be coupled with thrusters for desaturation. In this case, thrusters are only used periodically, minimizing propellant consumption to sustainable levels over the 5 year mission.

Sensor Selection In the absence of a lunar magnetic field, attitude determination must rely on celestial references:

1. **Sun Sensor + Moon Horizon Sensor + Gyroscopes:** A multi-sensor fusion approach combining analog sun sensors, Moon horizon sensor for nadir reference, and gyroscopes for rate sensing could achieve $\pm 0.5^\circ$ attitude knowledge at low cost and power. However, this architecture requires complex sensor fusion algorithms and provides degraded performance during eclipse periods when sun sensors are inactive. The horizon sensor's accuracy is also sensitive to lunar terrain variations and albedo changes, introducing additional measurement uncertainty that must be filtered out.
2. **Star Tracker:** A star tracker provides absolute three-axis attitude knowledge by matching observed star patterns against an onboard catalog, achieving higher accuracy. While the precision significantly exceeds the $\pm 1^\circ$ requirement, the star tracker eliminates sensor fusion complexity and provides robust attitude determination during eclipse periods. The higher cost and power were accepted given the critical nature of attitude knowledge for maintaining communication links and the 5 year operational lifetime where sensor reliability is necessary. Sun sensors are selected nevertheless because the solar panels pointing needs.

ADCS Simulation Software Selection

The ADCS simulation must validate both actuators and sensors performance through software implementation:

1. **Python/MATLAB Scripts:** Custom scripting in Python or MATLAB provides flexibility, but requires manual implementation of all dynamics, sensor models, and control algorithms.
2. **Simulink:** Simulink's block-diagram environment provides two key advantages. First, the Aerospace Blockset includes pre-validated models for quaternion algebra, coordinate transformations, and spacecraft dynamics, eliminating errors in manual implementation. Second, and most importantly, the Simulink blocks directly represent the flight software architecture, each control block maps to a software module that will execute on the OBC.

Solar Array Configuration: Rotating vs Body-Mounted

The solar array architecture directly impacts power generation efficiency and ADCS complexity:

1. **Body-Mounted Fixed Arrays:** Solar panels rigidly mounted to the spacecraft body eliminate all mechanical articulation, reducing mass, cost, and simplify the ADCS control. However, the ADCS must prioritize antennas pointing located in four faces of the satellite, preventing the spacecraft from orienting toward the Sun for optimal power generation. Since the solar incidence angle varies significantly throughout the orbit, oversized arrays would be required, canceling out the mass savings from eliminating articulation mechanisms.
2. **Single-Axis Rotating Solar Arrays:** Solar panels that track the Sun maximize power generation across all orbital phases. However, rotating mechanisms add mass, require continuous ADCS sun-tracking computation and generate disturbance torques during rotation that must be compensated by the reaction wheels. Nevertheless, this configuration was selected as final because of the orbit

dynamics, causing long periods of eclipse for fixed arrays.

5.8.4 Baseline Design

The ADCS baseline design is comprised of the following components:

Sensors:

> **2 ST200 Star Trackers from Hyperion Technologies**[21]: Two units are selected both for single-failure redundancy and to ensure continuous attitude knowledge throughout the lunar year: as the Sun angle changes with the orbital plane's seasonal variation, one star tracker may be temporarily blinded by sunlight entering its field of view while the other maintains lock on the star field and their operational roles alternate as solar geometry evolves.

> **6 SS200 Sun Sensors from AAC Clyde Space**[2]: Placed one on each face of the spacecraft, they fulfill two functions: providing attitude reference during detumbling operations, when the star tracker cannot acquire lock on the star field and providing the position vector pointing towards the Sun, feeding it into the OBC[49] which will handle solar panels rotation together with SADA[9].

> **1 BMI085 Inertial Measurement Unit from Bosch Sensortec**[8]: Provides three-axis gyroscope and accelerometer measurements for angular rate sensing and is used in the attitude estimation and validation.

Actuators:

> **4 RW1 Reaction Wheels from Blue Canyon Technologies**[7]: Arranged in a pyramidal configuration to ensure full three-axis control with single-wheel failure tolerance. They provide sufficient torque and momentum storage capacity to maintain pointing accuracy throughout the mission while operating continuously during nominal operations.

> **5 Cold Gas Thrusters in a VACCO Propulsion System**[54]: Provides thrust for reaction wheel desaturation and emergency detumbling. Thruster placement is optimized to align thrust vectors through the spacecraft center of mass.

ADCS Computer:

> **1 OBC-P3 from Space Inventor**[49]: Serves as the ADCS processor, executing attitude determination and algorithms on its dual Cortex-M7 cores.

ADCS Simulation:

To transition from theoretical analysis to a practical assessment for the verification of the subsystem requirements, the selected hardware specifications were integrated into a custom ADCS simulation developed within the MATLAB/Simulink environment. Replacing generic spacecraft assumptions with targeted hardware parameters allows for a more accurate performance analysis. The logical flow and architecture of the simulation are structured as follows (Figure 24):

It starts from the Spacecraft Dynamics block, which returns the effective position of the satellite at any given epoch. In this block, spacecraft specifications are set: mass, inertia tensor, orbit parameters and initial position of the spacecraft (to verify detumbling capabilities). The Spacecraft Dynamics block, outputs among other things the Quaternion from the ICRF to the Body frame (q_{icrf2b}), which is the mathematical representation of the satellite's 3D orientation (attitude) relative to the International Celestial Reference Frame, an Inertial Frame with axes locked to distant, stationary background stars. This acts exactly as a star tracker, and can be fed straight into the star tracker noise model.

The noise model logic for this sensor follows this path: Gaussian Noise tailored on the star tracker datasheet specifications (3σ 0.055° roll, 0.0083° pitch and yaw[21]) → deg2rad → ZYX Rotation to convert the three noise angles into a noise quaternion → Quaternion multiplication to apply the noise

→ Quaternion normalize to obtain a unit quaternion representing a pure 3D rotation → Quaternion conjugate to invert the rotation from q_{icrf2b} to q_{b2icrf}.

The noisy q_{b2icrf} now inputs the Attitude Profile block along with position and velocity straight from the Spacecraft Dynamics block. The Attitude Profile block, calculates the orientation of the Local Vertical Local Horizontal frame in 3D space, it applies the primary and secondary body-frame constraints set by the user and it solves for how the 3D orientation of the satellite must be to satisfy the constraints. This block's output is the quaternion q_{tgt_b}, which represents the ideal commanded orientation of the spacecraft's body frame relative to the inertial ICRF at any given simulation time step.

q_{tgt_b} goes into the Attitude Controller block, which contains a Rotation XYZ to convert the quaternion into Euler Angles (Roll, Pitch, Yaw), a PID Controller and outputs the torque (M, a 3-element vector measured in Nm), which quantifies of how much the satellite needs to twist to fix the pointing error.

The torque M follows two separate paths: RW path and Thrusters path. The first one consist in a Saturation block ($\pm 0.06Nm$ [7]) and a Random Gaussian Noise block. The former flattens the output strictly to the RW's maximum capability in case the Attitude Controller block asked for more Momentum, this ensures the simulation doesn't perform maneuvers that the real satellite couldn't actually perform. The Noise block acts as the RW jitter, and it's tailored with the informations found in the component's datasheet ([7]). The Thrusters path is also divided into two paths. The first one is comprised of just a Sign block, which outputs +1 or -1 depending on which direction the thrusters needs to fire, and 0 if no torque is commanded. The second path consists of an Abs block to evaluate the pure magnitude and a Relay block, which is multiplied by a Random Gaussian Noise block, to make sure that the noise is taken into account only when the thrusters are firing. The Relay block acts like a valve, if the commanded magnitude crosses the Switch On threshold, it outputs 1 (Valve Open), and it stays open until the command drops below the Switch Off threshold, and ouputs 0 (Valve Closed). This makes sure that the thrusters activates just when the RWs are saturated (Switch On threshold at 90% of the RW saturation $= 0.054Nm$ [7]). The Random Gaussian Noise block takes as variance:

$$\sigma_F = \frac{0.0006N}{3} = 0.0002N \rightarrow \sigma_F^2 = 4 \cdot 10^{-8} N^2 \rightarrow \sigma_M^2 = \sigma_F^2 \cdot (0.226m)^2 = 2.04 \cdot 10^{-9} N^2 m^2$$

where 0.0006N comes from the assumptions and 0.226m is the distance of the thruster's nozzle from CoM.

The output product of these two paths goes into a gain block which fires with a nominal thrust of $10mN \cdot 0.226m = 2.26 \cdot 10^{-3} Nm$[54]. The RW block and the Thruster block are added together, assembling the input torque of the Spacecraft Dynamics block and closing the simulation loop.

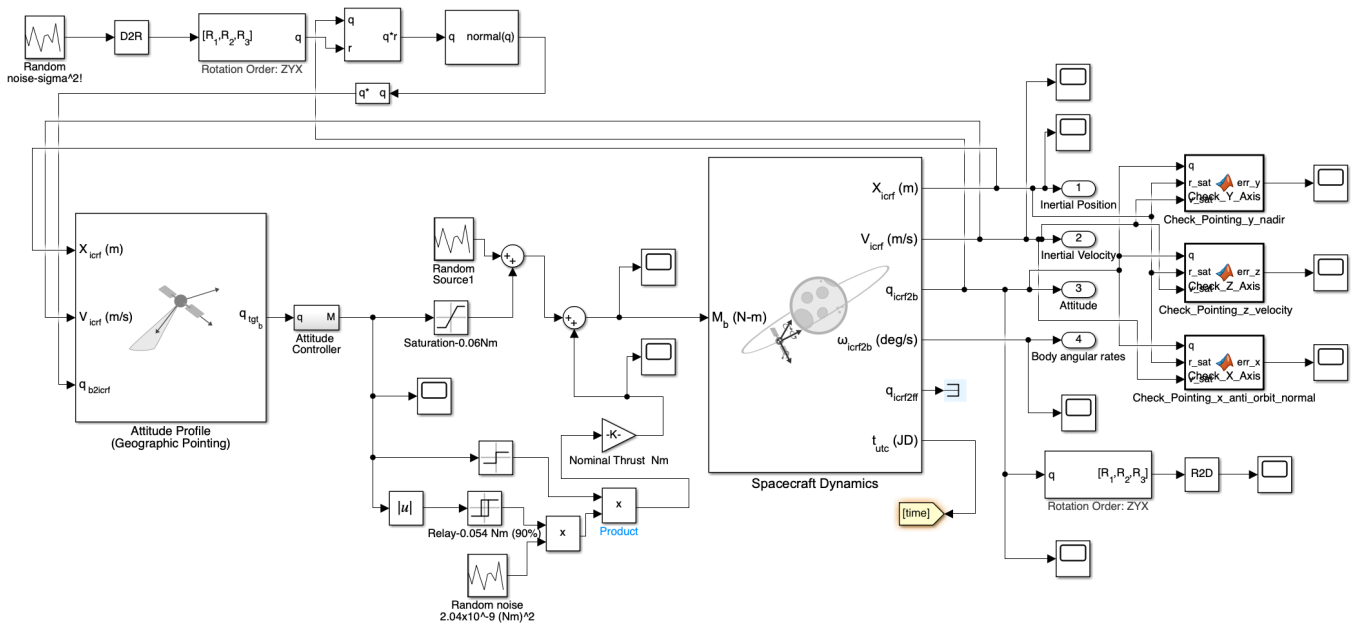

Figure 24: Simulink ADCS simulation.

Results:

Table 24: Antenna Beamwidth Specifications Across LICOS Network

Platform	**Antenna Gain**	**Beamwidth (HPBW)**	**Application**
Constellation Satellite			
7.5 dBi S-Band Patch	7.5 dBi	80°	Ground Link
7.5 dBi S-Band Patch	7.5 dBi	80°	ISL
13 dBi S-Band Patch	13 dBi	40° × 40°	Relay Link
Relay Satellite			
18 dBi S-Band Array	18 dBi	13° × 40°	Constellation Link
15 dBi X-Band Patch	15 dBi	20°	Earth Link

Actuators and Sensor Influence, Figure 25
The observed high-frequency oscillations in the angular rate telemetry ($t > 200$s) are attributed to the superposition of two primary sources: Reaction Wheel Jitter and Sensor Noise. The presence of discrete spikes in the angular rate plot confirms the operational logic of the cold gas thrusters, which provide impulsive restorative torques when the attitude error exceeds the defined relay thresholds.

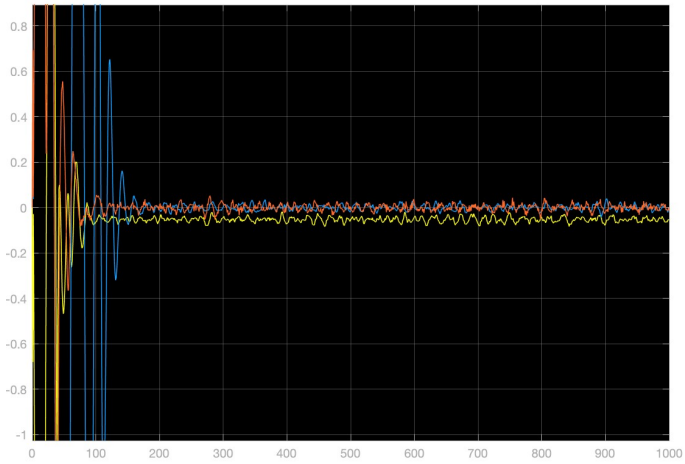

Figure 25: Satellite angular rates in y axis (deg/s) vs. time in x axis (s).

Maneuver Convergence and Stability, Figure 26
The spacecraft's transition from the initial toumbling state to a stable Nadir-pointing orientation is analyzed across three distinct phases:

- **Detumbling Phase** ($0 < t < 50$**s):** The PID controller commands maximum torque (saturated) to arrest high initial angular rates. This is evidenced by the large-magnitude oscillations in the angular rate telemetry.
- **Slew and Acquisition** ($50 < t < 150$**s):** The attitude error plots for the X (Anti Orbit Normal), Y (Nadir), and Z (Velocity) axes show a synchronized decay. The Y-axis (Primary Constraint) exhibits the fastest convergence, while the X and Z axes show minor coupling as the secondary constraint is resolved.
- **Steady-State Pointing** ($t > 150$**s):** The controller successfully maintains the Local Vertical Local Horizontal (LVLH) frame. The sawtooth behavior observed in the quaternion telemetry is consistent with a Nadir-locked body rotating at the orbital mean motion.

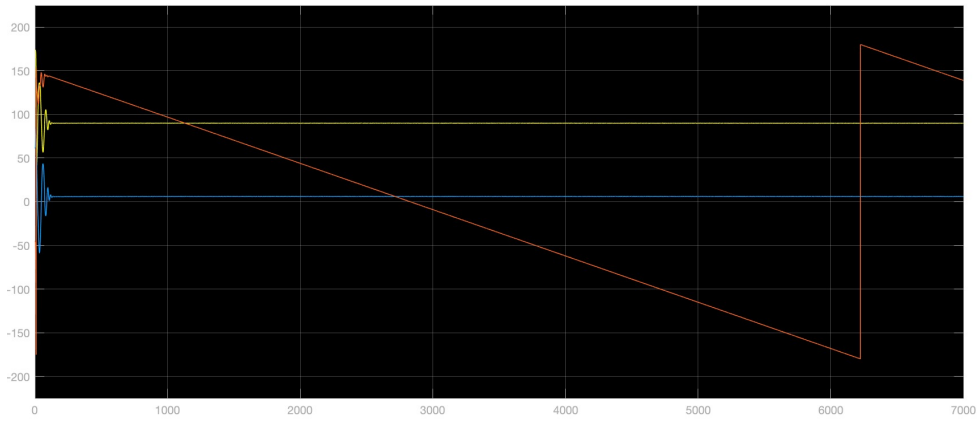

Figure 26: Satellite Attitude in y axis (deg) vs. time in x axis (s).

Pointing Performance Summary, Figures 27,28
The final steady-state performance is reached in less than $\sim 200s$, pointing results are summarized in Table 25.

Table 25: Steady-State Attitude Error Performance

Axis	**Reference Vector**	**Steady-State Error (RMS)**
Y Axis(Primary)	Lunar Nadir	$< 0.15°$
Z Axis (Secondary)	Velocity Vector	$< 0.50°$
X Axis (Tertiary)	Anti Orbit Normal	$< 0.50°$

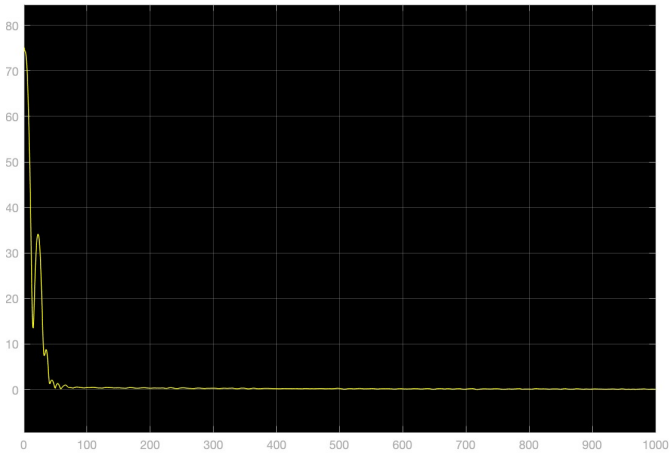

Figure 27: Y axis pointing error (deg) vs. time (s).

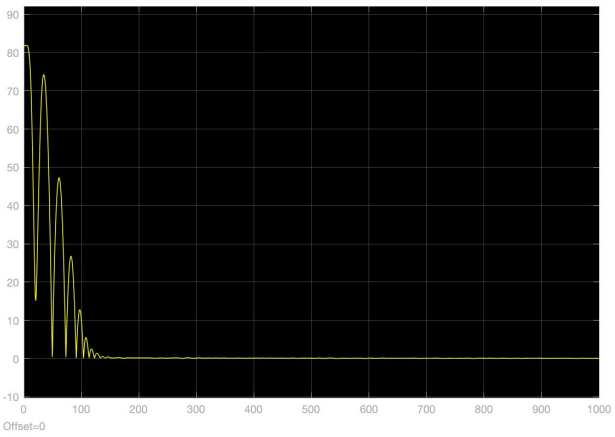

(a) X axis pointing error (deg) vs. time (s).

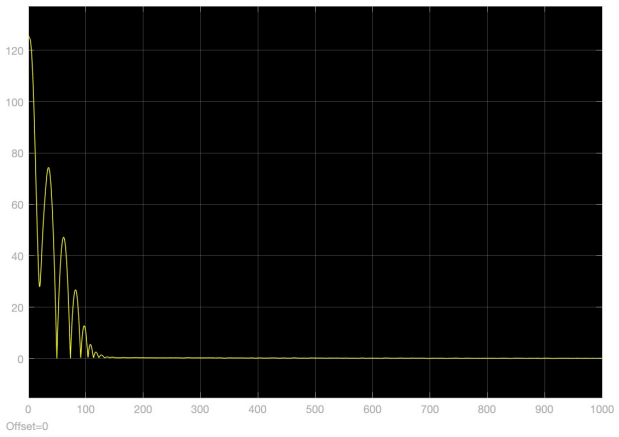

(b) Z axis pointing error (deg) vs. time (s).

Figure 28

5.9 On-Board Data Handling - Author: Simone Borzaga

The OBDH subsystem serves as the central data management system of the lunar IoT constellation, coordinating communication between lunar surface users, constellation satellites, the relay satellite, and Earth ground stations.

5.9.1 Design Drivers

The OBDH subsystem design is shaped by the unique challenges of establishing a lunar IoT network with distributed ground users, multi-hop architecture, payload characteristics, performance goals and

the lunar operational environment. The key drivers are:

• **Multi-Hop Communication Architecture**

The architecture requires the OBDH to manage data aggregation, packet routing, and protocol handling across multiple interfaces operating on different frequency bands and data rates. The constellation must coordinate data flow from hundreds of independent IoT assets on the ground, relay information between satellites via Inter-Satellite Link, and aggregate traffic for transmission to the relay satellite, which then forwards data to Earth ground stations.

• **LoRa Half-Duplex Constraints and Link Closure**

The selected LoRa transceiver technology operates in half-duplex mode, meaning each radio can only transmit or receive at any given time [47]. The OBDH must implement time-division strategies to coordinate reception from ground IoT devices, inter-satellite communication, and relay transmission without signal collisions. Additionally, the protocol must minimize the header to align with LoRa's small data optimization, ensuring sufficient link margins and reliable delivery for all traffic types.

• **High User Capacity and Low Latency**

The lunar IoT network must support the anticipated lunar missions over the next decade, accommodating a growing number of assets including rovers, habitats, scientific instruments, and astronaut suits transmitting periodic sensor telemetry and interactive data requests. End-to-end latency from lunar surface to Earth must be minimized to enable near-real-time monitoring applications, while user-to-user request processing must occur within the minute to support interactive IoT services. These performance requirements drive the need for efficient packet routing algorithms, priority scheduling and a communication protocol with sufficient address space to accommodate future network growth.

• **Autonomous Operation and Data Buffering**

The OBDH must ensure continuous system operation during ground communication outages by maintaining time-tagged command sequences for station-keeping in storage, triggering their release to the satellite bus at the specific epoch. Sufficient memory must be provided to buffer user IoT data for interactive request fulfillment, host user authorization databases and maintain system logs. Furthermore, strict clock synchronization is mandatory to maintain the alignment of time allocation and guarantee the accuracy of the command schedule.

• **Radiation Tolerance and Network Security**

The harsh radiation environment in lunar orbit requires fault-tolerant architectures including redundant firmware storage, memory scrubbing routines, and autonomous error recovery mechanisms to mitigate radiation-induced bit errors and component failures. Additionally, the nature of the lunar IoT network, where any LoRa-enabled device can potentially request data, necessitates cryptographic authentication for user data requests to prevent unauthorized access to sensitive information.

5.9.2 OBDH Requirements

Based on these drivers, the subsystem requirements are defined in Table 26.

Table 26: OBDH Subsystem Requirements

ID	Requirement
REQ-OBDH-001	The OBDH shall manage concurrent data traffic between all communication interfaces without data loss.
REQ-OBDH-002	The OBDH shall forward received data packets to the next link interface within 5 seconds of reception.

ID	Requirement
REQ-OBDH-003	The OBDH shall implement a communication protocol supporting at least 5,000 unique lunar surface user IDs.
REQ-OBDH-004	The OBDH shall deliver lunar surface data to Earth with end-to-end latency not exceeding 1 minute under clear Earth visibility conditions.
REQ-OBDH-005	The OBDH shall process user-to-user data requests with latency not exceeding 1 minute.
REQ-OBDH-006	The OBDH shall support at least 150 simultaneous users per satellite.
REQ-OBDH-007	The OBDH shall prioritize in order: telecommands, user requests, user data, satellite telemetry.
REQ-OBDH-008	The OBDH shall authenticate all user requests prior to execution.
REQ-OBDH-009	The OBDH shall provide sufficient storage to buffer at least 5,000 data packets.
REQ-OBDH-010	The OBDH shall provide at least 1 GB memory storage for flight software, user authorization database, and system logs.
REQ-OBDH-011	The OBDH shall implement error detection on all transmitted data packets.
REQ-OBDH-012	The OBDH shall maintain at least 3 copies of flight firmware in non-volatile storage.
REQ-OBDH-013	The OBDH shall coordinate multiple access control across all radio interfaces to prevent signal collisions.
REQ-OBDH-014	The relay satellite OBDH shall be capable of aggregating at least 50 MB of data from multiple constellation satellites.
REQ-OBDH-015	The OBDH shall enforce a maximum user transmission duty cycle of 10

5.9.3 Assumptions and trade-off

Assumptions

The OBDH baseline design is based on the following assumptions:

• **Hardware and Component Compatibility**

Commercial off-the-shelf components including the OBC-P3 and LR1121 transceiver meet datasheet typical specifications and are compatible with the satellite bus interfaces. The OBDH receives stable regulated voltage from the power subsystem and operates within temperature ranges throughout all mission phases.

• **Communication Reliability**

All transmitted messages (e.g. relay beacons, telecommands, user data) are received with sufficient reliability to maintain network operations. The clock drift remains within ±1.0 ppm specification, requiring ground re-synchronization no more than once per month [49]. Ground station contact occurs with sufficient frequency to provide necessary synchronizations and firmware updates.

• **User Compliance**

Lunar surface users comply with the defined transmission protocol, respecting duty cycle constraints and packet size limits. Data packages from users do not exceed the maximum payload size defined by the system architecture. Users do not intentionally interfere with constellation communications beyond

what cryptographic authentication can mitigate.

Trade-off

• Communication Protocol Selection

The OBDH requires a lightweight packet routing protocol with minimal header, sufficient address space to support thousands of lunar IoT devices, and compatibility with LoRa's constrained data rates. The options considered are stated in Table 27.

Table 27: Communication Protocol Trade Study Comparison

Protocol	Header Size	Address Space	Standard	Space Heritage	Complexity
LoRaWAN [30]	13 bytes	32-bit	ITU standard	Limited	High
Meshtastic [34]	24-32 bytes	32-bit	Open-source	None	Medium
Custom	Flexible	Customizable	None	None	Medium
MAVLink v2 [33] [32]	14 bytes	8-bit	Industry	Drone/rover	Medium
CSP 1.0 [29]	4 bytes	5-bit	ECSS	CubeSat	Low
CSP 2.x[29]	6 bytes	14-bit	ECSS	CubeSat	Low

LoRaWAN was initially attractive due to its terrestrial IoT maturity, but the 13-byte header represents a large overhead on 30-byte payloads, and its network server architecture is incompatible with the store-and-forward relay model [30]. MAVLink is widely used in robotics but optimized for high-bandwidth vehicular telemetry rather than low-power sensor networks, with header sizes comparable to LoRaWAN [33]. Custom protocols offer maximum flexibility but lack standardization, complicate interoperability with future lunar infrastructure, and require extensive validation effort.

Cubesat Space Protocol emerged as the optimal choice. Initially developed for inter-CubeSat communication, CSP is explicitly designed for small-packet, low-power space networks and has ECSS heritage. CSP 1.0 has a 5-bit addressing (32 IDs), insufficient for the anticipated user growth, but CSP 2.x extends this to 14-bit (16,384 unique IDs) while maintaining a compact 6-byte header. The protocol provides built-in priority levels for telecommand/telemetry/requests differentiation and supports connectionless data transmission suitable for LoRa's half-duplex constraints [29].

• Multiple User Access Control: TDMA vs LR-FHSS

The lunar IoT constellation requires a multiple access control strategy for the ground uplink (lunar surface users → constellation satellites) that supports the required user capacity while maintaining compatibility with the CSP 2.x protocol and LoRa's half-duplex constraints.

Option 1 - TDMA: Initial analysis using standard LoRa modulation (SF12, BW = 250 kHz, CR = 4/5) revealed a fundamental capacity constraint. The time-on-air for a 36-byte CSP packet is approximately 0.9 seconds [46]. In a strict time-division multiple access (TDMA) scheme, each user requires two transmission slots: a telemetry uplink slot and a request slot. If users transmit for example every 5 minutes (300 seconds), the maximum user capacity per satellite is:

$$N_{\text{users, TDMA}} = \frac{T_{\text{cycle}}}{T_{\text{telemetry}} + T_{\text{request}}} = \frac{300 \text{ s}}{0.82 \text{ s} + 0.82 \text{ s}} \approx 183 \text{ users} \tag{9}$$

This calculation assumes perfect scheduling with no guard intervals or overhead. In practice, guard

times between slots (typically 10/15%) reduce capacity to approximately 160 users per satellite. While this marginally satisfies the user capacity requirement, it provides minimal margin and limits the constellation's scalability to support growing mission demands.

Option 2 - LR-FHSS Modulation: Long Range Frequency Hopping Spread Spectrum (LR-FHSS) is a modulation scheme supported by the LR1121 transceiver that addresses the user capacity limitation through intra-packet frequency hopping [46]. Unlike standard LoRa, which transmits a packet on a single frequency, LR-FHSS spreads the packet content across multiple pseudo-random frequencies within the allocated bandwidth. This technique "provides improved capacity and an even longer range than LoRa" and offers "even better robustness in the presence of interferences" by enabling concurrent transmissions without strict time-slot coordination [46].

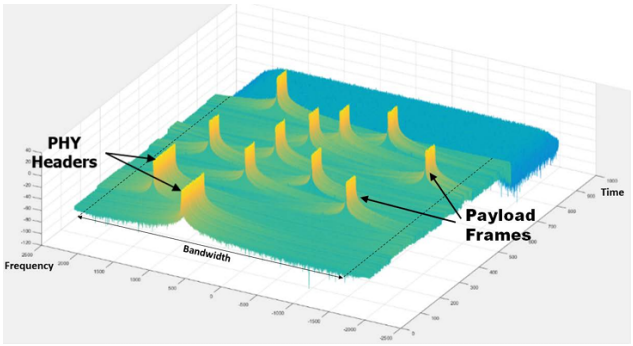

Figure 29: LR-FHSS Spectral Plot Example

The maximum number of users per satellite supported by LR-FHSS can be estimated by analyzing the available spectral resources versus user demand. The total data throughput capacity is determined by the satellite's visibility time, available bandwidth, and modulation spectral efficiency. Dividing this capacity by each user's data requirement yields the maximum supportable user count:

$$N_{\text{users}} = \frac{T_{\text{visible}} \times BW_{\text{total}} \times \eta_{\text{spec}}}{L_{\text{packet}} \times N_{\text{daily\_msgs}}} \tag{10}$$

where T_{visible} is the satellite visibility time per day, BW_{total} is the total available bandwidth, η_{spec} is the spectral efficiency of LR-FHSS, L_{packet} is the message size, and $N_{\text{daily\_msgs}}$ is the number of messages each user sends per day. For the lunar IoT ground uplink, substituting $T_{\text{visible}} \approx 86,400$ s/day, $BW_{\text{total}} = 250,000$ Hz, $\eta_{\text{spec}} \approx 0.5$ bits/s/Hz [46], $L_{\text{packet}} = 288$ bits, and $N_{\text{daily\_msgs}} = 288$ messages/day yields:

$$N_{\text{users, LR-FHSS}} = \frac{86,400 \times 250,000 \times 0.5}{288 \times 288} \approx 13,020 \text{ users} \tag{11}$$

This calculation provides a theoretical upper bound assuming ideal channel utilization. Practical capacity will be reduced by collision probability and guard intervals, but remains orders of magnitude higher than TDMA capacity.

However, the ultimate constraint is set by the CSP 2.x addressing scheme, which provides 14-bit node addresses (16,384 unique IDs for users and nodes). Therefore, while LR-FHSS modulation enables high spectral efficiency, the practical limit is 16,346 users constellation-wide, distributed across all satellites based on geographic coverage and demand.

- **On-Board Computer Selection**

The lunar IoT constellation requires an On-Board Computer capable of managing concurrent data flows across three communication interfaces (Ground, ISL, Relay), buffering a high number of packets in the storage, and executing time-tagged commands autonomously. This trade study evaluates the selection between discrete components versus different integrated OBC solutions.

The baseline architecture initially specified discrete commercial components to minimize cost and maximize flexibility:

- **Microcontroller:** STM32H743/753 (ARM Cortex-M7, 480 MHz, 1 MB Flash, 1 MB RAM) [51] for data routing between three LR1121 transceivers and RAM buffering
- **External Flash Memory:** Winbond W25Q128JV (128 Mbit NOR Flash) [56] for user authorization database, firmware storage, and system logs
- **Real-Time Clock:** External 32.768 kHz crystal oscillator [3] for time-tagged command execution

This architecture offered modularity and low component cost but was discarded following preliminary data flow analysis. The single-core microcontroller created a processing bottleneck when handling three simultaneous LoRa transceivers, risking packet loss during high-traffic intervals. Furthermore, the 1 MB internal RAM was insufficient to buffer the required data, and the reliance on custom firmware development introduced schedule risks compared to flight-proven integrated solutions.

On the other hand, integrated on-board computers provide flight-proven platforms with pre-validated hardware, radiation-tolerant designs, and heritage software stacks. The following OBC options were evaluated:

Table 28: On-Board Computer Selection Comparison

Criterion	**Discrete Comp.**	**OBC-P3**	**NanoMind Z7000**	**ISIS-OBC**
Processing Power	480 MHz single-core	300 MHz dual Cortex-M7	800 MHz dual Cortex-A9	400 MHz ARM9
RAM Capacity	1 MB	384 kB x 2	1 GB	64 MB
Non-Volatile Storage	128 Mbit	64 GB x 2	32 GB	4 GB
Interfaces	Custom	I2C, SPI, UART, CAN	I2C, SPI, UART, CAN	I2C, SPI, UART
Space Heritage	None	CubeSat missions	100+ missions	CubeSat missions
Radiation Tolerance	Commercial-grade	Rad-tested EEE parts	SEU/SEL tolerant	Radiation-tested
Power Consumption	∼500 mW	∼1 W	∼2.3 W	∼400 mW
Mass	∼50 g	120 g	77 g	100 g
Cost (relative)	Low	Medium	High	Medium

The NanoMind Z7000 was rejected due to higher cost, increased power consumption, and unnecessary FPGA complexity for this application, while the ISIS-OBC lacks the dual-module redundancy architecture required for mission-critical OBDH operations. [16, 23]

The OBC-P3 from Space Inventor was selected as the baseline on-board computer for both constellation and relay satellites. The dual-module architecture with two independent ARM Cortex-M7 processors (300 MHz each) provides hardware redundancy for mission-critical operations and sufficient

processing capability to manage concurrent LoRa interfaces. Each module has 384 kB SRAM and 64 GB storage, with the large non-volatile storage accommodating firmware redundancy, user authorization databases, network maps and extensive system logs. [49]

5.9.4 Baseline Design

Based on the trade-off analysis and system requirements, the OBDH baseline design is defined as follows:

• **OBC Architecture and Functions**

The selected Space Inventor OBC-P3 serves as a highly integrated central processing unit that consolidates both OBDH and ADCS functionalities, thereby minimizing system mass and complexity while ensuring robust performance. Powered by dual ARM Cortex-M7 processors running at 300 MHz, the OBC ensures sufficient computational throughput to handle concurrent mission-critical operations without processing bottlenecks. This processing capability enables the unit to perform demodulation of complex LR-FHSS signals and real-time execution of attitude control loops, while simultaneously managing data routing and protocol encapsulation. Crucially, the unit integrates a clock to synchronize constellation timing and Time-Division windows. However, to maintain the strict timing accuracy required for these network operations, the on-board reference requires monthly synchronization commands from Earth to correct for natural oscillator drift.

Moreover, the 64 GB OBC memory is partitioned to support:

- **Firmware Redundancy:** Storage of multiple firmware copies to ensure system recovery from corruption or failed updates.
- **Operational Databases:** Non-volatile lookup tables for user authorization keys, user locations, and constellation orbital parameters.
- **Autonomous Operations:** Time-tagged sequences for autonomous maneuvering and mode switching, requiring only monthly ground synchronization.
- **Transient Data Cache:** Temporary buffer for user data requests, automatically discarding packets older than 5 minutes to ensure data freshness.

• **Data Packages and Communication Protocols**

To maximize network efficiency under the data rate constraints of the link using LoRa, the baseline design implements the CSP 2.x protocol, with a compact 6-byte header to handle four distinct traffic types:

- **User Data ($\leq$ 36 Bytes):** This is the primary uplink data product. Users are allowed to insert sensor readings from habitats, rovers, spacesuits and other ground assets. Keeping the total size under 40 bytes ensures a ToA of < 1 second between lunar ground and constellation under nominal modulation settings.
- **User Requests (18 bytes):** To enable IoT interactivity, users can request data from other users. This short format is optimized for rapid transmission and prioritized by the scheduling logic to ensure low latency. The 12-byte payload contains the Target Node ID, the access window requested and the authorization token.
- **Satellite Housekeeping (36 bytes):** Telemetry generated by the satellite (e.g. Battery voltage, ADCS state, Thermal) is formatted with the same packet size as Ground Data. This uniformity simplifies the OBDH tasks, allowing the same packaging for the Earth downlink without complex switching logic.
- **Relay Coordination Beacons (18 Bytes):** The Relay Satellite broadcasts visibility windows and time-slot allocations to the constellation. By restricting these beacons to a short frame, the system minimize the Relay's transmission duty cycle, thereby maximizing the time available for data

reception.

For the high-speed X-Band link between the Relay Satellite and Earth, the system transitions to the standardized CCSDS protocol to ensure compatibility with major ground station networks. The Relay Satellite functions as the protocol gateway, performing the encapsulation of downlink traffic and the translation of uplinked Earth Updates and Commands (32 Bytes), critical for clock synchronization, firmware updates, and emergency maneuvers, from CCSDS frames back into the internal CSP format.

• **Network Routing Logic and Data Flow**

The OBDH subsystem implements a dynamic routing architecture designed to manage the large data flow of the network. The data flow logic is defined for nominal and request operational scenarios:

Nominal Uplink and Forwarding: Upon reception of a CSP packet from a lunar surface user, the OBC first buffers the data in his memory. The storage queues the data for downlink and holds it for potential user-to-user requests (with a 5-minute discard time). Then, if the Relay Satellite is visible, the packet is forwarded directly. If not, the packet is routed via the ISL to the next node in the orbital plane, hopping along the constellation until it reaches a node with Relay visibility. Simultaneously, locally generated satellite housekeeping telemetry is injected into this same stream, following an identical routing path to the Relay and finally Earth.

User-to-User Request Handling: To support interactive IoT services, users may transmit request packets during their allocated slots. The OBC first authenticates the request against the on-board Authorization Database, so that unauthorized requests trigger an immediate "Access Denied" response to prevent network flooding. Valid requests are forwarded according to the on-board User Map. If the target data resides on a different orbital plane, the request is routed to the polar regions where orbital planes converge, allowing cross-plane transfer via ISL. Once the node holding the target data is reached, the requested payload is retrieved from memory and routed back to the requesting user following the reverse path.

The network capacity and user operational constraints are defined by the modulation scheme and the available link budget:

Surface-to-Satellite Link (Uplink): The system leverages LR-FHSS modulation to support high-density uplink traffic. While the protocol addressing space allows for up to 16,384 unique users (around 450 per satellite footprint), the physical link capacity is managed via a strict duty cycle. Each user is allocated one transmission slot for telemetry and one optional slot for requests every 90 seconds. This ensures that the ISL does not accumulate data in the queue.

Satellite-to-Surface Link (Downlink): A critical constraint is identified in the downlink path to the user. As LR-FHSS is an uplink-only modulation, the satellite must revert to standard LoRa for replies, resulting in a low data rate of ≈ 586 bps. Consequently, the volume of User-to-User replies must be strictly rate-limited by user request limitations to prevent saturation of the single downlink transmission channel.

High-speed LoRa links (5.5 kbps) are utilized for the satellite network to ensure rapid buffer clearing:

ISL Management: The ISL transceivers operate on a time-division duplex basis, switching between transmitting forwarded user data, requests and housekeeping via the forward antenna and receiving similar streams from the backward antenna. The low ToA (< 0.1 sec) of these high-rate packets allows the network to clear the large volume of data efficiently.

Constellation-to-Relay Coordination: The link to the Relay is coordinated via the reception of Relay Coordination Beacons. Satellites in the same orbital plane coordinate their transmissions to avoid collision at the their Relay receiver. The duty cycle is highly asymmetric: the link is primarily active in transmission mode (uploading aggregated ground and housekeeping data) and switches to reception mode only to capture visibility checks, clock updates, and telecommands.

• **Latency and Eclipse Management Strategy**

The network architecture is designed to manage two critical latency scenarios: the predictable signal propagation delays during nominal operations and the delay caused by the Relay Satellite's eclipse.

Nominal Operation: During nominal visibility, user telemetry is routed via ISL, which operates at 5.5 kbps with a 50% duty cycle to provide a fixed effective throughput of 2.75 kbps. To maintain network stability within this constraint, the transmission interval for the 455 users per satellite is scaled to 90 seconds, limiting the aggregate data inflow to 2.18 kbps. This configuration yields a positive safety margin of 20.7%, ensuring that buffers clear rapidly even during peak usage. Consequently, the multi-hop latency is minimized, resulting in a worst-case end-to-end latency of 5.20 seconds from the Lunar Surface to Earth, well within the 10-minute requirement.

Eclipse Mode (Store-and-Forward): During the 69-minute eclipse, the Relay Satellite switches to a buffering mode. The Relay's OBDH aggregates incoming streams from all three orbital planes, accumulating approximately 83.2 Mb of data (including CCSDS protocol overhead). Upon re-acquisition of Earth Line-of-Sight, the system utilizes the high-speed X-Band downlink (800 kbps) to dump the entire buffer in just 104 seconds, ensuring rapid restoration of real-time data flow.

Request Handling (Downlink Bottleneck): The critical path for User-to-User interaction is the satellite-to-ground downlink. The response ToA is 0.91 seconds per packet, limiting the saturation capacity to approximately 53 responses per minute. Under a worst-case peak load (10% of users requesting simultaneously), the queuing delay reaches around 41 seconds. The total user request latency is calculated to be 50.6 seconds, which satisfy the requirement. However, due to the half-duplex architecture of the LoRa transceiver, the downlink duty cycle directly occupies the radio interface, blocking the reception of new uplink data during transmission intervals. This conflict represents the primary scalability limitation of the current baseline.

Table 29: System Performance Summary: Data Budget & Latency

Metric	Value	Description
Users	455 Users	Max active users per satellite
Data Interval	90 s	Selected interval to maintain stability
User Inflow	2.18 kbps	Total load (36B Telemetry + 18B Request)
ISL Capacity	2.75 kbps	Effective Throughput
Safety Margin	+20.7%	ISL Capacity vs. User Inflow
Eclipse Storage	83.22 Mb	Data Volume (CSP + 22.5% CCSDS Overhead)
Dump Time	104.0 s	Time to clear buffer via X-Band (800 kbps)
Data Latency	2.39 s	Best Case (Direct visibility to Relay)
	5.20 s	Normal Worst Case (11 ISL Hops)
	70.8 min	Eclipse Worst Case (Storage + Dump)
Request Latency	$\approx$ 2 s	Best Case (Satellite already has data)
	8.62 s	Request Round-Trip (without Downlink Queue)
	50.62 s	Request Round-Trip (with Downlink Queue)

6 Ground Segment and Operations - Author: Atharva Dhore

6.1 Ground Segment and Operations Requirements and Design Drivers

6.1.1 Ground Segment and Operations Requirements

Table 30: Ground Segment Requirements

Requirement ID	Requirement Statement
REQ-GS-001	The Ground Segment shall provide Telemetry, Tracking and Command (TT&C) capability for the Relay satellite.
REQ-GS-002	The Ground Segment shall receive aggregated IoT payload data from the Relay satellite via X-band downlink.
REQ-GS-003	The Ground Segment shall uplink telecommands to the Relay satellite for constellation management, including time synchronization, firmware updates and configuration updates.
REQ-GS-004	The Ground Segment shall interface with the Mission Operations Center (MOC) to process, archive and distribute payload data.
REQ-GS-005	The Ground Segment shall maintain a minimum average communication availability of 99% with the Relay satellite over one year.
REQ-GS-006	The Ground Segment shall support X-band uplink frequencies within 7.145–7.235 GHz and downlink frequencies within 8.400–8.500 GHz.
REQ-GS-007	All Earth–Relay communication links shall close with a minimum link margin of 2 dB under worst-case geometry during nominal operations.
REQ-GS-008	The Ground Segment shall support a minimum sustained downlink data rate of 800 kbps to enable Relay buffer dump after eclipse periods.
REQ-GS-009	The Ground Segment shall ensure that end-to-end data latency does not exceed $T_{eclipse} + T_{next\_contact}$ under nominal operations.
REQ-GS-010	The Ground Segment shall support store-and-forward operations to ensure no data loss during Relay Earth occultation periods.
REQ-GS-011	The Ground Segment shall operate in Primary Receive Mode, Command Uplink Mode and Periodic TT&C Monitoring Mode.
REQ-GS-012	The Ground Segment shall implement secure and authenticated command uplink mechanisms to prevent unauthorized access.

6.1.2 Design Drivers

The Ground Segment architecture is driven by the system-level constraints imposed by the Earth–Moon geometry, the Relay-based communication architecture, and the operational concept of store-and-forward data handling.

Earth–Moon Distance

The average Earth–Moon distance of approximately 384,400 km introduces significant free-space path loss. This drives the requirement for high-gain X-band antennas, high G/T performance, and robust link margins to ensure reliable communication under worst-case geometry conditions.

Relay-Based Architecture

The constellation does not directly communicate with Earth; instead, all traffic is routed through a single Relay satellite operating in Circular Polar Lunar Orbit. This makes the Relay a critical communication node, driving high TT&C reliability, secure command uplink capability, and high availability requirements.

Periodic Earth Occultation

Due to the selected polar relay orbit, deterministic Earth occultation periods occur. Continuous real-time communication is therefore not guaranteed. This drives the implementation of a store-and-forward communication concept, where data buffering onboard the Relay and high-rate post-eclipse dump capability are essential.

Data Rate and Buffer Management

During eclipse periods, IoT data accumulates onboard the Relay. After Earth re-acquisition, the Ground Segment must support sufficiently high downlink data rates to clear the buffer within a short contact window. Therefore, link margin is used to shorten dump time rather than to increase throughput.

Frequency Allocation Constraints

The use of X-band frequencies (7.145–7.235 GHz uplink and 8.400–8.500 GHz downlink) drives compatibility with established deep-space ground networks and dictates RF front-end design constraints.

Global Availability Requirement

To achieve annual communication availability above 99%, geographically distributed deep-space ground stations are required. This drives the selection of established networks such as DSN, ESTRACK or NSN.

Security and Command Integrity

Since the Relay manages the entire constellation, secure and authenticated telecommand uplink is mandatory. This drives encryption, authentication mechanisms, and controlled ground access procedures.

6.2 Assumptions and trade-off

6.2.1 Assumptions

The Ground Segment baseline design is based on the following assumptions:

Established Deep-Space Network Availability

It is assumed that access to an existing deep-space ground network (e.g., DSN, ESTRACK or equivalent commercial provider) is available throughout the mission lifetime. No dedicated proprietary antenna infrastructure is assumed to be developed by the mission.

X-Band Compatibility

It is assumed that the selected ground network supports X-band uplink (7.145–7.235 GHz) and downlink (8.400–8.500 GHz) frequencies with sufficient G/T to close the Relay–Earth link with margin.

Store-and-Forward Communication Model

Continuous Earth visibility is not required. The Relay satellite is assumed to buffer IoT data during eclipse periods and dump accumulated data during subsequent ground station contacts.

Predictable Relay Orbit Geometry

The Relay Circular Polar Lunar Orbit is assumed to maintain stable and predictable Earth visibility windows, enabling deterministic pass scheduling.

Data Volume Consistency

The IoT data generation rate is assumed to remain within the analyzed limits used in the buffer sizing calculations. No unexpected high-rate scientific payload data is considered.

Clock Drift Correction via Ground Updates

It is assumed that periodic telecommands from the Ground Segment are sufficient to maintain time synchronization of the Relay and constellation clocks.

6.2.2 Trade-Off Analysis

Several architectural trade-offs were performed to define the Ground Segment baseline.

Dedicated Ground Infrastructure vs. Established Networks

A trade-off was performed between building a mission-dedicated ground station and leasing services from established deep-space networks. While a dedicated station would provide operational independence, the development cost, certification effort, and long-term maintenance complexity are prohibitive. Therefore, the baseline selects established deep-space infrastructure to minimize cost and schedule risk.

Continuous Downlink vs. Store-and-Forward

A continuous real-time communication architecture was evaluated. However, due to periodic Earth occultations from the selected Relay orbit, continuous contact cannot be guaranteed without multiple Relay spacecraft or halo-type orbits [26]. The store-and-forward concept was selected as it reduces orbital complexity while maintaining data integrity.

High Throughput vs. High Reliability

Increasing downlink throughput beyond the required buffer dump rate would increase power demand and RF complexity without significant operational benefit. Instead, link margin is allocated to ensure reliable and deterministic buffer clearing rather than maximizing peak throughput.

Large Aperture vs. Moderate Aperture Ground Stations

Larger antennas improve link margin and reduce contact duration. However, mission analysis shows that moderate deep-space apertures (20 m class, 35 m preferred) provide sufficient performance [40]. Therefore, extremely large aperture infrastructure is not required.

6.3 Baseline Design

The Ground Segment baseline architecture is designed to support reliable Earth–Relay communication in X-band while enabling store-and-forward lunar IoT operations. The architecture consists of three main elements: the Earth X-band Ground Station, the Mission Operations Center (MOC), and the selected Deep-Space Network provider.

Ground Network Selection:

The primary ground station network selected for the mission baseline is the NASA Deep Space Network (DSN) [40]. X-band capable DSN stations include Goldstone (USA), Madrid (Spain), and Canberra (Australia), providing geographically distributed global coverage and high annual availability.

Alternative networks considered include ESA ESTRACK (Cebreros - Spain, New Norcia - Australia, Malargüe - Argentina) and the NASA Near Space Network (NSN). Final selection is driven by X-band compatibility, scheduling availability, cost, and mission timeline.

Frequency Allocation:

The Earth–Relay link operates in X-band [19] with: Downlink (Relay → Earth): 8.400–8.500 GHz;

Uplink (Earth → Relay): 7.145–7.235 GHz.

Deep-Space Station Performance:

The baseline assumes a 35 m class deep-space X-band station with representative parameters summarized in Table 31. Mission analysis confirms sufficient link margin for deterministic Relay buffer clearance.

Table 31: Representative 35 m Deep-Space X-Band Station Performance

Parameter	Value
Antenna gain @ 7.2 GHz (TX)	66.22 dBi
Antenna gain @ 8.45 GHz (RX)	67.61 dBi
RX performance (G/T)	48.6–50.6 dB/K
Typical data rate (uplink)	1–16 kbps
Typical data rate (downlink)	0.256–10+ Mbps

Operational Modes:

The Ground Segment operates in three modes: **GS Rx (Primary)** - high-rate payload reception; **GS Tx (Secondary)** - telecommand uplink; **GS TT&C (Periodic)** - health monitoring.

Store-and-Forward Architecture:

Due to periodic Earth occultations [26], continuous real-time communication is not guaranteed. The baseline adopts store-and-forward operation: data is buffered onboard during eclipse and dumped at high rate during the next contact; no real-time requirement exists during eclipse.

Latency Requirement:

$$T_{latency} \leq T_{eclipse} + T_{next\_contact}$$

This ensures buffered data delivery within one eclipse cycle under nominal conditions.

Scheduling Model:

Each contact follows a deterministic sequence: acquisition/lock/synchronization (10 s), high-rate downlink phase, and command uplink window.

Availability and Fault Tolerance:

The philosophy assumes minimum 95% station availability; a missed pass is not mission failure; temporary outages are survivable due to onboard buffering.

7 Concept of Operation - Author: Jakub Czerniej

7.1 Mission Overview

7.1.1 Mission Statement

The mission aims to establish a high-availability lunar IoT telecommunications infrastructure. The system consists of 36 microsatellites in Low Lunar Orbit (LLO) and a primary Relay satellite in High Polar Orbit. The constellation provides global LoRaWAN/S-band connectivity for lunar surface assets (landers, rovers, sensors), while the Relay satellite ensures continuous high-bandwidth backhaul to Earth ground stations.

7.2 System Architecture

7.2.1 Space Segment

- **IoT Orbiters (36 units):** 50.0 kg (Wet Mass) platforms equipped with low-thrust Electric Propulsion (≈ 30 mN). Primary payload: LoRaWAN transceivers.
- **Relay Satellite (1 unit):** High-power bus with Bipropellant propulsion for high-energy maneuvers (BLT/LOI). Primary payload: High-gain X/Ka-band Earth-link and Inter-Satellite Link (ISL) aggregation.
- **Orbital Transfer Vehicle (OTV):** Heavy-duty dispenser utilizing the Leros 1b engine for the 4.5-day direct transfer and circularization of 12-satellite batches.

7.2.2 Ground Segment (Operational Assumption)

- **Mission Operations Center (MOC):** A centralized, cloud-supported facility responsible for automated telemetry monitoring, orbit determination (OD), and command uplink.
- **Ground Station Network (GSN):** Deep Space Network (DSN) for LEOP, TLI, and LOI maneuvers.

7.2.3 Communications Architecture

The mission employs a store-and-forward architecture. Surface IoT data is collected by the LLO constellation, transferred via ISL to the high-altitude Relay satellite, and subsequently downlinked to Earth Ground Stations. Command and Control (C2) follows the reverse path, with critical contingency commands accessible via direct-to-Earth low-rate links on the IoT orbiters.

7.3 Mission Phases

Phase 1: Relay Satellite Deployment (RFA One)

The Relay mission serves as the precursor to the constellation deployment, ensuring backhaul availability.

- **Launch and TLI:** RFA One performs a Ballistic Lunar Transfer (BLT) to minimize propellant consumption.
- **Cruise (110 Days):** Low-energy transit allowing for precise trajectory corrections.
- **Lunar Orbit Insertion (LOI):** Bipropellant burn into a high polar elliptical orbit ($h \approx 6500$ km).
- **Commissioning (30 Days):** System checkouts and verification of Inter-Satellite Link (ISL) readiness.

Phase 2: Constellation Deployment (Neutron Launch)

Each of the three Neutron launches delivers a batch of 12 satellites. The timeline below represents a nominal flight sequence.

- **T-00:00:00:** Liftoff from Wallops Flight Facility.
- **T+01:00: Trans-Lunar Injection (TLI).** Upper stage burn sets the vehicle on a direct transfer trajectory.
- **T+01:30: OTV Separation.** The dispenser separates axially from the Neutron upper stage.
- **T+02:00: Solar Array Deployment (Critical Event).** OTV wings deploy to generate power.

- **T+24:00: MCC-1 (Calibration Burn).** Leros 1b engine firing for trajectory correction ($\Delta v <$ 50 m/s).
- **T+04.0 Days: MCC-2 (Fine Navigation).** RCS maneuvers to target perilune altitude (500 km) and inclination (84°).
- **T+04.5 Days: Lunar Orbit Insertion (LOI).** 10–14 minute retrograde burn ($\Delta v \approx 850$ m/s).
- **T+05.0 Days: Circularization.** Apoapsis burn to achieve nominal orbit ($a = 2250$ km, $e \approx 0$).
- **T+05.5 to T+05.6 Days: Payload Deployment.** Sequential release of Batch 1 (Face A) and Batch 2 (Face B) separated by a 180-degree Yaw Slew.

Phase 3: OTV Disposal Sequence

Immediately following deployment, the OTV initiates its self-disposal campaign.

- $T_{Sep} + 00 : 10$ **min: Collision Avoidance.** RCS maneuver to drift safely away from the deployed constellation.
- $T_{Sep}+12$ **hrs to 14 days: Ground Track Phasing.** Wait phase for lunar rotation to align Oceanus Procellarum with the orbital plane.
- $T_{Deorbit} - 00 : 00$**: Deorbit Burn.** 60–90 second Leros 1b ignition on the lunar Far Side ($\Delta v \approx$ 100 m/s).
- $T_{Deorbit} + 00 : 05$ **min: Passivation.** Venting of propellant/pressurant and battery discharge.
- $T_{Deorbit} + 60$ **min: Impact.** Hard kinetic impact into Oceanus Procellarum at ≈ 1.7 km/s.

Phase 4: Constellation Phasing and Slot Acquisition

Following the separation from the OTV, the 12 satellites must transition from a cluster to their designated orbital slots.

- $T_{Sep} + 0$ **to 2 hrs**: **Initial Acquisition.** Satellites perform autonomous detumbling and establish Inter-Satellite Links (ISL) with the Relay satellite to verify health and timing.
- $T_{Sep}+2$ **hrs to 10 hrs (3 orbits)**: **Differential Drift Maneuver.** Satellites use Electric Propulsion to modify their semi-major axis (a). By operating at slightly different altitudes, they utilize orbital mechanics to drift into their 30° angular separation slots.
- **Day 7 (3 orbits)**: **Slot Acquisition (Circularization & Locking).** Satellites use Electric Propulsion again to reach the target position, each orbiter executes a final burn to return to the nominal 500 km altitude, "locking" its position in the plane.
- **Deployment Complete**: **Transition to FOC.** Upon successful positioning, the satellites activate their LoRaWAN payloads and transition to the 5-year operational phase.

Phase 5: Nominal Operations (FOC)

The 5-year operational phase focuses on IoT service delivery and fleet maintenance.

- **Autonomous Data Collection:** 36 satellites collect surface LoRaWAN packets and route them via ISL to the Relay satellite.
- **Station Keeping:** Autonomous Electric Propulsion burns to maintain frozen orbit parameters against lunar mascon perturbations.

Phase 6: Orbiter End-of-Life (EOL) Disposal

Controlled disposal of individual IoT satellites via multi-stage deorbiting.

- **Day 1–7 (Perilune Lowering):** Multi-burn retrograde sequence at Apolune. Perilune altitude reduced from 522 km to 10 km (30–40 min duty cycles).
- **Day 8 (Phasing):** Passive drift to synchronize with target impact zone (Oceanus Procellarum).
- **Day 9 (Terminal Descent):** A continuous 1.3-hour retrograde burn lowers virtual perilune to −50 km.
- **Impact:** Grazing incidence impact at ≈ 1.7 km/s; Loss of Signal (LOS) confirmed.

Phase 6.2: Relay End-of-Life (EOL) Disposal

Following the disposal of the IoT constellation, the Relay satellite performs its final deorbit campaign to clear the high-altitude polar orbit.

- **Sept 15 – Sept 22, 2035**: **Relay Deorbit Campaign.** A 7-day operational window dedicated to the final decommissioning of the backhaul infrastructure.
- **Maneuver**: **Retrograde Burn.** Utilizing its high-thrust bipropellant engine, the Relay satellite executes a significant retrograde maneuver to lower its perilune from 6500 km to a sub-surface altitude.
- **Target**: **Oceanus Procellarum.** The impact trajectory is synchronized with the established "mission graveyard" zone to ensure all hardware is consolidated in a single region.
- **Conclusion**: **Final Passivation & Impact.** All remaining fuel is depleted during the burn, and batteries are discharged prior to the kinetic impact. Loss of Signal (LOS) marks the formal end of the mission.

7.4 Operational Modes

The spacecraft state machine is designed to manage power and subsystem priorities across different mission phases. The following modes define the operational "states of consciousness" for both the IoT Orbiters and the Relay satellite.

Nominal Mode This is the default state during the 5-year operational phase.

- **Payload Activity:** LoRaWAN and S-band transceivers are active for surface data collection.
- **Attitude:** Nadir-pointing to maintain optimal link margins with the lunar surface.
- **Communication:** Inter-satellite links (ISL) are active for data routing to the Relay satellite.

Safe Mode (Survival) An autonomous state triggered by the FDIR system in response to critical anomalies.

- **Load Shedding:** All non-essential payloads and subsystems are powered down.
- **Attitude:** Sun-pointing to maximize power generation via solar arrays.
- **Communication:** Switches to the Low-Gain Antenna (LGA) to broadcast a "Beacon" health tone to Earth.

7.5 Contingency & FDIR

The Failure Detection, Isolation, and Recovery (FDIR) system ensures mission survival during off-nominal events through autonomous onboard logic.

Autonomous Recovery Logic (FDIR) The system monitors telemetry against predefined "Red Limits" (e.g., battery voltage < 24 V or CPU temperature $> 60°$C).

- **Detection:** Onboard sensors detect a violation of safety parameters.
- **Isolation:** The faulty subsystem is isolated (e.g., switching to a redundant transceiver).
- **Recovery:** If isolation fails, the spacecraft enters Safe Mode and awaits Ground Station intervention.

Specific Contingency Scenarios

- **Loss of Signal (LOS):** If no command is received for a predefined period (> 72 hours), the spacecraft initiates a "Comm-Sweep," cycling through all radio frequencies and antenna orientations to re-establish contact with the Mission Operations Center (MOC).
- **Under-voltage / Power Contingency:** If power generation drops below critical levels (e.g., during an extended eclipse), the spacecraft enters a "Deep Sleep" state, maintaining only the flight computer and clock, until solar intensity increases.
- **Propulsion Degradation:** In the event of electric thruster performance loss, the MOC will initiate an accelerated EOL campaign while the spacecraft still possesses sufficient Δv to achieve a controlled lunar impact.

7.6 Ground Segment & Data Flow

This section describes the infrastructure and logical paths required to manage the fleet of 36 satellites and deliver lunar data to the end-user.

Mission Operations Center (MOC) The primary MOC is the central hub for mission command and control. It utilizes a cloud-based Mission Control System (MCS) for:

- **Command Generation:** Planning and uplinking weekly time-tagged command schedules.
- **Telemetry Processing:** Real-time monitoring of spacecraft health and automated anomaly detection.
- **Orbit Determination (OD):** Processing tracking data to refine orbital parameters for station-keeping.

Ground Station Network (GSN)

- **Critical Phase Support:** Utilization of the Deep Space Network (DSN) or high-gain Tier-1 stations during LEOP, TLI, and LOI to ensure stable links during high-dynamic maneuvers.
- **Routine Operations:** Utilization of commercial Ground Segment as a Service (GSaaS) providers (e.g., KSAT, SSC). The Relay satellite acts as the primary downlink node, performing high-bandwidth bulk data dumps during scheduled Earth visibility windows.

Data Flow Path The mission employs a multi-hop "Store-and-Forward" architecture:

1. **Surface-to-Orbit:** Lunar surface assets transmit IoT packets via LoRaWAN to the nearest IoT Orbiter.
2. **In-Orbit Aggregation:** The IoT Orbiter stores the data and transfers it to the Relay satellite via the Inter-Satellite Link (ISL).
3. **Backhaul Downlink:** The Relay satellite compresses and transmits the aggregated data to Earth via Ka-band.
4. **User Delivery:** The Ground Station routes the raw data to the MOC, where it is decrypted and delivered to the end-user.

7.7 Risk Analysis

The following table outlines the critical operational risks and the corresponding mitigation strategies implemented in the mission design.

8 Launch and Deployment - Author: Gonzalo Cuesta & Jakub Czerniej

The launch and deployment of the constellation satellites is divided in three main phases. First, the main launcher is used to get from the earth's surface to lower earth orbit and afterwards the trans

Risk Event	Impact	Mitigation Strategy
OTV Engine Failure during LOI	Critical	Rigorous qualification of the Leros 1b engine and implementation of an automated RCS-based "Rescue Burn" for emergency capture.
Loss of Relay Satellite	High	Implementation of an emergency "Direct-to-Earth" low-rate communication mode for individual IoT Orbiters.
Lunar Mascon Perturbations	Medium	Use of autonomous onboard station-keeping scripts to maintain frozen orbit parameters with minimal ground intervention.
Deployment Collision	High	Precise OTV "Back-off" maneuvers and timed sequential separation of satellites to ensure physical clearance.

Table 32: Operational Risk Matrix

lunar injection is performed. Secondly, an Orbiter Transfer Vehicle (OTV) separates from the launcher and transports the satellites to their correct orbit. Lastly, the satellites separate from each other in their orbit by orbit phasing.

Launch The launcher must transport the Orbiter Transfer Vehicle to a trajectory towards the moon. For the payload mass for this mission, the launcher that is the most cost-effective is the "RocketLab Neutron". This rocket has the ability to put a payload with a mass of 2000kg on a trajectory towards the moon which is enough for the requirements of this mission. It also has a reasonable launch price.

Orbiter Transfer Vehicle The Orbiter Transfer Vehicle must transport the satellites that correspond to an orbital plane from lunar transfer to their orbit. This means it must perform trajectory correction maneuvers, the lunar orbit insertion, satellite deployment correction maneuvers and the disposal burn. This equates to 1071 m/s of delta-v capability. The Orbiter Transfer Vehicle that was designed has a wet mass of 735.5 kg.

9 Mass Budget - Author: Jakub Czerniej & Atharva Dhore

Mass Estimation Approach

An initial top-down mass allocation based on SMAD statistical models targeted a wet mass of 50 kg. A detailed bottom-up estimation derived from the CAD model results in a predicted wet mass of 55.6 kg, corresponding to a 10% growth. The increase is attributed to higher model fidelity, inclusion of harness and mechanisms, and the use of COTS components.

Dry and Wet Mass

The total dry mass of the spacecraft is 52.1 kg. With 3.5 kg of propellant allocated for orbit maintenance and disposal maneuvers, the resulting launch (wet) mass is 55.6 kg.

Subsystem Mass Drivers

The dominant contributors are Structure and Mechanisms (36%), Power subsystem (24%), and ADCS (11%). The structural mass reflects lunar load requirements and deployable elements. The power mass is driven by solar array sizing and battery capacity for eclipse operations. The payload mass fraction remains low due to the lightweight LoRa communication architecture.

Table 33 presents the detailed bottom-up mass budget derived from the CAD model, including Current Best Estimate (CBE), applied subsystem-level contingencies, and predicted mass. The analysis results in a total dry mass of 52.13 kg and a wet mass of 55.63 kg including 3.5 kg of propellant. Structure, power, and propulsion are the dominant mass contributors, reflecting the requirements of lunar orbit

operations and electric propulsion integration.

Contingency Policy

Subsystem-level contingencies between 5% and 20% were applied depending on design maturity and structural criticality. Higher margins were assigned to primary structure and propellant tanks, while lower margins were used for qualified COTS electronics.

Mass Compliance Assessment

Although the predicted wet mass exceeds the initial 50 kg allocation, the selected launch vehicle provides sufficient lift capability margin. The mass growth is therefore considered acceptable and does not compromise mission feasibility.

Table 33: Detailed Bottom-Up Mass Budget with Subsystem-Level Contingencies

Detailed Bottom-Up Mass Budget (CBE from CAD Model)							
No	Subsystem / Component	Quantity	Unit Mass [kg]	CBE Total [kg]	Contingency (%)	Growth [kg]	Predicted Mass (kg)
1	**Structure & Mechanisms**			**17,03**		**3,217**	**20,247**
	SADM	2	0,465	0,93	5	0,0465	0,9765
	HDRM	4	0,025	0,1	5	0,005	0,105
	Separation Ring	1	0,23	0,23	5	0,0115	0,2415
	Structure	1	11,35	11,35	20	2,27	13,62
	Yoke	2	0,01	0,02	20	0,004	0,024
	Triangle	2	2,2	4,4	20	0,88	5,28
2	**Propulsion**			**6,505**		**0,67925**	**7,18425**
	Hall-Effect Thruster	1	0,83	0,83	5	0,0415	0,8715
	PPU	1	1,88	1,88	5	0,094	1,974
	PFC	1	0,86	0,86	5	0,043	0,903
	PMA	1	0,575	0,575	5	0,02875	0,60375
	Tank	1	2,36	2,36	20	0,472	2,832
3	**Power**			**12,6208**		**1,03604**	**13,65684**
	Battery	4	0,48	1,92	5	0,096	2,016
	EPS	1	0,5	0,5	5	0,025	0,525
	Battery (Miscallenous)	1	0,2	0,2	5	0,01	0,21
	Solar Panel	6	1,35	8,1	10	0,81	8,91
	Solar Cell	528	0,0036	1,9008	5	0,09504	1,99584
4	**ADCS**			**5,752**		**0,2876**	**6,0396**
	Thruster	1	1,25	1,25	5	0,0625	1,3125
	Star Tracker	2	0,042	0,084	5	0,0042	0,0882
	Sun Sensor	6	0,003	0,018	5	0,0009	0,0189
	Reaction Wheel	4	1,1	4,4	5	0,22	4,62
5	**Thermal**			**2,120072**		**0,244**	**2,3640756**
	OSR 1	2	0,000025	0,00005	5	2,5E-06	0,0000525
	OSR 2	1	0,000022	0,000022	5	1,1E-06	0,0000231
	Radiator Mechanism	1	0,64	0,64	15	0,096	0,736
	Deployable Radiator	2	0,74	1,48	10	0,148	1,628
6	**Payload**			**1**		**0,05**	**1,05**
	Payload	1	1	1	5	0,05	1,05
7	**Telecom**			**0,44**		**0,022**	**0,462**
	S-Band Antenna (13 db)	1	0,17	0,17	5	0,0085	0,1785
	S-Band Antenna (7.5 db)	3	0,09	0,27	5	0,0135	0,2835
8	**ODH**			**0,12**		**0,006**	**0,126**
	OBC-ADCS Computer	1	0,12	0,12	5	0,006	0,126
9	**Others (wires, fasteners)**	1	1	**1**	**0**	**0**	**1**
A	**TOTAL DRY MASS**						**52,1297656**
10	**Fuel**	1	3,5	**3,5**	**0**	**0**	**3,5**
B	**TOTAL WET MASS**						**55,6297656**

10 Cost and Schedule - Author: Jakub Czerniej

Operational Concept and Mission Profile

The Lunar IoT Mission is scheduled to span from mid-2026 to 2035, beginning with an intensive initiation phase focused on regulatory compliance and infrastructure acquisition. A critical path activity in the early stages is the immediate filing for frequency allocations with the ITU, a process that requires a minimum two-year lead time. Simultaneously, negotiations for ground segment support must commence in early 2027. Due to the high utilization of the NASA Deep Space Network (DSN), the mission strategy prioritizes securing support from networks to ensure reliable Telemetry, Tracking, and Command (TT&C) capabilities.

The mission architecture employs a hybrid launch strategy designed to optimize the performance of two distinct payload types. The Relay Satellite is scheduled for launch in Q1 2030 aboard an RFA One vehicle. Given the launch vehicle's trans-lunar injection (TLI) capacity of approximately 300 kg relative to the satellite's 250 kg mass, a direct high-energy transfer is not feasible. Consequently, the

mission will utilize a low-energy Ballistic Lunar Transfer (BLT). While this extends the cruise duration to 3–4 months, it significantly reduces the Delta-V required for capture, allowing the satellite to safely achieve the target 6,500 km polar orbit.

In contrast, the deployment of the 36-satellite IoT constellation will execute a rapid transit profile starting in mid-2030. Three Neutron launches will occur at one-month intervals, utilizing a Direct Transfer trajectory with a flight time of approximately 4.5 days. A custom Orbital Transfer Vehicle (OTV) will perform the critical Lunar Orbit Insertion (LOI) burn ($\Delta v \approx 850$ m/s) and sequentially dispense the satellites into a 500 km circular polar orbit. The operational phase is planned for five years, concluding with a controlled end-of-life (EOL) sequence in 2035. To mitigate orbital debris, the constellation will perform perigee-lowering maneuvers to -10 km, resulting in a targeted impact within the Oceanus Procellarum region.

Master Project Schedule

The following table outlines the detailed project roadmap, encompassing development phases, launch campaigns, and operational milestones.

Table 34: Master Mission Schedule

ID	Task Name	Duration	Start	End	Notes
1	**PHASE 1: INITIATION**	**456 days**	**01.07.26**	**30.09.27**	
1.1	Project Kick-off & Fundraising	92 days	01.07.26	30.09.26	Initial funding tranche
1.2	Mission Definition Review (MDR)	92 days	01.10.26	31.12.26	Architecture freeze
1.3	Launch Slot Reservation	181 days	01.01.27	30.06.27	1xRFA One, 3xNeutron
1.4	Ground Segment Negotiation	273 days	01.01.27	30.09.27	DSN vs. Commercial
1.5	ITU Frequency Application	730 days	01.03.27	01.03.29	Regulatory process 2yrs
2	**PHASE 2: DEVELOPMENT**	**1096 days**	**01.10.27**	**30.09.30**	
2.1	Preliminary Design Review (PDR)	1 day	30.09.27	30.09.27	
2.2	Engineering Model (EM) & FlatSat	366 days	01.10.27	30.09.28	Electronics validation
2.3	Critical Design Review (CDR)	1 day	30.09.28	30.09.28	Final design freeze
2.4	Series Production (36 Sats)	455 days	01.10.28	31.12.29	Integration of payloads
2.5	Relay Satellite Construction	365 days	01.10.28	30.09.29	Integration Biprop eng
2.6	OTV Construction (3 Units)	365 days	01.01.29	31.12.29	Transfer vehicles
2.7	Environmental Testing	180 days	01.01.30	30.06.30	TVAC, Vibration
3	**PHASE 3: RELAY MISSION**	**150 days**	**01.01.30**	**31.05.30**	**Target: 6500 km**
3.1	Relay Shipment & Integration	14 days	01.01.30	14.01.30	
3.2	**LAUNCH: RFA One (Relay)**	**1 day**	**15.01.30**	**15.01.30**	window for BLT
3.3	BLT Cruise (Ballistic Transfer)	110 days	16.01.30	05.05.30	Low-energy (3-4 mnth)
3.4	LOI (Lunar Orbit Insertion)	1 day	06.05.30	06.05.30	Biprop capture burn
3.5	Relay Commissioning	30 days	07.05.30	06.06.30	Ready for constellation
4	**PHASE 4: CONSTELLATION**	**100 days**	**01.06.30**	**10.09.30**	**Target: 500 km, 84°**
4A	**Plane A Deployment**	**15 days**	**01.06.30**	**15.06.30**	
4A.1	**LAUNCH: Neutron 1**	0 days	01.06.30	01.06.30	T-0

ID	Task Name	Duration	Start	End	Notes
4A.2	TLI Burn & Separation	1 day	01.06.30	01.06.30	T+1h to T+2h
4A.3	Direct Transfer Cruise	4 days	02.06.30	05.06.30	T+24h to T+4.5d
4A.4	LOI Burn (OTV Main Engine)	1 day	05.06.30	05.06.30	$\Delta v \approx 850$ m/s
4A.5	Deployment (12 Sats)	1 day	06.06.30	06.06.30	T+5.5 days
4A.6	OTV Disposal (Impact)	9 days	07.06.30	15.06.30	Oceanus Procellarum
4B	**Plane B Deployment**	**15 days**	**01.07.30**	**15.07.30**	**30 days post-L1**
4B.1	**LAUNCH: Neutron 2**	0 days	01.07.30	01.07.30	Target RAAN +30°
4C	**Plane C Deployment**	**15 days**	**01.08.30**	**15.08.30**	**30 days post-L2**
4C.1	**LAUNCH: Neutron 3**	0 days	01.08.30	01.08.30	Target RAAN +60°
5	**PHASE 5: OPERATIONS**	**5 years**	**01.09.30**	**31.08.35**	
5.1	Full Operational Capability	1825 days	01.09.30	31.08.35	Commercial IoT Live
5.2	Replenishment Decision	1 day	01.01.34	01.01.34	Decision on Gen-2
6	**PHASE 6: END OF LIFE**	**30 days**	**01.09.35**	**30.09.35**	
6.1	Constellation Deorbit	14 days	01.09.35	14.09.35	Perilune to -10 km
6.2	Relay Deorbit	7 days	15.09.35	22.09.35	Retrograde burn

10.1 Cost budget

10.1.1 Financial Methodology and Tools

The financial projection for the Lunar IoT Constellation utilizes a hybrid estimation approach, aligning with the project's commercial "NewSpace" philosophy. To ensure high fidelity in the cost model, the analysis was supported by access to industry-standard governmental tools and a detailed hierarchical breakdown of the system.

The cost model is derived using three primary methods:

- **Product Breakdown Structure (PBS) Alignment:** The budget is strictly mapped to the subsystems defined in the project's Product Breakdown Structure. This ensures that every hardware element is accounted for.
- **Parametric Modeling (NICM & PCEC):**
  - Payload instrumentation costs were cross-referenced using the **NASA Instrument Cost Model (NICM)** to validate the estimates for the LoRa and Inter-Satellite Link (ISL) modules.
  - Subsystem integration and Non-Recurring Engineering (NRE) costs were benchmarked against the **NASA Project Cost Estimating Capability (PCEC)**. These governmental baselines were then calibrated with "Commercial Class D" complexity factors to reflect the streamlined documentation and higher risk tolerance of this mission.
- **Catalog Pricing:** Major COTS hardware elements (e.g., satellite buses, sensors) and launch services were estimated using 2026 market projections for providers such as Rocket Lab and RFA.

10.1.2 Architectural Baseline for Costing

The budget is predicated on the following architectural configuration, as defined in the PBS:

- **Space Segment:** 36x Microsatellite Orbiters (Low Lunar Orbit), 1x High-Power Relay (High Lunar Orbit), and 3x Orbital Transfer Vehicles (OTVs) for orbit insertion.
- **Launch Segment:** A multi-launch strategy utilizing **Rocket Lab Neutron** (for the constellation) and **RFA One** (for the Relay).
- **Timeline:** A 4-year development phase followed by a 5-year operational phase.

10.1.3 Capital Expenditure (CAPEX)

The total Capital Expenditure required to reach Initial Operating Capability (IOC) in Q3 2030 is estimated at **$216.5 Million (USD)**.

Table 35: CAPEX Breakdown (Investment to Orbit)

Cost Category	Item Description	Cost (USD)	Notes
Launch Services	3x Rocket Lab Neutron (Dedicated)	$150,000,000	Includes OTV
	1x RFA One (Dedicated Relay Launch)	$6,000,000	HLO Injection
Space Segment	36x Orbiters	$16,200,000	Vol. Pricing
	3x Orbital Transfer Vehicles (OTV)	$12,000,000	Lunar Insertion
	1x Relay Satellite	$8,000,000	Custom Design
	Payload Integration & NRE	$3,800,000	PCEC Calibrated
Risk & Insurance	Launch Insurance (10% Premium)	$20,000,000	Launch + HW
Ground Segment	Initial Mission Control Setup	$500,000	SW Licenses
TOTAL CAPEX		**$216,500,000**	

10.1.4 Operational Expenditure (OPEX)

The estimated annual OPEX during the service life (2030–2035) is **$4.2 Million (USD)** per year.

- **Ground Station Services ($3.0 M/year):** Allocation for a premium "Deep Space Network" service tier (e.g., KSAT or commercial equivalents). This high-cost item ensures priority access to large-aperture antennas, critical for maintaining the link with the HLO Relay and OTVs.
- **Engineering & Operations ($1.2 M/year):**
  - *Personnel:* Lean team of 6 FTEs (Flight Dynamics, Mission Operators, Systems Engineers) based in Munich.
  - *Overhead:* Spectrum licensing fees (ITU), office administration, and software maintenance.

10.1.5 Financial Phasing (Spend Profile)

Based on the Master Schedule, the CAPEX spending is distributed as follows:

- **Phase 1 (2026–2027): ∼10% of CAPEX.** Initial fundraising, reservation deposits for launch vehicles (RFA/Neutron), and Kick-off NRE.
- **Phase 2 (2027–2029): ∼60% of CAPEX.** The peak spending period covering series production of 36 satellites, Relay manufacturing, and OTV construction.
- **Phase 3/4 (2030): ∼30% of CAPEX.** Final launch milestone payments and insurance premiums due upon launch.

11 Limitations - Authors: Fiorenza Ferrante & Simone Borzaga

While the comprehensive analysis in this document confirms the feasibility of the overall mission concept, the system design imposes operational limitations driven by the selection of LoRa technology and the orbital geometry:

- **Small Data Rate and Packets:**
  The utilization of LoRa implies that the network is strictly limited to low-data-rate communication. The maximum attainable bit-rate is insufficient for high-definition scientific payloads, real-time video, or large file transfers, restricting the system's utility to short burst data applications as sensors data transmission.
- **Network Capacity & Scalability:**
  The current architecture has a finite user capacity before packet collision rates degrade network performance. While scalable up to 16.346 users, the network may not sustain future lunar missions needs without significant packet loss if LoRa assets on the ground overflow this number.
- **Single Point of Failure Risk:**
  The architecture relies on one Relay Satellite for communication to Earth. Unlike the distributed redundancy of the constellation itself, the Relay segment represents a potential single point of failure. A malfunction of the Relay payload would force the network to relay on other services to communicate with Earth (e.g. Lunar Gateway).
- **Connectivity Gaps:**
  The selection of a Polar Relay orbit introduces deterministic Earth occultation periods (up to 69 minutes per orbit during specific sessions). This necessitates a Store-and-Forward operational concept, precluding continuous near-real-time communication or immediate emergency intervention from Earth during these specific occultation windows.
- **User Constraints:**
  Some User Constraints are necessary to guarantee link closure while communicating with the constellation: 29 dBm for transmitting, 4 dBm in receiving, usage of correct frequencies. Others regard the data network (modulation, duty cycle, limited requests and data packets) and can limit the communication and data flow windows due to the necessity of not overloading the network.
- **Downlink Bottleneck:**
  The LoRa transceiver's half-duplex architecture creates a critical resource contention: the radio cannot receive uplink signals while transmitting downlink packets. Consequently, since a long time is spent during downlink transmission, the available uplink capacity is reduced, serving as the primary bottleneck for network scalability.

12 Future Work - Authors: Simone Borzaga & Fiorenza Ferrante

This section suggests future research efforts, aimed to improve the following key areas other than already mentioned limitations:

Hardware Evolution

To overcome the scalability limitations identified in the half-duplex LoRa baseline, future iterations of the system design should assess the integration of dual-transceiver payloads or advanced full-duplex hardware to enable simultaneous uplink and downlink operations, significantly reducing latency.

Navigation Capabilities Assessment

Given the stable orbital geometry of the Walker Delta 36/3/0 constellation, the network possesses the potential to provide positioning services alongside communication in the polar regions [35]. Future work

should quantify the system's performance as a Lunar Navigation Satellite System, assessing the onboard clock stability requirements needed to support precise orbit determination and user localization, and clearly defining the polar areas where navigation services could be guaranteed.

Deeper Relay Analysis

While the current study validated the relevance of the Relay satellite, a deeper level analysis is required define all aspects of its design. For instance, a detailed thermal modeling could be implemented to ensure the satellite can survive the lunar environment.

13 Conclusion - Author: Fiorenza Ferrante

The primary goal of this project was to achieve the mission objectives described in subsection 3.2. We successfully reached this goal, providing IoT coverage across the lunar surface and closing communication links with LoRa devices in all types of communications involving the constellation and ground assets. We established a bidirectional communication path between lunar surface, constellation, relay and Earth's selected ground stations, supporting all mission data transfer requirements. Moreover, we achieved to design a scalable system, that ensures compatibility between network and users through preassigned protocol, users duty cycle and communication modulation.

While the analysis identified specific operational limitations inherent to the chosen technology and orbital geometry, these constraints do not diminish the fundamental validity of the architecture. Instead, they serve to define the boundaries of the current baseline while highlighting improvement possibilities for future optimization. This work demonstrates the substantial potential of the proposed network, providing a robust and flexible foundation that can be expanded to support the growing complexity of future lunar exploration.

References

[1] Lunar thermal environment design guide, 2020.

[2] AAC Clyde Space. SS200 Fine Sun Sensor, 2026. Accessed: 2026-02-18.

[3] Abracon LLC. Real-time clock with integrated 32.768khz crystal oscillator, 2024.

[4] Anywaves. Compact x-band payload telemetry antenna. Product Datasheet, 2024.

[5] ITU Radiocommunication Assembly. Recommendation ITU-R RA.479-5: Protection of frequencies for radioastronomical measurements in the shielded zone of the Moon. *ITU*, 2003.

[6] AZUR SPACE Solar Power GmbH. Tj3g30 advanced triple junction solar cell (8x8 cm) datasheet. `https://www.azurspace.com/media/uploads/file_links/file/bdb_00010892-01-00_tj3g30-advanced_8x8.pdf`, 2024. Accessed: 2026-02-18.

[7] Blue Canyon Technologies. Spacecraft reaction wheels, 2026. Accessed: 2026-02-18.

[8] Bosch Sensortec. *BMI085 6-axis Inertial Measurement Unit Datasheet*, 2026. Document Revision 1.0. Accessed: 2026-02-18.

[9] COMAT. Solar array drive mechanism (sadm). `https://comat.space/wp-content/uploads/2021/09/SADM_compressed.pdf`, 2021. Accessed: 2026-02-18.

[10] M.A. Woodard D.C. Folta and D. Cosgrove. "Stationkeeping of the First Earth-Moon Libration Orbiters: The ARTEMIS Mission". *NTRS - NASA Technical Reports Server*, 2011.

[11] Kathleen C. Howell Emily M. Zimovan and Diane C. Davis. "Near Rectilinear Halo Orbits and their application in cis-lunar space". *ResearchGate*, 2017.

[12] European Space Agency. Moonlight services. `https://www.esa.int/Applications/Connectivity_and_Secure_Communications/Moonlight/Moonlight_services_seeking_feedback_for_updated_LunaNet_framework`, 2023.

[13] ExoTerra. Exoterra hallo data sheet, n.d. Accessed: 2026.

[14] David Folta. "Lunar Frozen Orbits". *NTRS - NASA Technical Reports Server*, 2008.

[15] David G. Gilmore. *Spacecraft Thermal Control Handbook*. Aerospace Press, 2002.

[16] GomSpace. Nanomind z7000 on-board computer. Product Datasheet, 2024.

[17] GomSpace A/S. Nanopower bpx battery module – product page and datasheet. `https://gomspace.com/product/nanopower-bpx/`, 2024. Accessed: 2026-02-18.

[18] GomSpace A/S. Nanopower p80 electrical power system – product page and datasheet. `https://gomspace.com/product/nanopower-p80/`, 2024. Accessed: 2026-02-18.

[19] Space Frequency Coordination Group. Recommendation SFCG 32-2R6: Communication and Positioning, Navigation, and Timing Frequency Allocations and Sharing in the Lunar Region. *Space Frequency Coordination Group*, 2025.

[20] Daniel Matthiae Guenther Reitz, Thomas Berger. Radiation exposure in the moon environment. *Planetary and Space Science*, 2012.

[21] Hyperion Technologies and Berlin Space Technologies. ST200 Star Tracker, 2026. Accessed: 2026-02-18.

[22] IMT S.r.l. X-band transponder. Product Datasheet, 2024.

[23] Innovative Solutions in Space. Isis-obc on-board computer. Product Datasheet, 2023.

[24] David J. Israel, Jason W. Mitchell, Michael A. Johnson, Kendall D. Mauldin, Antti A. Pulkkinen, Steven D. Christe, Christopher J. Roberts, La Vida D. Cooper, and Cheryl J. Gramling. Lunanet: A flexible and extensible lunar exploration communications and navigation infrastructure. In *IEEE Aerospace Conference*. IEEE, 2020.

[25] O. Ivanchuk. Estudio del acabado superficial de un cubesat, 2021.

[26] Jonathan Verville Grant Ryden Jaime Espera, Gregory Heckler. "NASA's Lunar Communications Relay and Navigation Systems (LCRNS)". *18th International Conference on Space Operations*, 2025.

[27] E. Jang et al. Study on optimal orbit phasing for neonsat constellation. *Acta Astronautica*, 239:685–695, 2026.

[28] E. M. Leonardi, G. de Angelis, and M. Pontani. Guidance strategies to deploy a lunar navigation constellation from gateway. *Acta Astronautica*, 232:143–153, 2025.

[29] LibCSP Contributors. libcsp: Cubesat space protocol, 2023.

[30] LoRa Alliance. Lorawan® l2 1.0.4 specification. Technical Report TS001-1.0.4, October 2020.

[31] Bruno Mattos, Lucas Anderson, Randy Jost, Charles Swenson, Denis Vieira, and Renan Menezes. Thermal and radiation design considerations for cubesats in low lunar orbit, 2023.

[32] MAVLink Development Team. *MAVLink 2 Packet Format and Serialization*, 2023.

[33] MAVLink Development Team. *MAVLink Developer Guide - Protocol Overview*, 2023.

[34] Meshtastic Project. *Mesh Broadcast Algorithm - Meshtastic Protocol Documentation*, 2024.

[35] Maksim Shirobokov Mikhail Ovchinnikov and Sergey Trofimov. "Lunar Satellite Constellations in Frozen Low Orbits". *Aerospace*, 2024.

[36] Mini-Circuits. Cbp-2150an+ bandpass filter. Product Datasheet, 2024.

[37] Mini-Circuits. X-band rf filters. Product Catalog, 2024.

[38] William Anthony Morad Nazari and Eric A. Butcher. "Continuous Thrust Stationkeeping in Earth-Moon L1 Halo Orbits Based on LQR control and Floquet Theory". *ResearchGate*, 2014.

[39] NASA. Artemis program overview. `https://www.nasa.gov/artemis`, 2023.

[40] NASA Jet Propulsion Laboratory. Deep space network telecommunications link design handbook. Technical Report 810-005, Jet Propulsion Laboratory, California Institute of Technology, 2023. Revision E.

[41] NASA Johnson Space Center. Lunar near rectilinear halo orbit (gateway). NASA Website, 2024. Accessed: February 18, 2026.

[42] M. Ovchinnikov, M. Shirobokov, and S. Trofimov. Lunar satellite constellations in frozen low orbits. *Aerospace*, 11(11):918, 2024.

[43] Christian Poivey. Radiation hardness assurance for space systems. *EEE NSREC*, 2002.

[44] Qorvo. Qpc1022 sp4t rf switch. Product Datasheet, 2023.

[45] Seiko Epson Corporation. *TG-5006CG TCXO: Crystal Oscillator Datasheet*, 2025. Accessed: 2026-02-17.

[46] Semtech Corporation. *LR1121 Datasheet - Long Range, Low Power, Multi-band LoRa Transceiver*, April 2025. Rev. 2.1.

[47] Semtech Corporation. *LR1121 User Manual*, 2025.

[48] Skyworks Solutions. Sky67151-396lf ultra low noise amplifier. Product Datasheet, 2023.

[49] Space Inventor. Obc-p3 on-board computer - technical specifications. SatCatalog, 2024.

[50] Space Inventor. S-band 2×2 antenna array. Product Datasheet, 2024.

[51] STMicroelectronics. Stm32h743/753 high-performance mcus, 2023.

[52] Texas Instruments. Tps25982 current-limiting power switch. Product Datasheet, 2024.

[53] Triad RF Systems. Ta1295 high power amplifier datasheet. Product Datasheet, 2023.

[54] VACCO Industries. Standard micro cubesat propulsion system (mips), 2026. Accessed: 2026-02-18.

[55] James R. Wertz and Wiley J. Larson. *Space Mission Analysis and Design*. Microcosm Press, 3rd edition, 1999.

[56] Winbond Electronics Corporation. *W25Q128JV 128M-bit Serial Flash Memory Datasheet*, 2021. Rev. G.

[57] WIRAN. S-band patch antenna. Product Datasheet, 2024.